DYNAMIC MODULUS TEST – LABORATORY INVESTIGATION AND FUTURE

IMPLEMENTATION IN THE STATE OF WASHINGTON

By

MUTHUKUMARAN ANBILPADUGAI ELANGOVAN

A thesis submitted in partial fulfillment of
the requirements for the degree of

MASTER OF SCIENCE IN CIVIL ENGINEERING

WASHINGTON STATE UNIVERSITY
Department of Civil and Environmental Engineering

AUGUST 2008

To the Faculty of Washington State University:

      The members of the Committee appointed to examine the thesis of MUTHUKUMARAN ANBILPADUGAI ELANGOVAN find it satisfactory and recommend that it be accepted.

_____

Chair

_____

_____

ACKNOWLEDGMENT

DYNAMIC MODULUS TEST – LABORATORY INVESTIGATION AND FUTURE IMPLEMENTATION IN THE STATE OF WASHINGTON

Abstract

by Muthukumaran Anbilpadugai Elangovan, M.S.
Washington State University
August 2008

Chair: Laith Tashman

The objectives of this study were to investigate and develop a database of dynamic modulus of the mixes widely used in the State of Washington, to investigate the sensitivity of dynamic modulus to aggregate gradation, and to evaluate the distress prediction accuracy of the *2002 Guide for the Design of New and Rehabilitated Pavement Structures* (MEPDG). Seven Hot Mix Asphalt (HMA) mixes, designated as Job Mix Formula (JMF) mixes, widely used in the State of Washington were first selected; a lower modified mix (LM) and an upper modified mix (UM), were derived from each JMF mix by decreasing percent-passing sieve #200 by 2% in the LM mix and increasing by 2% in the UM mix. Twenty-one mixes – two replicates in each mix – altogether forty-two specimens were prepared for the dynamic modulus tests; the mixes include seven JMF mixes, seven LM mixes and seven UM mixes. Target air voids in the test specimens were 7±1%. Dynamic Shear Rheometer (DSR) tests were conducted to measure the complex shear modulus (G^*) of the asphalt binders.

Sigmoidal master curves were constructed for all the mixes. The dynamic modulus data were analyzed statistically. Dynamic modulus of the JMF mixes showed significant variation at high temperatures. It was not sensitive to the ±2% variation in percent-passing sieve #200. Aggregate gradation influenced variation in dynamic modulus at high temperatures. A database

of dynamic modulus values of the mixes investigated and a database of sigmoidal fitting parameters for determining dynamic modulus of the mixes at any temperature and frequency were developed.

The performance of the mixes i.e. distresses were predicted using MEPDG. The predicted performance data were analyzed statistically. The MEPDG predicted rutting and alligator cracking reasonably well. Predicted IRI and measured IRI varied significantly; longitudinal cracking were inconsistent.

TABLE OF CONTENTS

LIST OF TABLES

LIST OF FIGURES

CHAPTER ONE

INTRODUCTION

1.1 Background

Over the years, since the construction of the first pavement in the United States in 1870 at Newark, New Jersey, pavement design has undergone many transformations. Especially, after the release of the 1986 AASHTO Design Guide at which time the need for a mechanistic based pavement design was recognized. Early pavement design methods were purely empirical and aimed at determining the optimum thicknesses of pavement structural layers to provide adequate strength and protection to the weak subgrade. With substantial changes in traffic volume and loading conditions, the emphasis shifted away to pavement performance (ride quality). In the late 1950's, construction of a series of test tracks was initiated, most importantly the AASHO Road Test. Subsequently, the 1961 Interim Guide, the 1972 Interim Guide, the 1986 and 1993 AASHTO Guides were developed. The 1972 version was the first attempt towards the design of overlays; the 1986 and 1993 versions of the AASHTO Guide addressed important issues like better characterization of subgrade and unbound layers, drainage, environmental effects and included reliability as a factor in the design. Even though empirical methods in the design were accurate, they were valid only for the materials and environmental conditions upon which they were developed.

The pavement community felt the need for a design method that will be valid over a broad range of materials, environmental and loading conditions and takes in to account the mechanical properties of pavement materials in the design. In 1988, the Strategic Highway Research Program (SHRP) began with the primary goal of developing a rational mix design

1

procedure that will address the limitations of the existing design methods. Consequently, in 1993 the Superpave system emerged with the following elements: new grading system for asphalt binders (performance graded (PG) grading system), guidelines for selection of aggregate, new mix design and mixture analysis procedures. The Department of Transportation (DOT) in many States in the country has adopted the Superpave method of design and many are in the process of implementing it in the routine design procedure.

A major limitation of the Superpave method at the time of its release was the lack of a strength test to evaluate the performance of compacted material. Instead, it relied mainly on specifications for material selection and volumetric mix criteria to ensure satisfactory performance. The industry realized the need for a strength test to ensure reliable mixture performance over a wide range of traffic and climatic conditions. Subsequently, in 1996, research began at the University of Maryland at College Park to identify and validate Simple Performance Tests (SPT) for permanent deformation, fatigue cracking, and thermal cracking to complement the Superpave volumetric mix design method. In 1999, the work was transferred to NCHRP Project 9-19 "Superpave Support and Performance Models Management." The research team assessed existing test methods for measuring HMA response characteristics. The principal evaluation criteria were (1) good correlation of the HMA response characteristics to actual field performance; (2) reliability; (3) ease of use; and (4) reasonable equipment cost.

A comprehensive laboratory program was conducted in which material responses of specimens prepared for 33 test method-test parameter combinations were measured. The measured responses were statistically correlated with the performance data from accelerated pavement testing projects, namely, WesTrack in Nevada, MnRoad in Minnesota, and FHWA Accelerated Loading Facility (ALF) experiments. NCHRP Report 465 summarizes the

experimental and analytical work performed for this study, which recommends the following SPT method-response parameter combinations selected for comprehensive field validation.

1. HMA Rutting (testing conducted at 37.8 to 54.4 °F)

   - Dynamic complex modulus term, $E^*/\sin\varphi$, determined from the triaxial dynamic modulus test

   - Flow time, F_t, determined from the triaxial static creep test

   - Flow number, F_n, determined from triaxial repeated load test

2. HMA Fatigue Cracking (testing conducted at 4.4 to 15.5 °C)

   - Dynamic complex modulus, E^*, determined from triaxial dynamic modulus test

3. HMA Low-Temperature Cracking (testing conducted at 0, -10, -20°C)

   - Indirect tensile creep compliance, $D(t)$, determined from indirect tensile creep test.

Another important step towards the development of a mechanistic based pavement design procedure was the initiation of Project NCHRP 1-37A: *Development of the 2002 Guide for Design of New and Rehabilitated Pavement Structures*. The project called for developing a guide utilizing existing mechanistic-based models and databases, and reflecting current state-of-the-art pavement design procedures. The guide was to address all new and rehabilitation design issues and provide equitable design basis for all pavement types (NCHRP 1-37A). The NCHRP Project 1-37A concluded with the delivery of the *2002 Guide for Mechanistic-Empirical Design of New and Rehabilitated Pavements Structures* (MEPDG). The mechanistic-empirical numerical models in the MEPDG were calibrated using performance data from the Long Term Pavement Performance (LTPP) database. The numerical models require input data related to traffic,

climate, materials, and the proposed structure to predict damage accumulation over the service life of the pavement. The MEPDG includes software, referred to as the *Design Guide*, for analyzing existing pavements, identifying deficiencies in past designs, and predicting pavement performance over time. The pavement community envisages MEPDG will be a major improvement over the AASHTO 1993 guide in terms of achieving cost effective pavement designs and rehabilitation strategies (AASHTO Memorandum, 2004), and SPT will play a major role in quality control and selection of mixes with superior performance and improving the reliability of performance prediction.

There is currently a national effort to implement performance tests as part of the Superpave mix design for Hot-Mix-Asphalt (HMA), and to implement the *2002 Guide for Mechanistic-Empirical Design of New and Rehabilitated Pavements Structures*. Washington State Department of Transportation (WSDOT) is in the process of implementing both Superpave and MEPDG. It has created the need to investigate dynamic modulus of HMA mixes widely used in the State of Washington and evaluate the MEPDG using local conditions.

1.2 Objectives of the Study

Following are the objectives of this study:

1. To investigate and develop a database of dynamic modulus of widely used HMA mixes in the State of Washington,

2. To investigate the sensitivity of dynamic modulus to aggregate gradation,

3. To predict performance of the mixes using Design Guide (MEPDG software) with Level 1 and Level 3 inputs, and the ability of dynamic modulus to correlate with field performance, and

4. To evaluate the distress prediction accuracy of the MEPGD.

This study will help WSDOT to implement dynamic modulus as a performance test to complement the volumetric mix design of HMA. The database will present representative dynamic modulus values of the mixes investigated in this study, which can be used for evaluating existing pavements, as inputs to the MEPDG for the design/analysis of flexible pavements, and in future research.

1.3 Tasks

Following is the summary of the tasks carried out for the study:

- Selection of mixes; collection of materials and pavement performance data,

- Preparation of mixes,

- Specimen preparation for dynamic modulus tests; perform bulk specific gravity tests to determine air voids in the specimens,

- Conduct dynamic modulus tests and develop master curves for all mixes,

- Analyze dynamic modulus data and verify results statistically,

- Predict distresses using Design Guide (MEPDG software),

- Evaluate distress prediction accuracy of the MEPDG by comparing predicted distress data with measured distress data, and

- Create a database of dynamic modulus values of the mixes investigated, and a database of parameters for determining dynamic modulus of the mixes investigated at any temperature and frequency.

1.4 Organization of the Thesis

Chapter 2 focuses on dynamic modulus test and the salient features of the MEPDG. The chapter also focuses on literature related to these topics.

Chapter 3 deals with the experimental part, which includes selection of mixes, mixture volumetrics and material properties, mixture and specimen preparation, and the laboratory tests performed. Tables and figures are presented at the end of the chapter.

Chapter 4 presents dynamic modulus data and master curves for the mixes investigated in this study. Also presented are the results of the analysis of dynamic modulus data and Analysis of Variance of the dynamic modulus data. Tables and figures are presented at the end of the chapter.

Chapter 5 deals with the MEPDG Analysis, which includes a brief account of the distress prediction mechanism incorporated in the MPEDG, the predicted performances (distresses) of the mixes, results of the analysis of predicted distress data and statistical analyses of predicted distress data. Tables and figures are presented at the end of the chapter.

Chapter 6 summarizes the conclusions derived from this study followed by Bibliography.

Appendix 1 presents the Dynamic Modulus Database.

Appendix 2 presents sample dynamic modulus master curves.

Appendix 3 explains terminologies related to Analysis of Variance (ANOVA).

Appendix 4 presents the methodology for distress data collection.

CHAPTER TWO

REVIEW OF DYNAMIC MODULUS TEST AND MEPDG

2.1 Dynamic Modulus Test

The relationship of stress versus strain of any linear viscoelastic material under continuous sinusoidal loading is defined by a complex number called Complex Modulus denoted by E*. The real part of complex modulus represents the elastic stiffness of the material; the imaginary part represents the viscous behavior. Dynamic Modulus is the absolute value of complex modulus denoted by |E*|. The stress-strain relationship of asphalt concrete, which is a linear viscoelastic material, can be defined using dynamic modulus. Eq.2.1 shows the mathematical form of dynamic modulus.

$$\left|E*\right| = \frac{\sigma_o}{\varepsilon_o} \quad \text{... (2.1)}$$

where

σ_o = peak dynamic stress; and

ε_o = peak recoverable axial strain.

Dynamic modulus is determined by exerting sinusoidal (haversine) compressive load on a cylindrical specimen of asphalt concrete measuring the applied stress and the resulting recoverable strain. The test is performed at different temperatures and frequencies. Due to the viscous nature of asphalt concrete, peak strain lags behind peak stress called as the *phase angle* (φ), expressed in degrees. For pure elastic materials, φ equals zero; for pure viscous materials, φ equals 90°. Mathematically,

$$\varphi = \frac{t_i}{t_p} \times (360) \quad \text{..} \quad (2.2)$$

where

t_i = time lag between a cycle of stress and strain (seconds); and

t_p = time for a stress cycle (seconds).

It is important to understand that dynamic modulus is not a measure of strength; higher dynamic modulus does not necessarily indicate higher strength, but only an indication that a given applied stress produces lower strain in the mixture. The applications of dynamic modulus and phase angle include characterization of asphalt concrete based on the susceptibility of a mixture to distresses like permanent deformation and fatigue cracking, performance criteria in asphalt concrete mixture design and key input parameter to the MEPDG.

2.1.1. Factors affecting dynamic modulus

Dynamic modulus of asphalt concrete is a function of material properties like aggregate gradation, aggregate content, binder content, binder stiffness, and air voids; also, non-material properties like test temperature and frequency, age and possibly specimen geometry (specimen height-to-diameter ratio; MEPDG advocates using a height-to-diameter ratio of less than two) affect dynamic modulus.

Tarefdar et al. (2006) studied the influence of aggregate gradation, asphalt type, asphalt content, and air voids on dynamic modulus and rut potential. They investigated twelve "lab mixes" and ten "plant mixes" from the Oklahoma Department of Transportation. They observed no clear trend between modulus and asphalt content; modulus decreased with increase in air

voids. Rut potential increased with increase in asphalt content and with increase in air voids. The mixes with coarser aggregate gradation produced the lowest rut potential; possibly the result of better interlocking or higher stability provided by coarse aggregates. PG grade affected rutting but not modulus at low to medium temperatures.

Vivek et al. (2006) evaluated the effect of height-to-diameter ratio on the accuracy of measured dynamic modulus and the significance of end friction reducing (EFR) membranes on dynamic modulus. Specimens with a diameter of 152 mm instead of the standard 102 mm provided consistent results, especially if the ratio was less than two. EFR membranes increased the accuracy of measured dynamic modulus.

Christopher et al. (2006) examined the effects of testing history and method of specimen preparation, sawed/cored or compacted, on dynamic modulus. The two factors did not affect dynamic modulus significantly. Mohammed et al. (2007) characterized thirteen plant-produced HMA mixes based on dynamic modulus of the mixtures. Dynamic modulus was sensitive to nominal maximum aggregate size (NMAS); recycled asphalt combined with larger size aggregates exhibited higher dynamic modulus at high temperatures.

2.1.2 Predictive equations for dynamic modulus

Dynamic modulus test is laborious and not all situations demand measured dynamic modulus values; for instance, trial designs or preliminary stages of a design. For such cases, dynamic modulus can be predicted using regression models with the knowledge of certain material properties. Several regression models are available for the prediction of dynamic modulus; Witczak model and Hirsch model are the widely used predictive equations. HMA

volumetric properties and binder rheological properties are required for these models. The two models are presented in the following sections.

Witczak Model

      It is an empirical model developed based on the testing of 200 asphalt concrete mixtures. It requires viscosity of asphalt binder and volumetric properties of asphalt-aggregate mixture to predict dynamic modulus. It is capable of predicting |E*| over a range of temperatures, rates of loading (frequency) and aging conditions. The model uses a symmetrical sigmoidal function, presented in Eq.2.3:

$$\log E^* = -1.249937 + 0.02932(\rho_{200}) - 0.001767(\rho_{200})^2 - 0.002841(\rho_4)$$
$$-0.058097(V_a) \times \frac{0.802208 V_{beff}}{V_{beff} + V_a} +$$
$$\frac{3.871977 - 0.0021(\rho_4) + 0.003958(\rho_{38}) - 0.000017(\rho_{38})^2 + 0.00547(\rho_{34})}{1 + \exp(-0.603313 - 0.313351 \text{Log}(f) - 0.393532 \text{Log}(\eta))}$$

.... (2.3)

where

    |E*| = dynamic modulus, 10^5 psi

    η = viscosity of asphalt binder, 10^6 psi

    f = frequency of loading, Hz

    V_a = air void content, %

    V_{beff} = effective asphalt binder content, % by volume

    ρ_{34} = cumulative percent retained on the 19mm sieve

    ρ_{38} = cumulative percent retained on the 9.5mm sieve

ρ_4 = cumulative percent retained on the 4.76mm sieve

ρ_{200} = percent passing 0.075mm sieve

Hirsch model

Hirsch (1961) developed a model to calculate the modulus of elasticity of cement concrete or mortar using aggregate modulus, mix proportions and elastic modulus of cement. Christensen et al. (2003) extended this model for dynamic modulus of HMA. The model requires |G*| of asphalt binder and volumetric properties of aggregate mixture to predict dynamic modulus. They reported that the estimated standard error of the model was 41%. Eq.2.4 shows the mathematical form of Hirsch model:

$$| E^* |= P_c \left[4,200,000 \left(1 - \frac{VMA}{100} \right) + 3 | G^* |_{\text{binder}} \left(\frac{VMA \times VFA}{10,000} \right) \right]$$

$$+ \frac{1 - P_c}{\left[\frac{\left(1 - \frac{VMA}{100} \right)}{4,200,000} + \frac{VMA}{3 | G^* |_{\text{binder}} (VFA)} \right]}$$

.... (2.4)

where

$$P_c = \frac{\left(20 + \frac{3 | G^* | (VFA)}{VMA} \right)^{0.58}}{650 + \left(\frac{3 | G^* | (VFA)}{VMA} \right)^{0.58}}$$

$|E^*|_{\text{mix}}$ = absolute value of mixture dynamic modulus

$|G^*|_{binder}$ = absolute value of asphalt binder complex modulus

VMA = voids in mineral aggregate, %

VFA = voids filled with asphalt, %

Both models are based on limited data and require validation for other conditions. Moreover, the models are reliable only up to a lower limit of $|E^*|$ below which testing is required. Dongre et al. (2005) compared dynamic modulus of asphalt mixtures collected from five pavement construction sites measured in the laboratory with the predicted values to evaluate the prediction capacity of Witczak and Hirsch models. Both models were capable of predicting dynamic modulus reasonably well; however, Hirsch model was valid over a wide range. It uses $|G^*|$ data directly in the calculations reducing a source of error and is easier to use. They reported that both models require corrections/refinements to improve accuracy.

Mohammed et al. (2006) evaluated Witczak's model and Hirsch model by investigating twenty-three plant-produced HMA mixtures in the Louisiana region. The two models predicted dynamic modulus with reasonable reliability, which increased in Witczak's model as the nominal maximum aggregate size (NMAS) increased and increased in Hirsch model with decrease in NMAS.

2.1.3 Dynamic modulus test implementation

Dynamic modulus test is still in the implementation stages in many states. Prior to implementing the test, it is important to validate the test for local conditions, investigate dynamic modulus of widely used HMA mixes in a particular region, and create a database. Shah et al. (2005) measured dynamic modulus of eleven mixes commonly used in North Carolina. Dynamic

modulus was sensitive to binder content – higher sensitivity for modified binder. The study provided feedback for implementing the test. Zhou et al. (2003) used field pavement conditions to validate dynamic modulus test and the associated parameter, $E^*/\sin\phi$, to support implementation of the test in day-to-day Superpave design practice. Findings from this study showed that dynamic modulus test is capable of distinguishing between good and poor mixtures.

2.2 Mechanistic Empirical Guide

The *2002 Guide for Mechanistic-Empirical Design of New and Rehabilitated Pavement Structures* (MEPDG) is the latest guide for new/rehabilitated flexible/rigid pavement design. All design guides preceding the MEPDG employ empirical equations developed based on the AASHO Road Test in the late 1950's. Significant changes in construction materials, trucks and truck volumes, and pavement construction techniques demanded the need for a mechanistic-empirical design that will take in to account the mechanical properties of pavement materials, and climatic effects; capable of predicting important types of distresses, and adapts to new conditions. These factors laid the basis for the development of the MEPDG.

The MEPDG employs mechanistic models to predict structural responses that become inputs to the empirical distress prediction models. The models were subjected to comprehensive calibration routine until reasonable prediction of pavement performance was achieved. The impact of climate and aging on material properties are incorporated in the design as biweekly and monthly iterative predictions of pavement performance over the entire design life. The complex models and design concepts come in a user-friendly software package called the 'Design Guide'. Improvisations to the design procedure and Design Guide can be made over

time in a piecewise manner to any of the component models and incorporate them in the procedure after recalibration and validation.

2.2.1 Hierarchical Inputs

An important aspect of the MEDPG is that it classifies the inputs, required for design/analysis, in to three hierarchical levels – Level 1, Level 2, and Level 3. Level 1 inputs provide the highest level of accuracy, appropriate for heavily trafficked pavements or where safety and economic considerations for an early failure are a concern. Level 2 inputs provide an intermediate level of accuracy, appropriate when resources or testing equipments are not available. These are typically user-selected possibly from an agency database, derived from limited testing program, or estimated through correlations. Level 3 inputs provide the lowest level of accuracy, appropriate if the consequences of an early failure seems minimal. These are typically user-selected from experience or typical averages for the region. The hierarchical input system is upon the premise that design reliability increases when the level of engineering effort expended for garnering inputs increases. This concept was validated only for the thermal fracture module. The guide recommends initiatives to confirm this hypothesis for at least one major load-related distress thereby illustrating that additional time and effort will result in a lower cost and better performance of the pavement. Approximately 100 inputs are required for design/analysis of pavements, which fall into three major categories: traffic, climate, and materials. Prediction accuracy of the models, obviously, will not be sensitive to all inputs. Investigating the critical inputs that affect the prediction accuracy of the models will help reduce the level of efforts required to collect inputs.

Ali (2005) used laboratory measured material properties as inputs to investigate the influence of material type on pavement performance predicted by the MEPDG. Dynamic modulus estimated using predictive equations incorporated in the MEPDG differed substantially from the measured values that resulted in underestimation of permanent deformation. The models reflected sensitivity to HMA mix type, but not to variations in unbound material. They recommended using nonlinear analysis to capture the real behavior of unbound materials, and measured dynamic modulus (Level 1) rather than predicted values (Level 2).

Carvalho (2006) used Level 3 inputs to investigate the capacity of MEPDG to predict pavement performance. Variation in thickness of HMA layer had significant impact on prediction of performance. The influence of thickness of base layer on fatigue cracking and permanent deformation was insubstantial. The study recommended the development of a database of material property inputs for routine design applications.

Mohammad et al. (2006) investigated the sensitivity of dynamic modulus to predict rutting using the Design Guide (MEPDG software). They reported that the rutting model in the MEPDG requires more validation and calibration.

The MEPDG is versatile with provisions to choose combination of input levels, for instance, HMA mix properties from Level 1, traffic data from Level 2 and subgrade properties from Level 3. Nantung et al. (2005) reported that combinations of design input levels rather than using a single design input level can yield results that are more rational. They found the default traffic-load spectra (Level 3) in the Design Guide as too general lacking design accuracy and recommended using at least a traffic input Level 2.

2.2.2 Structural Responses

The MEPDG predicts the following structural distresses in flexible pavement design and analysis:

- Bottom-up fatigue (or alligator) cracking

- Surface-down fatigue (or longitudinal) cracking

- Permanent deformation (or rutting)

- Thermal cracking

- Fatigue in chemically stabilized layers (only considered in semi-rigid pavements)

2.2.3 Need for calibration/validation of the MEPDG

The MEPDG insists on calibrating/validating the mechanistic-empirical models to local conditions because the distress mechanisms are too complex to develop a practical model and developing empirical factors and subsequent calibration is necessary to obtain realistic performance predictions. The rutting, fatigue cracking, and thermal cracking models in the flexible design procedure have been calibrated using design inputs and performance data largely from the LTPP database; although the database covers sections located throughout many parts of North America it still may not be adequate for specific regions of the country. To address this issue, the guide senses a need for more local or regional calibration/validation.

2.2.4 Implementation

The guide identifies various issues that need to be addressed prior to implementing the MEPDG. The most important are to establish databases for inputs, to calibrate and validate

distress models for local conditions. The agency implementing the mechanistic-empirical design procedure must address the implementation issues identified by the MEPDG.

Ceylan et al. (2005) investigated the sensitivity of design inputs pertaining to both rigid and flexible pavements exhibiting particular sensitivity in Iowa using the Design Guide (MEPDG software). The inputs for longitudinal and transverse cracking, rutting, and roughness were categorized as *extremely sensitive* and *sensitive to very sensitive* and presented a strategic plan for implementing MEPDG in Iowa.

Uzan et al (2005) carried out a sensitivity study to determine input variables for MEPDG most important to Texas Department of Transportation (TxDOT). They found that the models predicted rut depth adequately, slightly over-predicted alligator cracking, and inconsistent with longitudinal cracking. The findings from this study supported the implementation of MEPDG into TxDOT's normal pavement design operations.

Gramajo (2005) used the Design Guide (MEPDG software) to predicted distress using input data from actual pavement sections in the Commonwealth of Virginia. Predicted distresses were higher than the field distresses. The study concluded that significant calibration and validation is required before implementing MEPDG.

2.3 Summary

Dynamic modulus is a useful parameter for complementing the volumetric mixture design and defining the stress-strain relationship of asphalt concrete. However, the test needs calibration for local conditions before implementation in the routine design procedure. Dynamic modulus can be predicted using Witczak's model and Hirsch's model. Hirsch's model is

comparatively simple and the associated source of errors is relatively less; however, both models need corrections/refinements for accurate prediction of dynamic modulus.

The *2002 Guide for Mechanistic-Empirical Design of New and Rehabilitated Pavement Structures* (MEPDG) is the recently developed guide for pavement design and a major step towards mechanistic-based pavement design. It addresses the limitations of the existing pavement design guides. The complex models and design concepts come in a user-friendly software package called the Design Guide, which requires a comprehensive set of inputs for predicting structural distresses. Depending upon the importance of the project, inputs could be one or combination of the following: site-specific, from databases, based upon local conditions or experience. The mechanistic-empirical models in the guide need calibration for local conditions to obtain realistic performance predictions.

CHAPTER THREE

EXPERIMENT

The foremost step in this study was the selection of HMA mixes and collection of materials followed by the experimental part, which comprised of dynamic modulus and dynamic shear rheometer testing, and preparation of specimens for these tests. This chapter presents details of the mixes selected for this study, properties of the materials, specimen preparation, and the laboratory tests performed.

3.1 Mixes and Material Properties

Seven HMA mixes widely used in the State of Washington for the construction of highways were selected for the study. For selecting the mixes, the criteria given below were employed:

1. Mixes must possess different properties due to different aggregate source, aggregate gradation, binder grade, binder content, or a combination of these,

2. Mixes used in the construction of highway sections with available performance data, and

3. Availability of aggregates and binder.

Table 3.1 lists the HMA mixes selected for the study and the pavement sections constructed using these mixes. The selected mixes, henceforth, are referred to as Job Mix Formula (JMF). Table 3.2 summarizes the volumetrics of the JMF mixes, and asphalt binder

information. The VMA and VFA of the mixes satisfy the Superpave requirements: VMA – min. 13%, VFA – 65 to 75%. Various types of aggregates and aggregate structures were part of the mixture design. Table 3.3 summarizes source, type, and other aggregate related properties. The aggregates passed the Superpave requirements – flat and elongated particles (max. 10%) – single fractured faces (min. 90%) – un-compacted voids in fine aggregate (min. 40%) – plastic fines in graded aggregate (min. 40%).

3.1.1 Modified mixes

The amount of mineral filler (passing sieve #200) in a mix is critical during HMA plant operations, which could influence the volumetrics of the mix significantly. In order to investigate the sensitivity of dynamic modulus to variations in mineral filler, a 'lower modified mix', designated as LM, and an 'upper modified mix', designated as UM, were prepared from each JMF mix. In the LM mixes, percent-passing sieve #200 was reduced by 2%; in the UM mixes it was increased by 2% (e.g. 7% becomes 5% in the LM mixes and 9% in the UM mixes). The modifications to percent passing sieve #200 are based upon WSDOT tolerance limits summarized in Table 3.4. Even though the tolerance limits include other sieve sizes and asphalt content, because of lack of materials the focus was restricted to percent-passing sieve #200.

3.2 Gradation Charts

Gradation is an important property of aggregates that affects HMA properties like stiffness, stability, and fatigue and frictional resistance. The best gradation is the one that gives the densest packing of particles allowing sufficient voids for asphalt cement, and unfilled air

voids to avoid bleeding and/or rutting. Fuller and Thompson (1907) proposed an equation for maximum density called as Fuller's maximum density curve – Eq.3.1 below.

$$P = 100 \times \left(\frac{d}{D}\right)^n \quad .... (3.1)$$

where,

d = diameter of the sieve size in question

D = maximum size of the aggregate

P = total percent passing or finer than the sieve

Federal Highway Administration (FHWA) used n=0.45 in Eq.3.1 and called it the 0.45 Power Gradation Chart. This chart is convenient for determining the maximum density line (MDL) and for adjusting aggregate gradation. Maximum density line is a straight line joining the origin with the percentage point of the maximum aggregate size. Fig.3.1 (a) through (g) illustrates the 0.45 power gradation charts for the JMF mixes. The gradation curves of the JMF mixes are close to MDL indicating that the aggregates are well graded.

Maximum density line is an ideal case, which might not always provide sufficient voids for enough asphalt to achieve adequate durability. A densely packed aggregate might also lead to a mixture more sensitive to even slight changes in asphalt. In such cases, a deviation from the MDL creates sufficient voids in the mineral aggregate (VMA). In Fig.3.1, the gradations of some of the mixes deviate from the MDL, which is a result of such adjustments. A combined gradation chart, illustrated in Figure 3.2, compares the gradation curves of all JMF mixes.

Table 3.5 summarizes aggregate gradations of all mixes. Modifying the percent-passing sieve #200 in the JMF mixes resulted in substantial reduction of mineral filler in the lower

modified mixes and vice versa in the upper modified mixes; approximately 25 to 40% by weight. To balance the aggregate content in the mixes same as in the JMF mixes, rest of the sieve sizes were proportionately adjusted. Table 3.6 summarizes the quantitative variations in the gradation of all LM and UM mixes. Figure 3.3 (a) through (g) illustrates the effect of the modifications on the gradation curves of LM and UM mixes. The gradation curves have shifted substantially in the finer sieve sizes compared to the coarser ones.

3.3 Grouping of Mixes

In this study, twenty-one mixes were investigated, which include seven JMF, seven LM and seven UM mixes. The mixes were grouped into seven Projects; each Project a combination of JMF, LM and UM mixes. Hereinafter, the projects are referred to by the Mix ID's listed in Table 3.1. For instance, Project #5381 comprises JMF Mix #5381 and the two derived mixes – LM and UM.

3.4 Laboratory Tests

The laboratory tests performed for the study include bulk specific gravity and dynamic modulus test on HMA specimens, and dynamic shear rheometer test on asphalt binders. Specimens for dynamic modulus tests, 100 mm in diameter and 150 mm in height, were cut and cored from gyratory specimens 150 mm in diameter and 170 mm in height. Gyratory specimens were compacted in the Superpave Gyratory Compactor (SGC) in accordance with AASHTO T 312. Bulk specific gravity, G_{mb}, of the specimens were measured in accordance with AASHTO T 166-05. Air voids in the gyratory and test specimens were determined using Eq.3.2. Table 3.7 summarizes G_{mb}, air voids, effective binder content, and unit weight of the test specimens.

Figure 3.4 illustrates the percent air voids in the test specimens. The target air voids in the test specimens was 7±1%; however, in projects 5295 and 5627 the air voids in some specimens did not meet this range, and replacement specimens were not possible because of lack of aggregates.

$$AV(\%) = \left[1 - \frac{G_{mb}}{G_{mm}}\right] \times 100 \quad \text{..} \quad (3.2)$$

where,

AV = air voids in the specimen, %

G_{mb} = bulk specific gravity of the specimen

G_{mm} = maximum specific gravity of mixture

Dynamic modulus tests were performed in accordance with AASHTO TP 62-03, which states that there is approximately 1.5 to 2.0 percent decrease in air voids when a specimen is cut-cored from a gyratory specimen. To accommodate this variation, the target air voids in the gyratory specimens was $9 \pm 0.5\%$ in order to achieve 7 ± 1.0 % air voids in the actual test specimens. For each mix, two replicates were tested. The tests were performed at temperatures 4.4, 21.1, 37.8, and 54.4 °C, and frequencies 0.1, 0.5, 1, 5, 10, and 25 Hz. Prior to testing at each temperature, the test specimens were conditioned in order to achieve uniform temperature. Three equidistantly spaced LVDT's were mounted on the test specimens to measure axial deformation during the test. Table 3.8 summarizes the dynamic modulus test conditions in this study.

The purpose of a DSR test is to measure the complex shear modulus (G^*) and phase angle (δ) of asphalt binders. Typically, a specimen of asphalt binder is sheared between two cylindrical plates; asphalt specimens are aged in the rolling thin film oven (RTFO) at 164 °C for

approximately 45 minutes prior to testing. The test is performed at different temperatures at a constant angular frequency of 1.59 Hz. The diameter of the plates and the thickness of specimen depend upon the test temperature. For all measurements taken at temperatures 46 °C and above, a 25 mm diameter plate and a specimen height of 2 mm are used. For temperatures 37.8 °C and lower, 8 mm diameter plate and a specimen height of 1 mm are used. Table 3.8 summarizes the DSR test conditions in this study.

3.5 Summary

Twenty-one mixes were prepared and grouped in to seven projects. Each project was a combination of seven JMF mixes, seven LM mixes and seven UM mixes. JMF mixes were the ones selected for the study; LM mixes were prepared by decreasing the percent-passing sieve #200 of the JMF mixes by 2%; increased by 2% in the UM mixes. Two replicates were prepared for each mix. Test specimens (100 mm diameter by 150 mm height) for dynamic modulus tests were cut-cored from gyratory specimens (150 mm diameter by 170 mm height). Target air voids in the gyratory specimens were 9±0.5% to achieve 7±1% in the test specimens. Air voids in the specimens were determined through bulk specific gravity tests. DSR tests were performed to determine the G* and δ of the asphalt binders.

Table 3.1: Details of the pavement sections constructed using the mixes investigated in this study

Mix ID.	Pavement section	Year	SR	Location/ County	Milepost begin/end	Tonnage (tons)
5381	Railroad Crossing to Canyon Road, WA	1998	512	Tacoma/ Pierce	4.38/5.59	5695
5295	Thomas St. to N 152nd St., WA	1998	99	Seattle/ King	34.85/35.46	30335
5192	MP 0.0 to King County Line, WA	1997	99	Tacoma/ Pierce	0.50/1.05	2250
5373	V Mall Blvd. To Yak Riv Br. & Wapato Cr. To Ahtanum Cr., WA	1998	82	Yakima/ Yakima	36.31/38.05	12796
5627	Vic. Lind Coulee Bridge to Vic. SR 90, WA	1999	17	Moses lake/ Grant	43.00/45.22	15553
5364	Vancouver City Limits to S.E. 164th Ave., WA	1998	14	Vancouver/ Clark	6.58/7.93	31633
5408	SR 182 to SR 395, WA	1998	240	Richland/ Benton	37.78/40.18	30805

Table 3.2: Volumetrics of the selected mixes and asphalt binder properties

	Mix ID						
	5381	5295	5192	5373	5627	5364	5408
NMAS, mm	12.5	12.5	12.5	19	19	12.5	12.5
MAS, mm	19	19	19	25	25	19	19
Asphalt content, %	5.7	5.3	5.1	5.4	4.5	5.6	5.4
Aggregate content, %	94.3	94.7	94.9	94.6	95.5	94.4	94.6
VFA, %	73	74.5	72.8	72.8	70.8	70.8	73.3
VMA, %	15.2	16.6	14.6	14.6	13.9	13.9	14.9
G_{mm}	2.492	2.486	2.483	2.551	2.616	2.502	2.523
G_{mb}	2.267	2.262	2.260	2.321	2.381	2.277	2.296
Asphalt							
PG	58-22	70-22	64-22	70-28	64-28	58-22	64-28
Mixing temp, °C	136-141	154-159	153-158	160-171	160-168	136-141	157-162
Compaction temp, °C	133-138	145-150	142-147	138-149	138-149	133-138	146-151
G_b	1.0269	1.038	1.02	1.021	1.035	1.02	1.03

Table 3.3: Aggregate source, type, and properties

	Mix ID						
	5381	5295	5192	5373	5627	5364	5408
Source	B-333	B-335	B-335	E-141	GT-18	G-106	R-7
County	Pierce	King	Pierce	Yakima	Grant	Clark	Benton
Type	Vashon recessional outwash gravels	Vashon glacial gravels	Vashon glacial gravels	Alluvial gravels/ terrace deposits	Outwash flood gravels	Outwash flood gravels	Alluvial gravels
G_{sb} (coarse aggregate)	2.681	2.703	2.65	2.712	2.783	2.718	2.643
G_{sb} (fine aggregate)	2.646	2.625	2.626	2.609	2.76	2.598	2.705
G_{sb} (aggregate blend)	2.653	2.646	2.631	2.653	2.771	2.603	2.699
Flat and elongated particles (%)	0[c]	0[b]	0[b]	0[b] 3[c]	4.15[a]	n/a	n/a
Single fractured faces (%)	100[b] 100[e]	100[f]	100[f]	94[b] 98[c] 100[e]	100[a] 100[b] 99.5[c] 98[e]	91[b] 93[c] 96[d]	96[b] 95[c] 100[g]
Un-compacted voids in fine aggregate (%)	47.9	49	49	46.3	49	n/a	n/a
Plastic fines in graded aggregate (%)	75	70	70	69	81	71	76

[a] (3/4" sieve); [b] (1/2" sieve); [c] (3/8" sieve); [d] (1/4" sieve); [e] (#4 sieve); [f] (#8 sieve); [g] (#10 sieve)
n/a – not available

26

Table 3.4: WSDOT tolerance limits for aggregate gradation and asphalt content

Sieve (mm)	Tolerance limits
19	± 6%
12.5	± 6%
9.5	± 6%
4.75	± 5%
2.36	± 4%
1.18	-
0.6	-
0.3	-
0.15	-
0.075	± 2%
AC	± 0.5%

Table 3.5: Aggregate gradation of the mixes

Project	Mix	Sieve sizes (mm)											
		25	19	12.5	9.5	4.75	2.36	1.18	0.6	0.3	0.15	0.075	<0.075
	JMF	-	-	6	9	30	18	12	7	6	4	3	5
5381	LM	-	-	6.1	9.2	30.6	18.4	12.2	7.1	6.1	4.1	3.1	3.1
	UM	-	-	5.9	8.8	29.4	17.6	11.8	6.9	5.9	3.9	2.9	6.9
	JMF	-	-	3	13	30	21	11	7	5	4	1.2	4.8
5295	LM	-	-	3.1	13.3	30.6	21.4	11.2	7.1	5.1	4.1	1.2	2.9
	UM	-	-	2.9	12.7	29.4	20.6	10.8	6.9	4.9	3.9	1.2	3.2
	JMF	-	-	2	9	35	11	9	7	13	8	2	5
5192	LM	-	-	2.2	8.5	35.1	11.7	9.1	73	13.5	7.5	1.6	5.2
	UM	-	-	2.2	8.5	35.0	11.2	8.8	7.0	13.0	7.5	1.6	3.2
	JMF	1	4	16	8	23	18	9	6	5	3	2	5
5373	LM	1.0	4.1	16.3	8.2	23.5	18.4	9.2	6.1	5.1	3.1	1.9	5.2
	UM	1.0	3.9	15.7	7.8	22.5	17.6	8.8	5.9	4.9	2.9	1.0	4.1
	JMF	-	4	21	12	16	15	11	7	4	3	1	6
5627	LM	-	4.1	21.4	12.2	16.3	15.3	11.2	7.1	4.1	3.1	1.0	3.2
	UM	-	3.9	20.6	11.8	15.7	14.7	10.8	6.9	3.9	2.9	1.0	7.8
	JMF	-	-	6	16	23	17	14	7	6	3	3	5
5364	LM	-	-	6.1	16.3	23.5	17.3	14.3	7.1	6.1	3.1	3.1	3.1
	UM	-	-	5.9	15.7	22.5	16.7	13.7	6.9	5.9	2.9	2.9	6.9
	JMF	-	-	5	13	32	17	10	7	5	4	2	5
5408	LM	-	-	5.1	13.3	32.7	17.3	10.2	7.1	5.1	4.1	2.0	3.1
	UM	-	-	4.9	12.7	31.4	16.7	9.8	6.9	4.9	3.9	2.0	6.9

JMF – Job Mix Formula; LM – lower modified mix; UM – upper modified mix

Table 3.6: Quantitative variation in gradation after modification

Size (mm)	Project													
	5381		5295		5192		5373		5627		5364		5408	
	LM	UM	LM	UM	LM	UM	LM	UM	LM	UM	LM	UM	LM	UM
25	-	-	-	-	-	-	2.0	-2.0	-	-	-	-	-	-
19	-	-	-	-	-	-	2.0	-2.0	-2.0	-2.0	-	-	-	-
12.5	2.0	-2.0	2.0	-2.0	-		2.0	-2.0	-2.0	-2.0	-2.0	-2.0	2.0	-2.0
9.5	2.0	-2.0	2.0	-2.0	-		2.0	-2.0	-2.0	-2.0	-2.0	-2.0	2.0	-2.0
4.75	2.0	-2.0	2.0	-2.0	2.0	-2.0	2.0	-2.0	-2.0	-2.0	-2.0	-2.0	2.0	-2.0
2.36	2.0	-2.0	2.0	-2.0	2.0	-2.0	2.0	-2.0	-2.0	-2.0	-2.0	-2.0	2.0	-2.0
1.18	2.0	-2.0	2.0	-2.0	2.0	-2.0	2.0	-2.0	-2.0	-2.0	-2.0	-2.0	2.0	-2.0
0.6	2.0	-2.0	2.0	-2.0	2.0	-2.0	2.0	-2.0	-2.0	-2.0	-2.0	-2.0	2.0	-2.0
0.3	2.0	-2.0	2.0	-2.0	2.0	-2.0	2.0	-2.0	-2.0	-2.0	-2.0	-2.0	2.0	-2.0
0.15	2.0	-2.0	2.0	-2.0	2.0	-2.0	2.0	-2.0	-2.0	-2.0	-2.0	-2.0	2.0	-2.0
0.075	2.0	-2.0	2.0	-2.0	2.0	-2.0	2.0	-2.0	-2.0	-2.0	-2.0	-2.0	2.0	-2.0
< 75µ	-38.8	37.3	-40.5	38.9	-25.5	24.5	-38.0	36.5	-32.0	30.7	-38.8	37.3	-38.8	37.3

LM – Lower modified mix; UM – Upper modified mix

All values are in percentage

Table 3.7: Properties of compacted test specimens

Project		Mix					
		JMF1	JMF2	LM1	LM2	UM1	UM2
5381	AV	7.9	6.6	7.0	7.1	7.2	7.8
	G_{mb}	2.296	2.324	2.316	2.315	2.313	2.298
	V_{beff}	12.7	12.9	12.9	12.8	12.8	12.8
	Unit wt.	143	145	145	145	144	143
5295	AV	8.1	7.1	7.5	8.2	7.6	7.2
	G_{mb}	2.282	2.31	2.299	2.282	2.297	2.306
	V_{beff}	11.7	11.8	11.7	11.7	11.7	11.8
	Unit wt.	142	144	7.5	142	143	144
5192	AV	7	6.8	7.3	7.3	7.2	6.8
	G_{mb}	2.31	2.314	2.301	2.301	2.305	2.315
	V_{beff}	11.6	11.6	11.5	11.5	11.5	11.6
	Unit wt.	144	144	144	144	144	145
5373	AV	6.1	7.3	7.2	6.3	7.2	7.1
	G_{mb}	2.393	2.363	2.364	2.389	2.328	2.37
	V_{beff}	12.7	12.5	12.5	12.6	12.5	12.5
	Unit wt.	149	148	148	149	148	148
5627	AV	7.5	7.4	8.6	5.7	6.2	6
	G_{mb}	2.421	2.423	2.39	2.466	2.455	2.459
	V_{beff}	10.5	10.5	10.4	10.7	10.7	10.7
	Unit wt.	151.1	151.3	149.2	154.0	153.3	153.3
5364	AV	6.4	6.4	7.1	7.1	6.8	6.3
	G_{mb}	2.343	2.343	3.324	2.325	2.333	2.343
	V_{beff}	12.2	12.2	12.2	12.2	12.2	12.2
	Unit wt.	146	146	145	145	146	146
5408	AV	7.4	7.3	7.9	7.8	7.2	7.5
	G_{mb}	2.335	2.339	2.324	2.326	2.342	2.334
	V_{beff}	12.0	12.0	12.0	12.0	12.1	12.0
	Unit wt.	146	146	145	145	146	146

JMF1, JMF2 – field mix replicates; LM1, LM2 – lower modified mix replicates
UM1, UM2 – upper modified mix replicates
AV in percentage; V_{beff} in percentage; Unit wt. in pcf

Table 3.8: Test conditions (temperature and frequency in the order of testing)

Temperature ° C	Mixture E*						Binder G* at 1.59 Hz
	25 Hz	10 Hz	5 Hz	1 Hz	0.5 Hz	0.1 Hz	
4.4	X	X	X	X	X	X	X
12.7							X
21.1	X	X	X	X	X	X	X
29.4							X
37.8	X	X	X	X	X	X	X
46.1							X
54.4	X	X	X	X	X	X	X

Table 3.9: G* and δ of the asphalt binders used in this study

Mix		Temperature (° C)							
		-10	4.4	12.7	21.1	29.4	37.8	46.1	54.4
5381	G*	-	43105	12524	3150.8	660.2	151.2	33.1	9.11
	δ	-	36.1	48.7	59.3	67.9	74.7	79.6	83.3
	η	7.2×10^{10}	9.51×10^{7}	5.51×10^{6}	5.05×10^{5}	7.27×10^{4}	1.42×10^{4}	3.7×10^{3}	1.19×10^{3}
5295	G*	-	56547	17859	4885.3	1218.8	298.2	76.7	23.8
	δ	-	33.3	44	53.8	60.7	66.6	68.6	73.6
	η	4.9×10^{10}	1.45×10^{8}	1.10×10^{7}	1.20×10^{6}	1.94×10^{5}	4.03×10^{4}	1.08×10^{4}	3.45×10^{3}
5192	G*	-	65321	22644	5052.8	1257.5	273.2	62.2	8.64
	δ	-	30.9	41.9	55.4	64.9	73.2	76.5	82.2
	H	6.4×10^{11}	3.78×10^{8}	1.6×10^{7}	1.14×10^{6}	1.36×10^{5}	2.29×10^{4}	5.31×10^{3}	1.56×103
5373	G*	-	18161	4905.4	1203.3	291.2	79.8	23.6	9.8
	δ	-	41.2	50.9	57.8	62.3	63.4	61.9	62
	H	1.8×10^{9}	1.43×10^{7}	1.66×10^{6}	2.57×10^{5}	5.45×10^{4}	1.42×10^{4}	4.58×10^{3}	1.71×10^{3}
5627	G*	-	26387	7486.5	1839.8	422	110	29.3	8.74
	δ	-	41.8	52.2	61.4	67.5	73	76.4	80.2
	η	9.1×10^{9}	2.94×10^{7}	2.4×10^{6}	2.87×10^{5}	5.03×10^{4}	1.14×10^{4}	3.32×10^{3}	1.16×10^{3}
5364	G*	-	29451	9229.9	2437.5	568.1	131.3	28.4	8.9
	δ	-	38.2	47.7	57.1	65.2	71.7	75.9	80.8
	H	3.1×10^{10}	6.04×10^{7}	4.03×10^{6}	4.11×10^{5}	6.4×10^{4}	1.33×10^{4}	3.61×10^{3}	1.2×10^{3}
5408	G*	-	31156	9275.5	2360.3	546	131	28.6	8.72
	δ	-	38.3	48.1	57.5	65.7	72	76.7	81.5
	η	3.2×10^{10}	6.01×10^{7}	3.98×10^{6}	4.03×10^{5}	6.26×10^{4}	1.3×10^{4}	3.52×10^{3}	1.17×10^{3}
	G* in kPa; δ in degrees; η in cP								
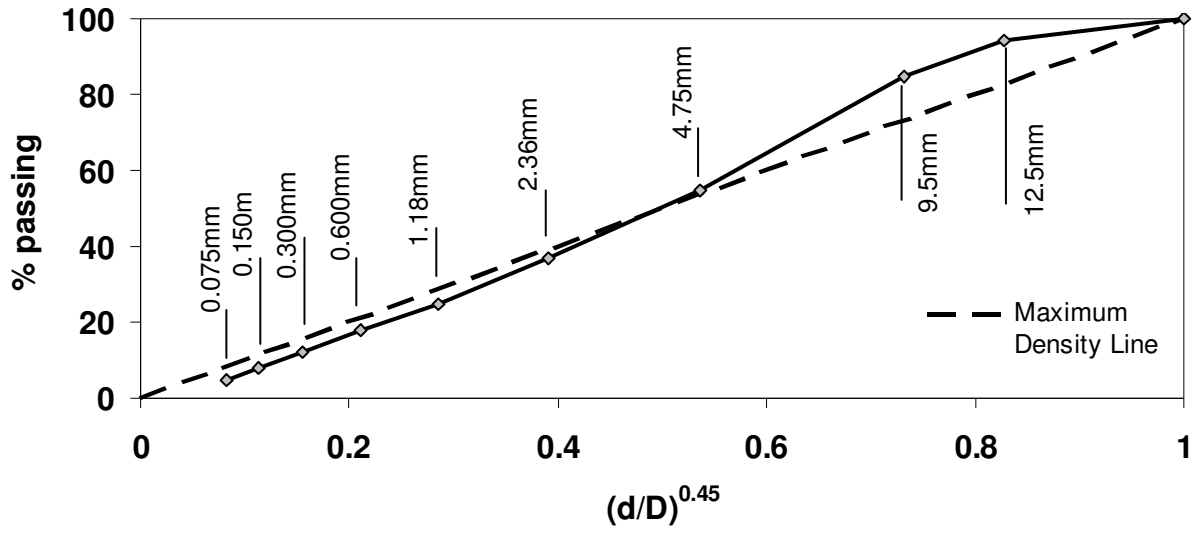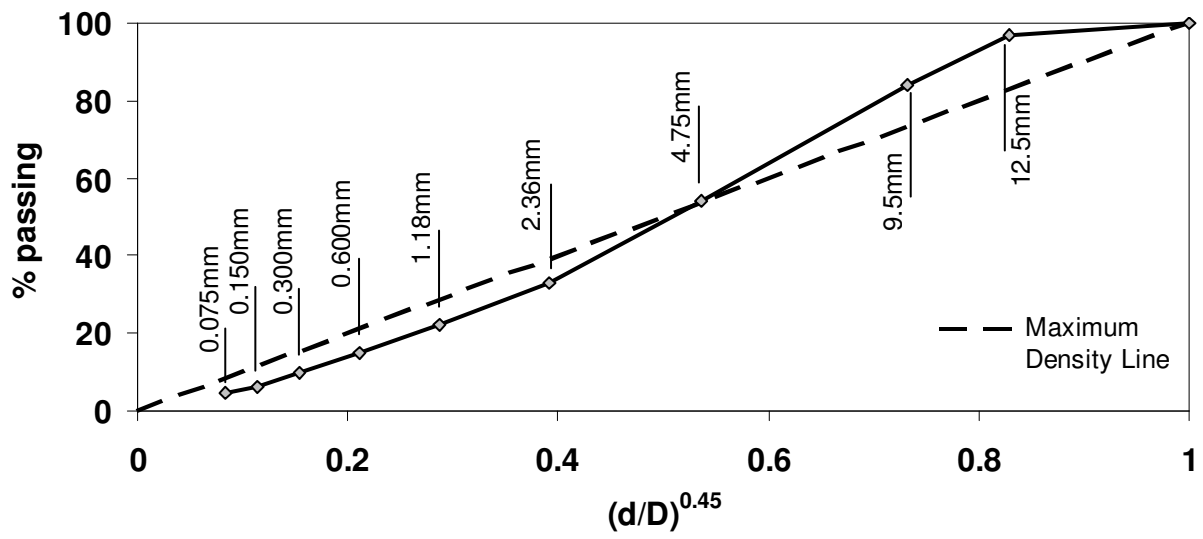
(a) Mix 5381

(b) Mix 5295
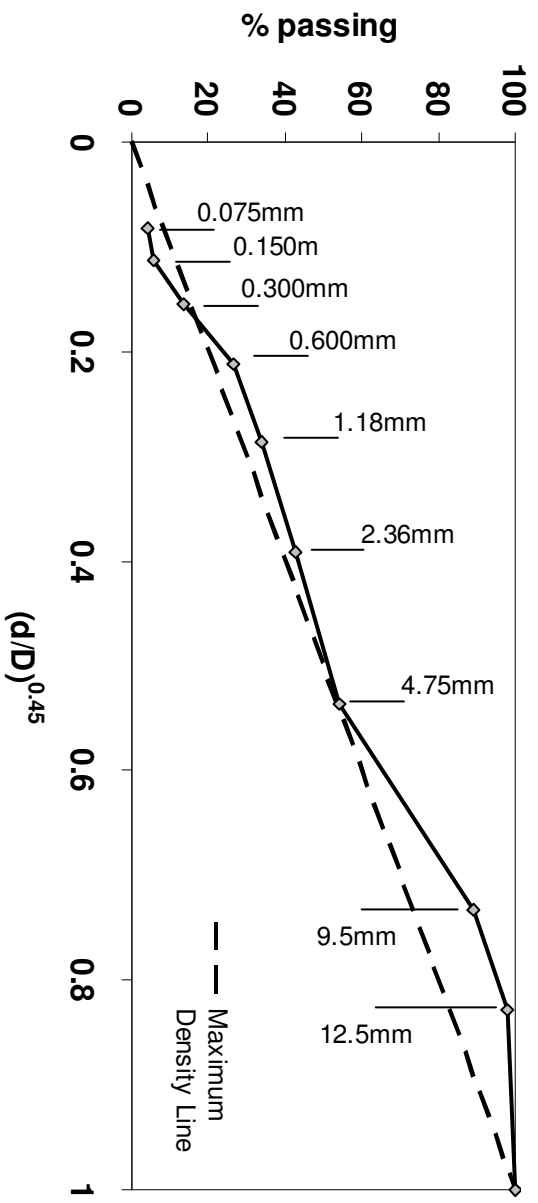
(c) Mix 5192

(d) Mix 5373

32
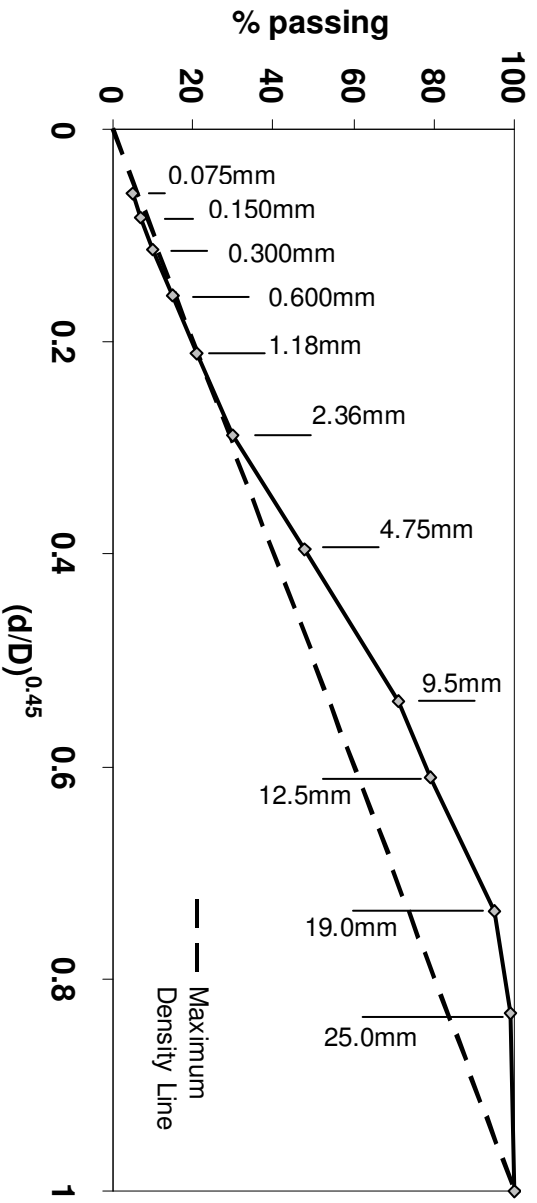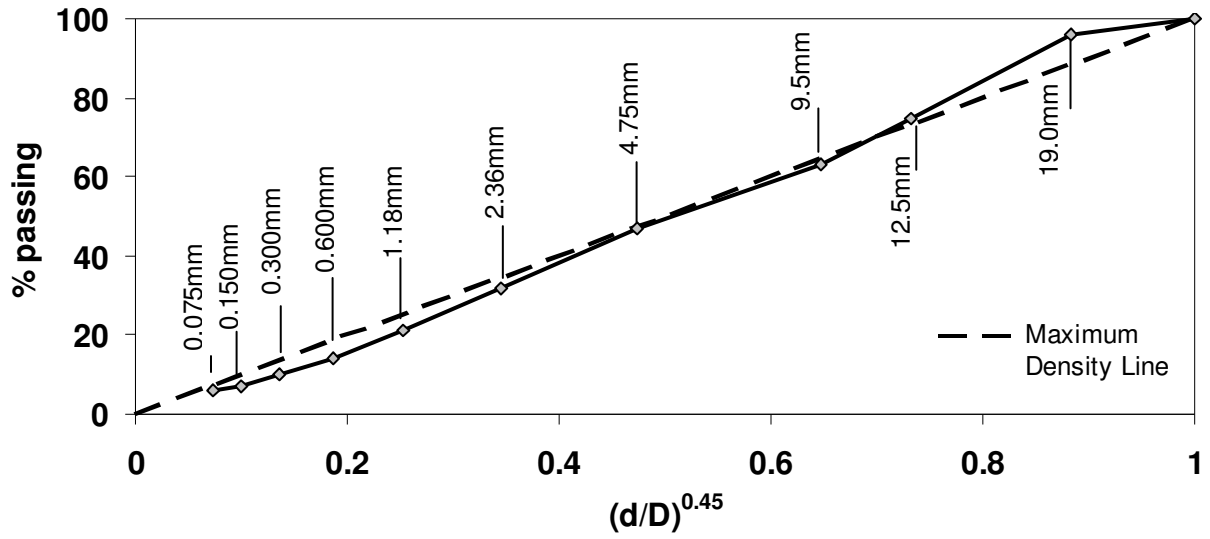
(e) Mix 5627
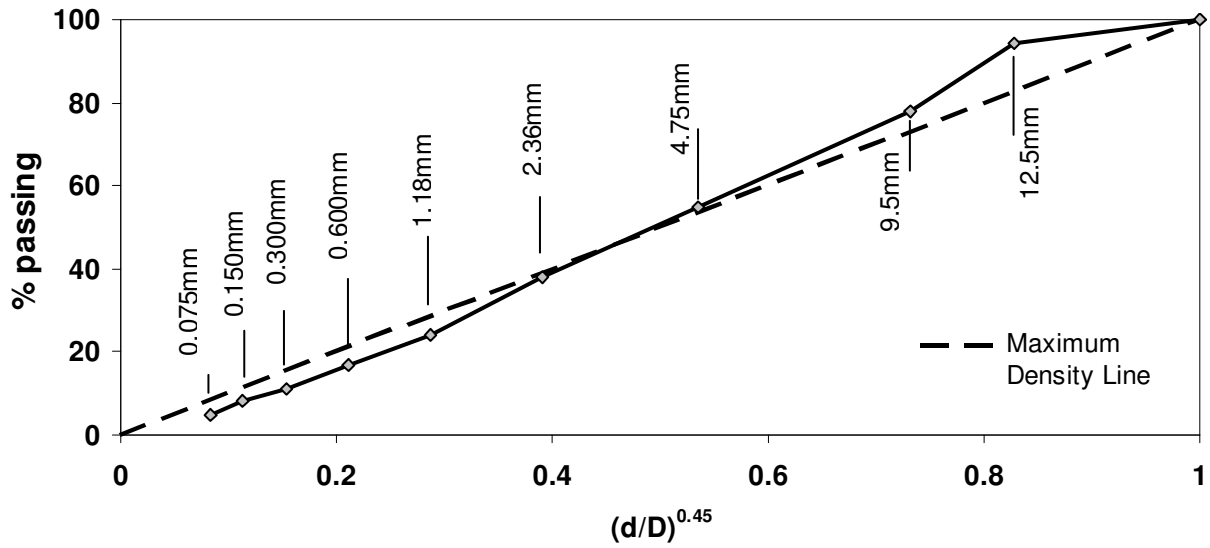
(f) Mix 5364
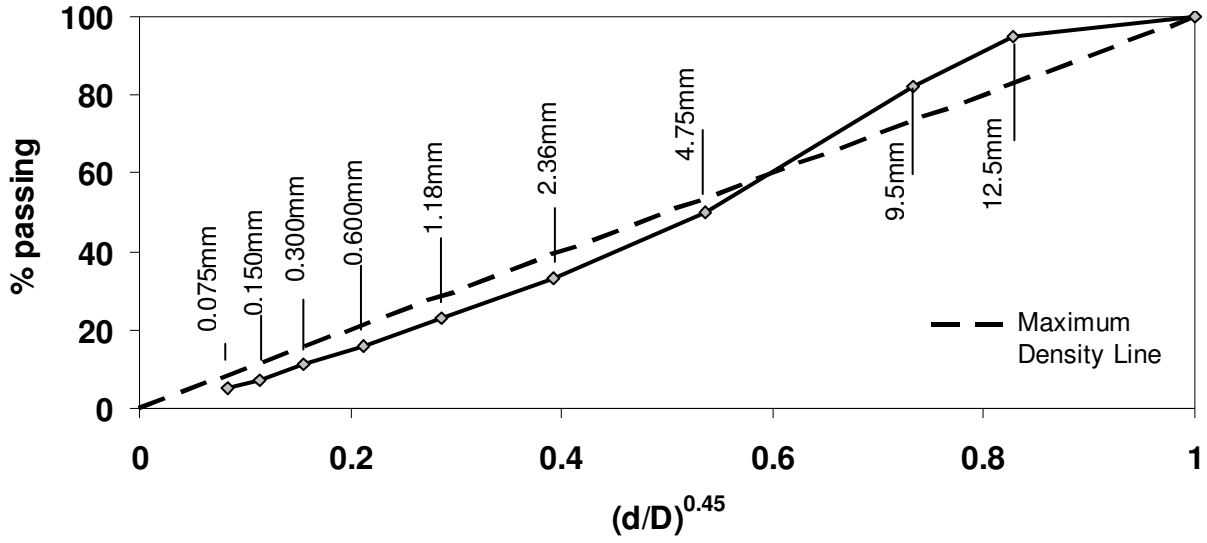
(g) Mix 5408

Figure 3.1: 0.45 Power gradation charts of JMF mixes
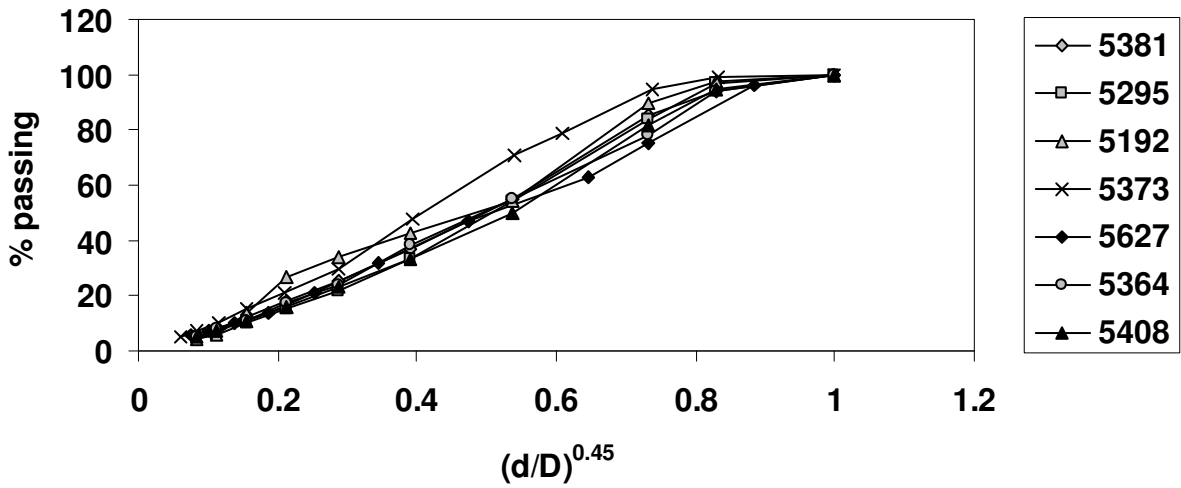
Figure 3.2: 0.45 Power gradation curves of all JMF mixes
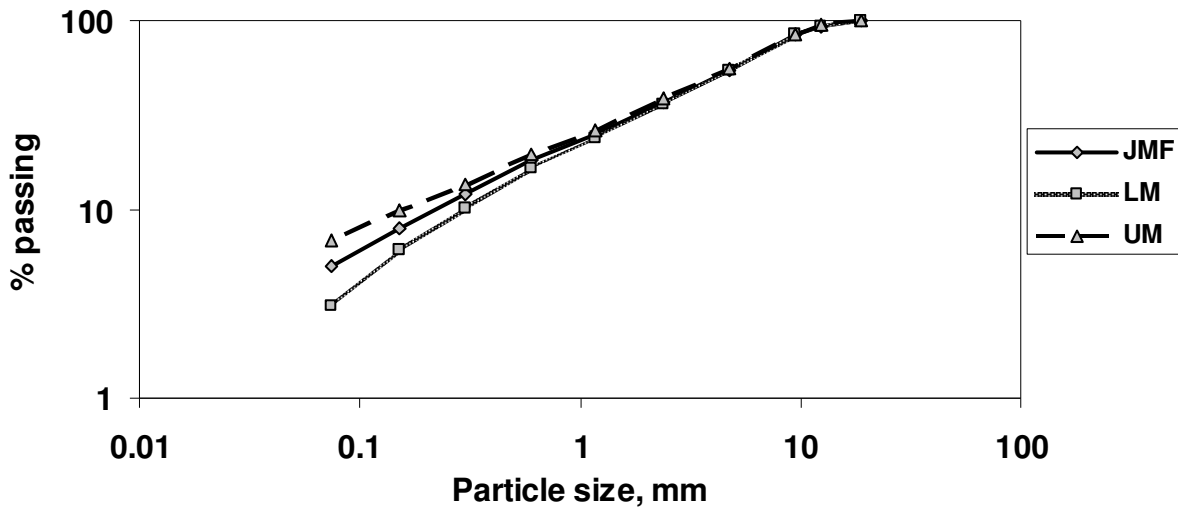
(a) Project 5381
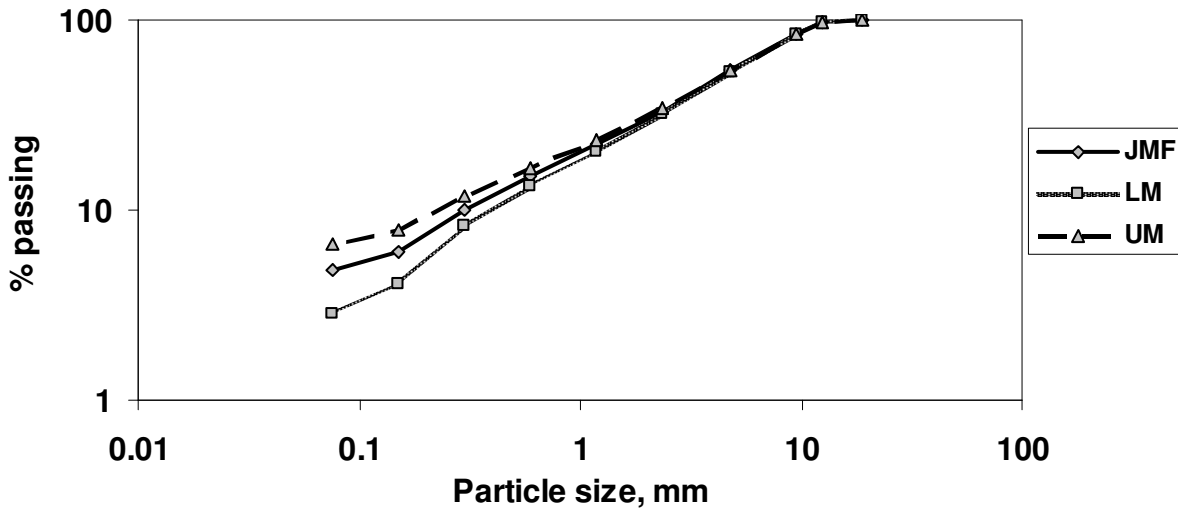
(b) Project 5295
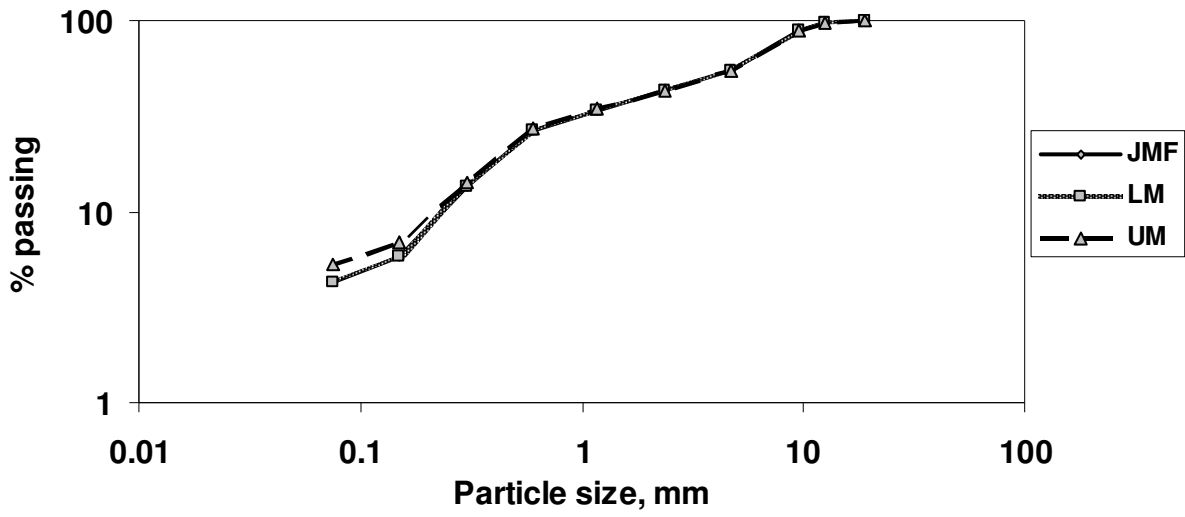
(c) Project 5192
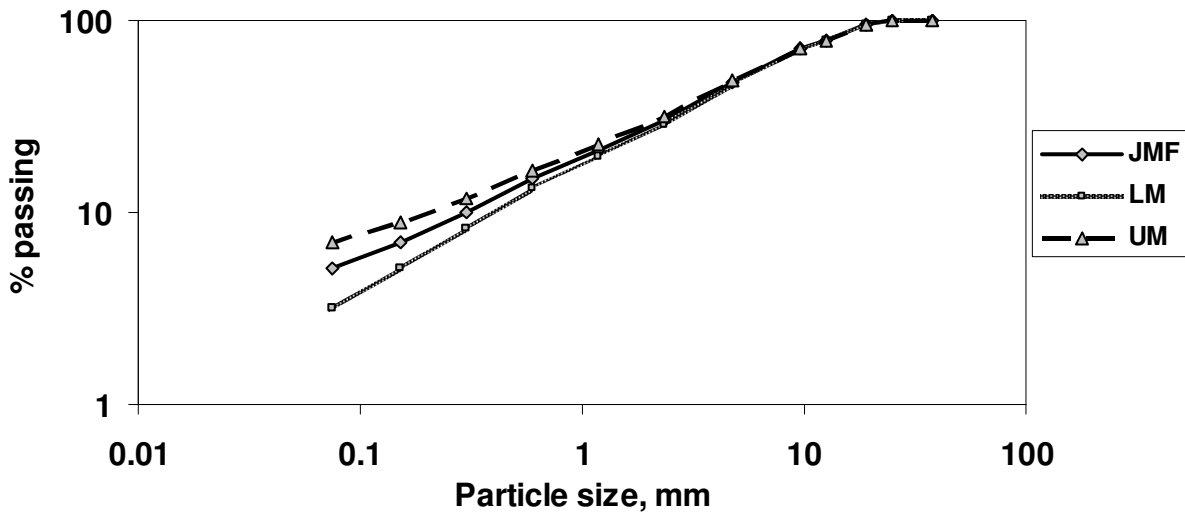
(d) Project 5373
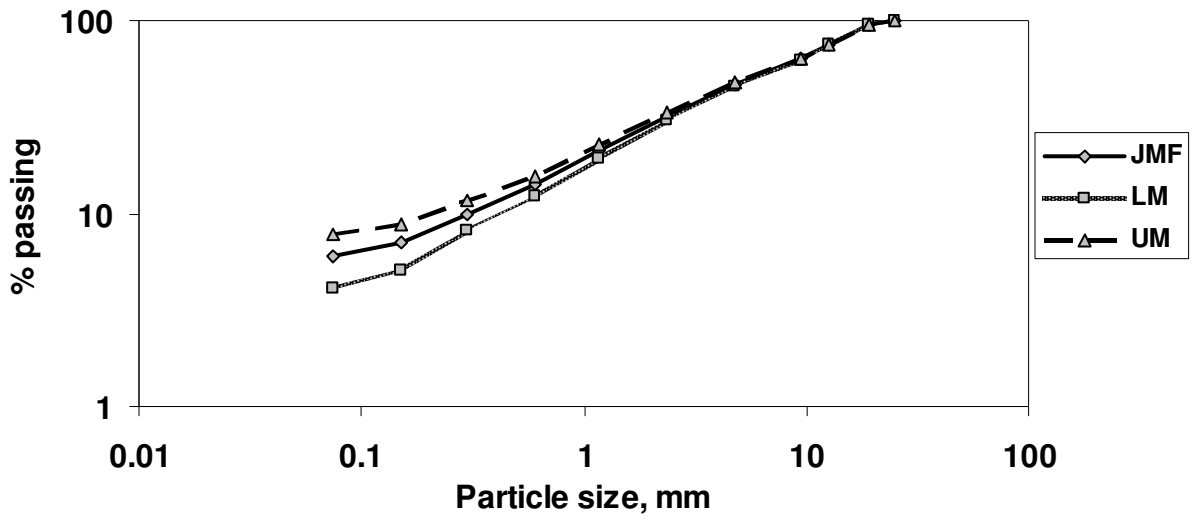
(e) Project 5627

(f) Project 5364

37
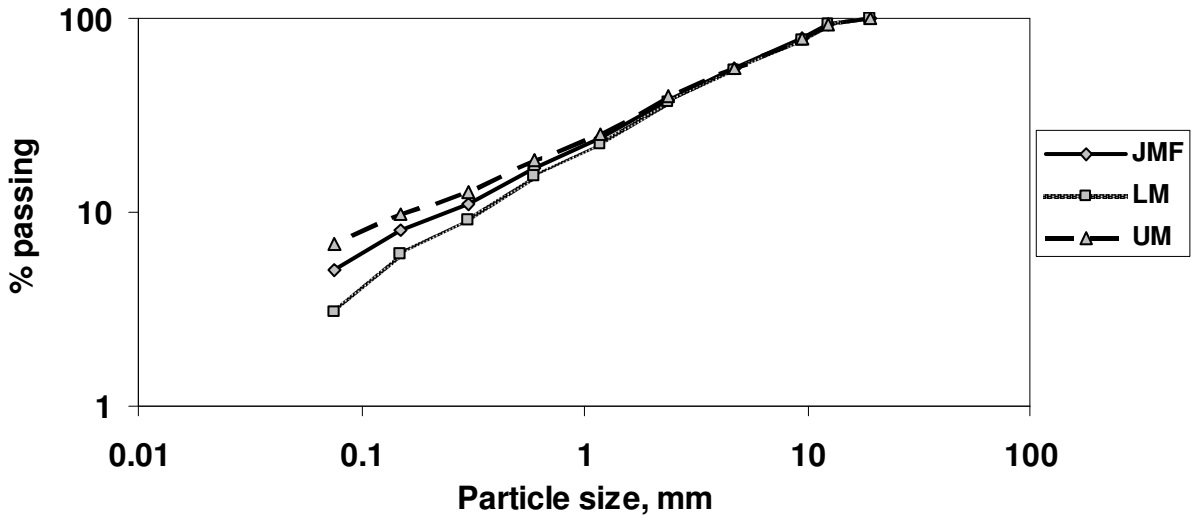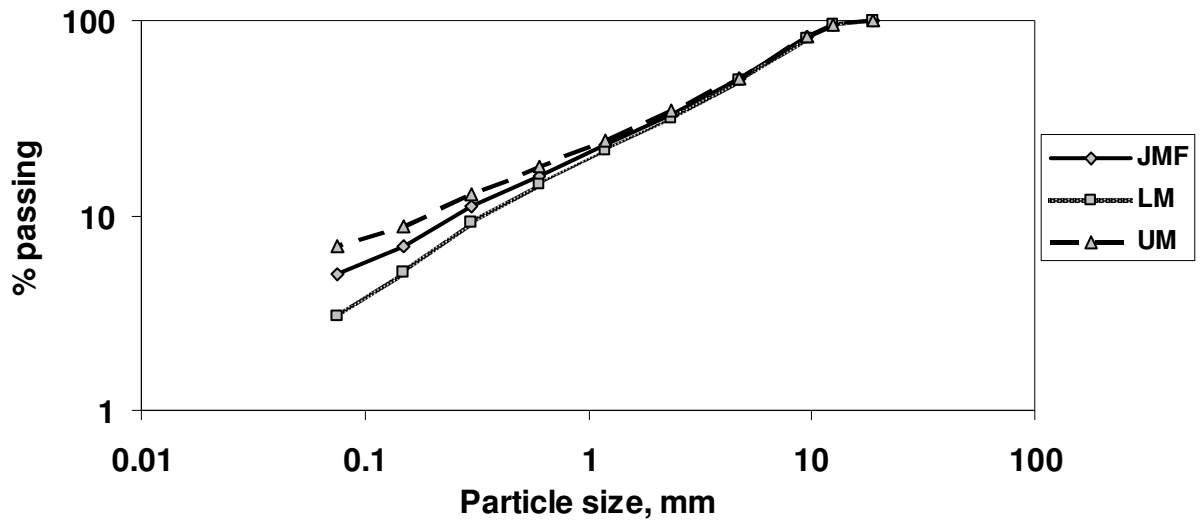
(g) Project 5408

Figure 3.3: Shift in aggregate gradation after modification
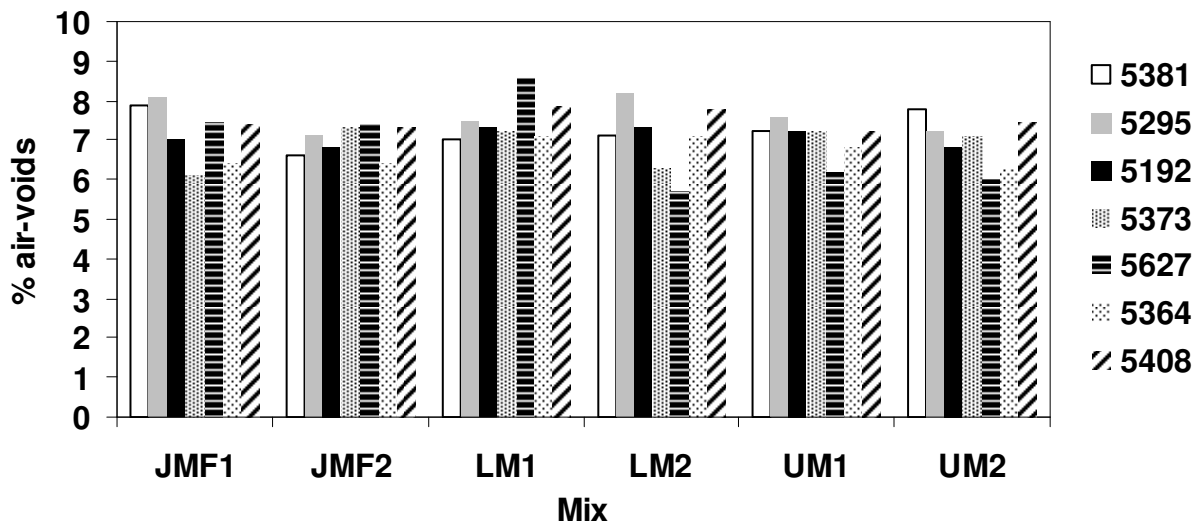
Figure 3.4: Air voids in test specimens (1 & 2 indicate replicates)

CHAPTER FOUR

ANALYSIS OF DYNAMIC MODULUS DATA

The step following the experimental part presented in Chapter 3 was the construction of master curves for the mixes investigated using the raw dynamic modulus data. The master curves were used for comparing the behavior of the mixes under load, and to investigate the sensitivity of dynamic modulus to aggregate gradation; all inferences were validated statistically. Details of the afore-mentioned tasks are presented in this chapter.

4.1 Dynamic Modulus Data and Master Curves

Dynamic modulus of the mixes investigated in this study is presented as a database in Table A1.1 (a) through (g) Appendix 1. The database includes all mixes and replicates, and projects. More details about the database and its applications are discussed in Appendix 1. One of the limitations of dynamic modulus test is that it is impossible to simulate all possible field conditions. Master curves are convenient tools for determining dynamic modulus at conditions not possible in the laboratory, constructed by shifting dynamic modulus data collected at different temperatures relative to time of loading, which is the inverse of frequency of loading.

4.1.1 Construction of Master Curves

There are different methods for constructing master curves. In this study, master curves were constructed in accordance with the method recommended by MEPDG. Dynamic modulus collected at 4.4, 37.7, and 54.4 °C were shifted relative to time of loading at 21.1 °C, which is the reference temperature. Time of loading at the reference temperature was computed using

Eq.4.1, which requires viscosity of asphalt binder. Viscosities of the asphalt binders at different temperatures and frequencies were computed using Eq.4.2, which is a correlation between viscosity (η), complex shear modulus (G*), and phase angle (δ). As the usage of Eq.4.2 is restricted to temperatures for which G* and δ data are known, viscosities at other temperatures were determined using Eq.4.3. The procedure to compute regression parameters 'A' and 'VTS' in Eq.4.3 is explained in Chapter 2, Part 2 of the MEPDG. Table A1.2 Appendix 1 summarizes the viscosities of the asphalt binders. The MEPDG states that viscosity of asphalt binders approach a maximum value at very low temperatures, and must be restricted to 2.70×10^{10} Poise, which was taken in to consideration for computing time of loading at the reference temperature.

$$\log(t_r) = \log(t) - c[\log(\eta) - \log(\eta_{T_r})] \quad \text{.............................. (4.1)}$$

where,

t$_r$ = time of loading at the reference temperature, sec

t = time of loading, sec

η = viscosity at temperature of interest, cP

η_{Tr} = viscosity at reference temperature, cP

$$\eta = \frac{G^*}{10}\left(\frac{1}{\sin\delta}\right)^{4.8628} \quad \text{...................................... .... (4.2)}$$

where

G* = binder complex shear modulus, Pa

40

δ = binder phase angle, degrees

η = viscosity, cP

$$\log\log\eta = A + VTS\log(T_R)\; .... (4.3)$$

where

η = viscosity, cP

T_R = temperature in Rankine at which the viscosity was determined

A, VTS = regression parameters

$$\log|E^*| = \chi + \frac{\alpha}{1 + e^{\beta + \gamma\log t_r}}\; .... (4.4)$$

where,

E* = dynamic modulus, MPa

t_r = time of loading at the reference temperature, sec (from Eq.4.2)

χ, α = fitting parameters; for a given set of data, χ represents the minimum value of log

(E*), and $\chi + \alpha$ represents the maximum value of log (E*)

β, γ = parameters describing the shape of the sigmoidal function

Sigmoidal curve fitting

The shifted dynamic modulus data points take the shape of a sigmoidal curve defined by

the function Eq.4.4. Fitting a sigmoidal function to the shifted data points reduces scatter and

creates a smooth master curve. The fitting parameters in Eq.4.4 define two things: the shape of

the curve, and the time-temperature dependency of dynamic modulus. The 'Solver' function in

Excel was used for computing the fitting parameters. Firstly, χ and α were determined from the dataset for which master curve is constructed; approximate values were assumed for parameters β and γ, and the parameter 'c' in Eq.4.1. All five parameters were solved iteratively in Solver until the sum of squared errors between measured and predicted dynamic modulus was close to zero. Table A1.3, Appendix 1 summarizes the fitting parameters for the master curves of the mixes investigated in this study, which can be used for determining dynamic modulus of a mix at any temperature and frequency. A systematic procedure is presented in Section A1.4, Appendix 1.

Sample dynamic modulus curves illustrating the construction of master curves are presented in Appendix 2. Fig.A2.1 is a typical dynamic modulus versus frequency plot; Fig.A2.2 illustrates the master curve before sigmoidal curve fitting; Fig.A2.3 illustrates the master curve after fitting a sigmoidal function. Fig. 4.1 (a) through (g) illustrates the master curves of the mixes after sigmoidal curve fitting.

4.1.2 Dynamic modulus at -10 °C

Dynamic modulus is a key input parameter to the MEPDG. The Design Guide (MEPDG software) Version 1.000 mandates that dynamic modulus data for distress prediction should consist at least one temperature in the range -17.7 to -6.7 °C. This temperature range is hard to achieve in the laboratory using the Simple Performance Tester currently available at the Washington Center for Asphalt Technology (WCAT); therefore, dynamic modulus values corresponding to -10 °C were predicted using Eq.4.3 and the fitting parameters presented in Table A1.2, Appendix 1.

4.2 Effect of air voids on dynamic modulus

Dynamic modulus of replicates of a mix could vary if there is significant variation in air voids. Air voids in some replicates in this study differed significantly: Mix 5381 – 1.3%, Mix 5295 – 1%, Mix 5373 – 1.2%, but marginal in the other mixes. Fig.4.2 (a) through (g) compares dynamic modulus curves of replicates of JMF mixes. The variation in dynamic modulus between replicates is not significant in most cases, even in mixes 5381, 5295, and 5373. It appears that variation in air voids had little effect on dynamic modulus of replicates although some cases showed noticeable difference at high temperatures, which could be the result of variations in experimental data.

4.3 Dynamic Modulus of JMF Mixes

Fig.4.3 (a) through (d) presents dynamic modulus curves of the JMF mixes at 4.4, 21.1, 37.8, and 54.4 °C. The curves are distinct at temperatures 37.8 and 54.4 °C, but not at 4.4 and 21.1 °C. This behavior could be attributed to aggregate interlocking and stiffness of asphalt. In general, at low temperatures, stiffness of asphalt binder governs dynamic modulus of a mix while at high temperatures it is governed by aggregate gradation and interlocking between particles.

Stiffness is a function of viscosity. Fig.4.4 illustrates viscosity versus temperature relationship for the asphalt binders used in this study. At low temperatures, viscosities of the asphalt binders show significant difference. As temperature increases, the difference becomes less significant, exhibiting approximately same stiffness at high temperatures. Thereby, any variation in dynamic modulus between the mixes at high temperatures (37.8 and 54.4 °C) must be a result of aggregate gradation and interlocking between particles.

4.4 Sensitivity of Dynamic Modulus to Percent Passing Sieve No.200

Dynamic modulus curves of JMF, LM and UM mixes is illustrated in Fig.4.5 through 4.8. The curves are distinct at 37.8 and 54.4 °C, but not at 4.4 and 21.1 °C, which is similar to the behavior of the JMF mixes. The same phenomenon described in Section 4.3 is valid in this case as well. However, in most cases, the LM and UM mixes do not follow a definite trend with the JMF mixes. Thus, ±2% variations in percent-passing sieve #200 did not have significant effect on dynamic modulus.

4.5 Statistical Analysis

The inferences in Section 4.4 and Section 4.5 were verified statistically. In general, statistical analysis refers to a collection of methods used to process large amounts of data and report overall trends. Some methods can be used to summarize or describe a collection of data called as 'descriptive statistics'. Some methods model the patterns in the data and draw inferences about the process or population being studied called as 'inferential statistics'. The statistical analysis performed in this study falls in the latter type i.e., inferential statistics. *Appendix 3* presents some basic terminologies related to the statistical analysis performed in this study.

4.5.1 Model

The objectives of the statistical analysis are to test if dynamic modulus of the JMF mixes show significant difference, and to test if dynamic modulus of JMF, LM and UM mixes vary significantly. A General Linear Model (GLM) was fitted to the dynamic modulus data and analyzed using multi-factor analysis of variance (ANOVA) using the statistical software SAS

Version 9.1. The treatment factors were one or combinations of project, mix, temperature and frequency – dynamic modulus was the response variable. Table 4.1 lists the levels of the treatment factors. For all pairwise comparisons, Tukey's Multiple Comparison Method was employed. For Null hypothesis (H_0), significance level of 0.05 was assumed. Section 4.6.3 presents the results of the analysis of the dynamic modulus data of the JMF mixes. Section 4.6.4 presents the results of the analysis of dynamic modulus data of JMF, LM and UM mixes.

4.5.2 JMF mixes

The dynamic modulus data of the JMF mixes was analyzed using Repeated Measures ANOVA. Repeated measures ANOVA was used because the same specimen was tested at all dynamic modulus test conditions – four temperatures and six frequencies, and a standard ANOVA would fail to model the correlation between the repeated measures; here repeated measures implies E* test conditions. The treatment factors were project, mix, temperature, and frequency. To test null hypothesis (i.e., there is no significant difference in dynamic modulus of the seven JMF mixes), p-values from Tukey's pairwise comparisons of the JMF mixes were compared with the significance level 0.05. Table 4.2 summarizes the p-values; majority is smaller than 0.05 indicating that the JMF mixes are significantly different. In addition, the Type I p-value is 0.0015, which is an overall indication that significant difference in dynamic modulus exists among the mixes. This supports Section 4.3, wherein it was shown that dynamic modulus of the JMF mixes exhibited variation. Fig.4.10 is a plot of the mean dynamic modulus of the seven mixes. Dynamic modulus of the JMF mixes follows the trend: 5364 < 5373 < 5408 < 5381 < 5627 < 5295 < 5192.

4.5.3 JMF, LM and UM Mixes

To test if dynamic modulus of JMF, LM and UM mixes vary significantly, dynamic modulus data of JMF, LM and UM mixes of each project were analyzed separately using Repeated Measures ANOVA. Table 4.3 summarizes the p-values from Tukey's pairwise comparisons of the three mixes; majority is larger than 0.05 indicating that dynamic modulus of the three mixes is not different. In addition, the Type I p-values of all the projects, except 5381 and 5364, are larger than 0.05, which also indicates that significant difference does not exist. This supports the inferences presented in Section 4.4, wherein it was shown that dynamic modulus was not sensitive to ±2% variation in percent-passing sieve #200.

4.6 Summary

Dynamic modulus of the JMF mixes varied significantly at high temperatures compared to low temperatures. Conversely, dynamic modulus of JMF, LM and UM mixes did not exhibit significant variation; also, LM and UM mixes did not follow a definite trend with JMF mixes. Thus, the behavior of the seven HMA mixes selected for this study was different under load, and varying percent-passing sieve #200 by ±2% did not have significant effect on dynamic modulus. Results from the Analysis of Variance of the dynamic modulus data supported these inferences. In some projects, air voids of replicates varied by approximately 1%, which did not have significant effect on dynamic modulus of replicates.

Table 4.1: Levels of treatment factors for ANOVA of dynamic modulus data

	Levels	
Block (Project)	7	5381, 5295, 5192, 5373, 5627, 5364, 5408
Mix	3	JMF, lower modified, upper modified
Temperature, ° C	4	4.4, 21.1, 37.8, 54.4
Frequency, Hz	6	25, 10, 5, 1, 0.5, 0.1

Table 4.2: *P*-values from pairwise comparisons of dynamic modulus of JMF mixes

Project	5381	5295	5192	5373	5637	5364	5408
5381	-	0.9295	0.4391	**0.0559**	0.9865	**0.0341**	0.1575
5295		-	0.9205	**0.0174**	0.9999	**0.0111**	**0.046**
5192			-	**0.0059**	0.7975	**0.0039**	**0.0141**
5373				-	**0.0245**	0.9991	0.9672
5627					-	**0.0154**	0.0665
5364						-	0.836
5408							-

Table 4.3: *P*-values from pairwise comparisons of JMF, LM and UM mixes

Project	Mix	UM	LM	Type I
5381	JMF	**0.0196**	0.0674	**0.0215**
	LM	0.2162	-	
5295	JMF	0.4824	0.6572	0.2259
	LM	0.2087	-	
5192	JMF	0.9999	0.8769	0.8514
	LM	0.872	-	
5373	JMF	0.1732	0.5857	0.1892
	LM	0.451	-	
5627	JMF	0.719	0.4825	0.5028
	LM	0.8817	-	
5364	JMF	0.4056	**0.0026**	**0.0016**
	LM	**0.0018**	-	
5408	JMF	0.8616	0.2081	0.2088
	LM	0.3342	-	

(a) 5381

(b) 5295

48

(c) 5192

(d) 5373

(e) 5627

(f) 5364

50
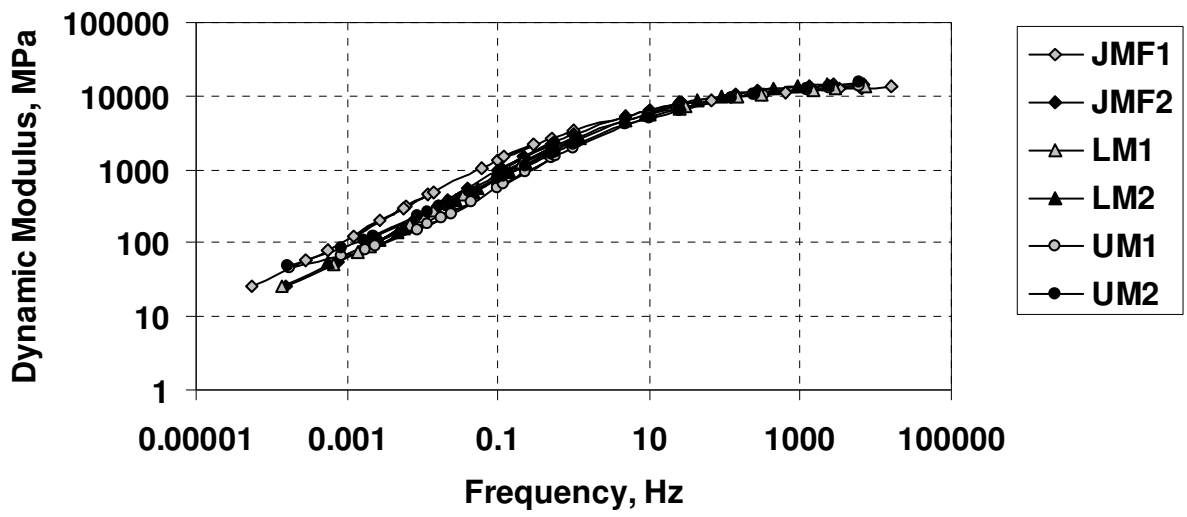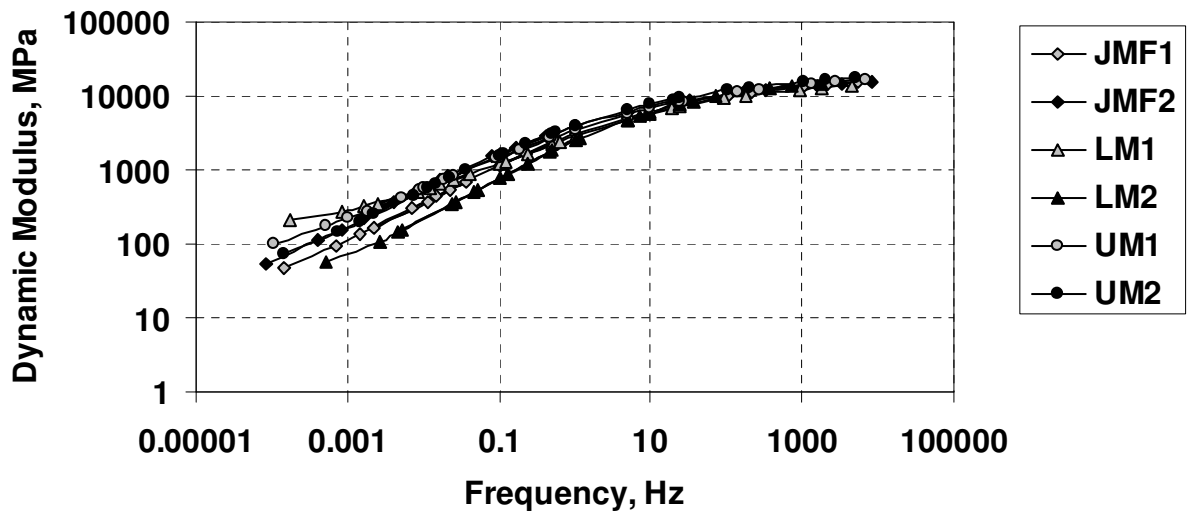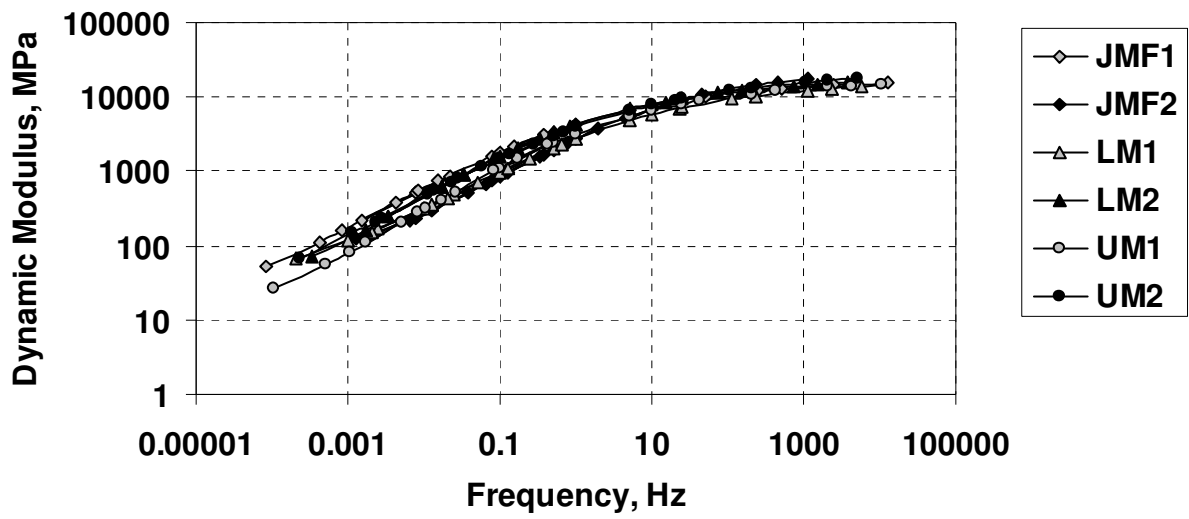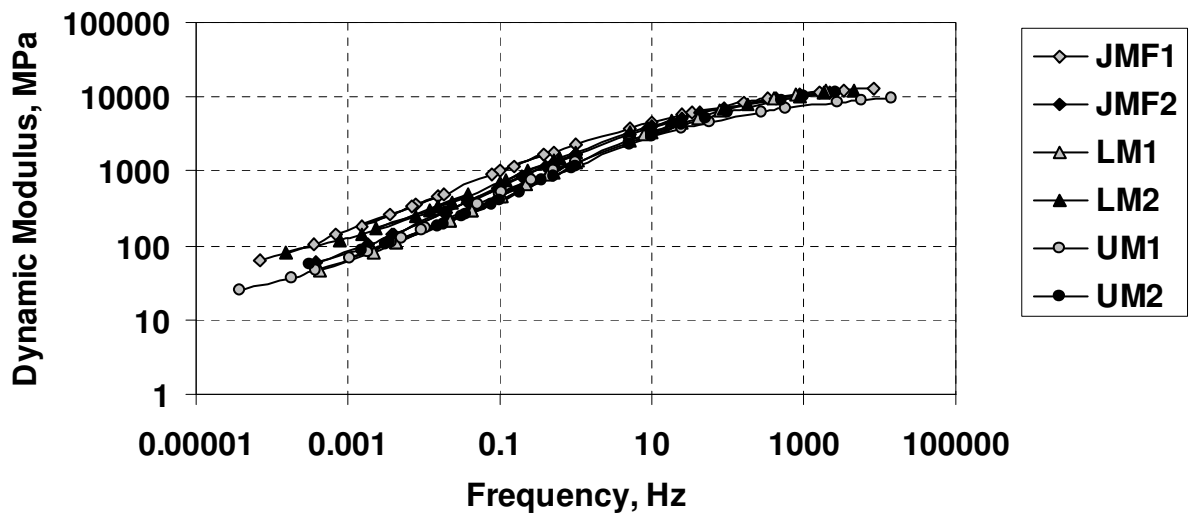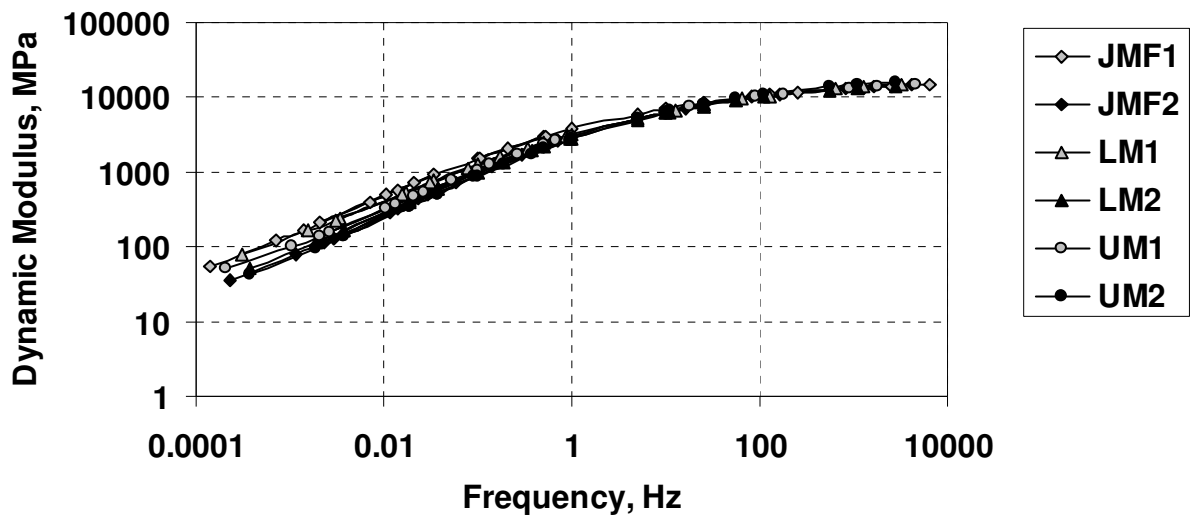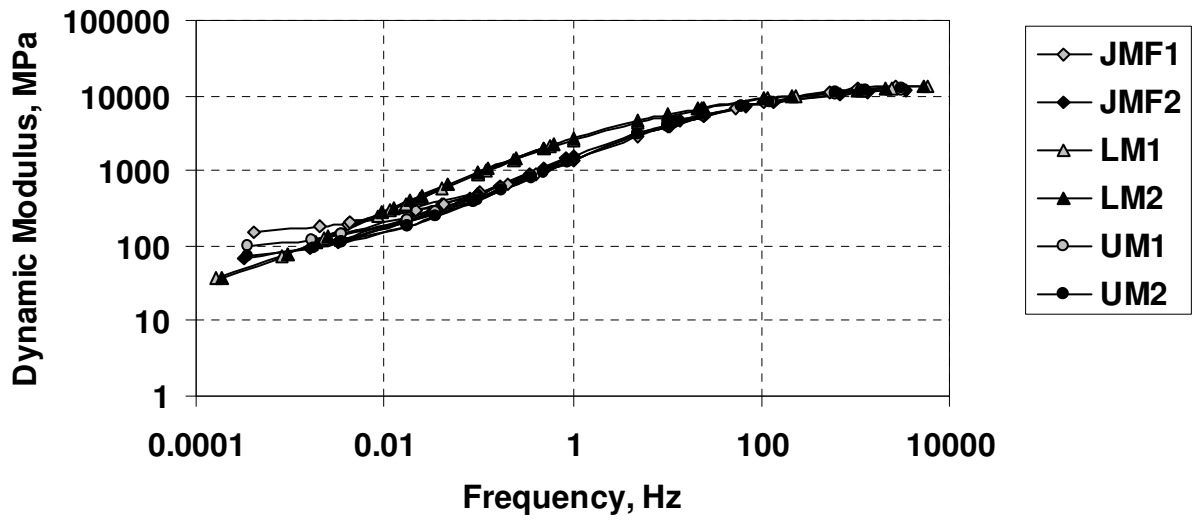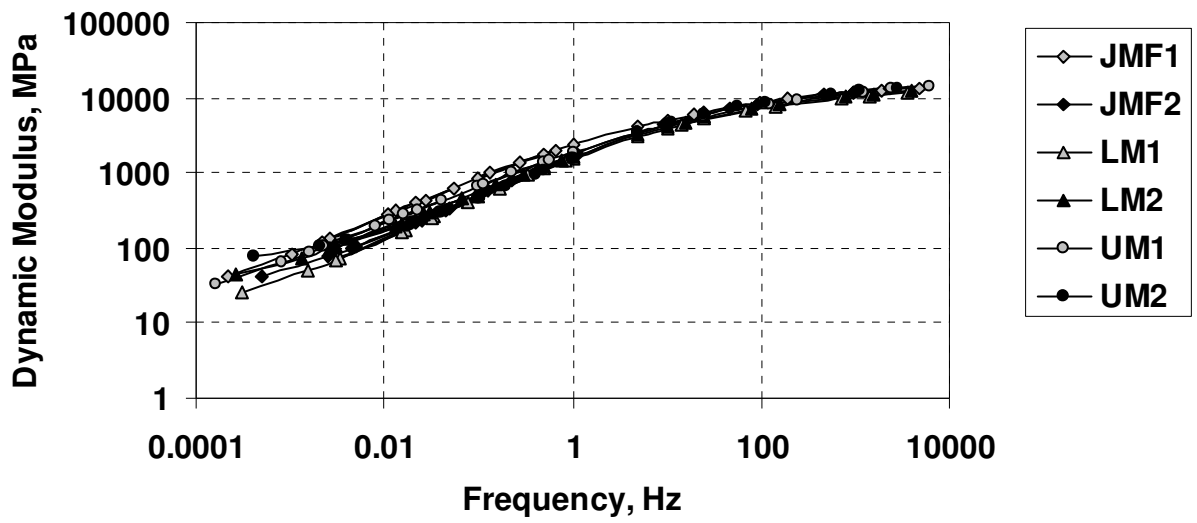
(g) 5408

Figure 4.1: Master curves of JMF, LM and UM mixes
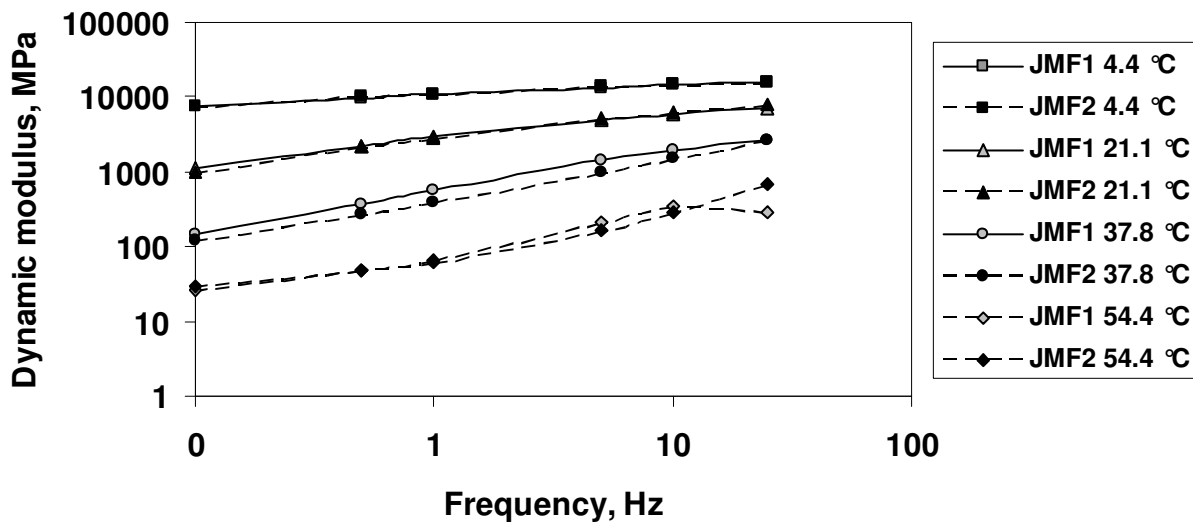
(a) Project 5381; JMF1 – 7.9% AV, JMF2 – 6.6% AV
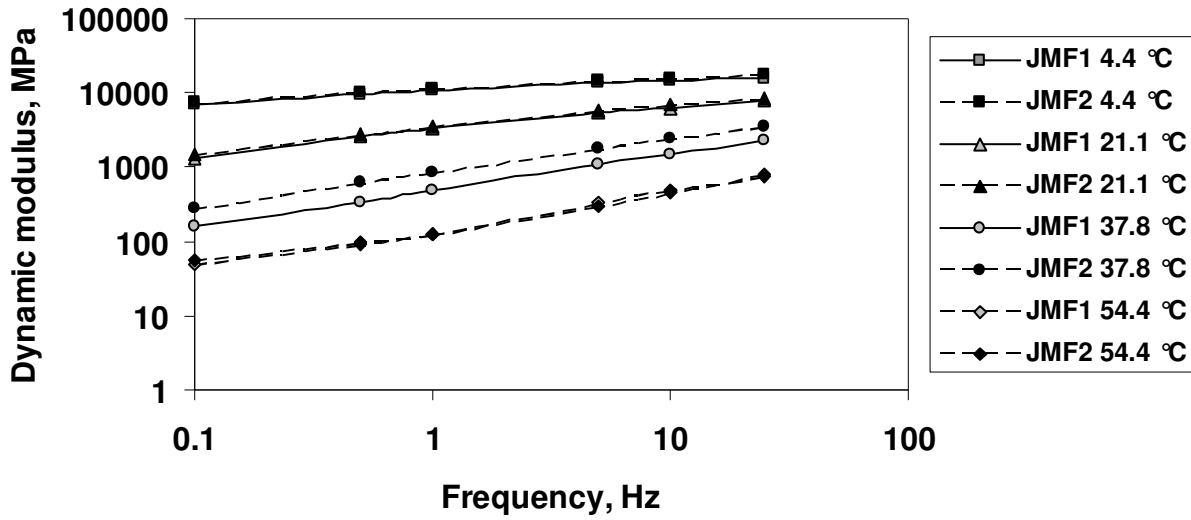
(b) Project 5295; JMF1 – 8.1% AV, JMF2 – 7.1% AV
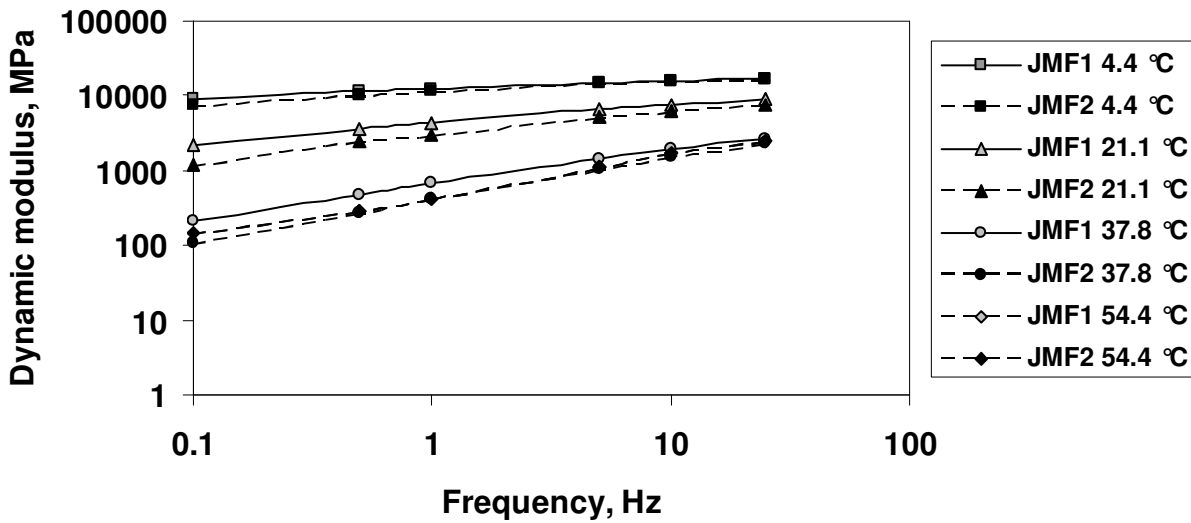
(c) Project 5192; JMF1 – 7.0% AV, JMF2 – 6.8% AV
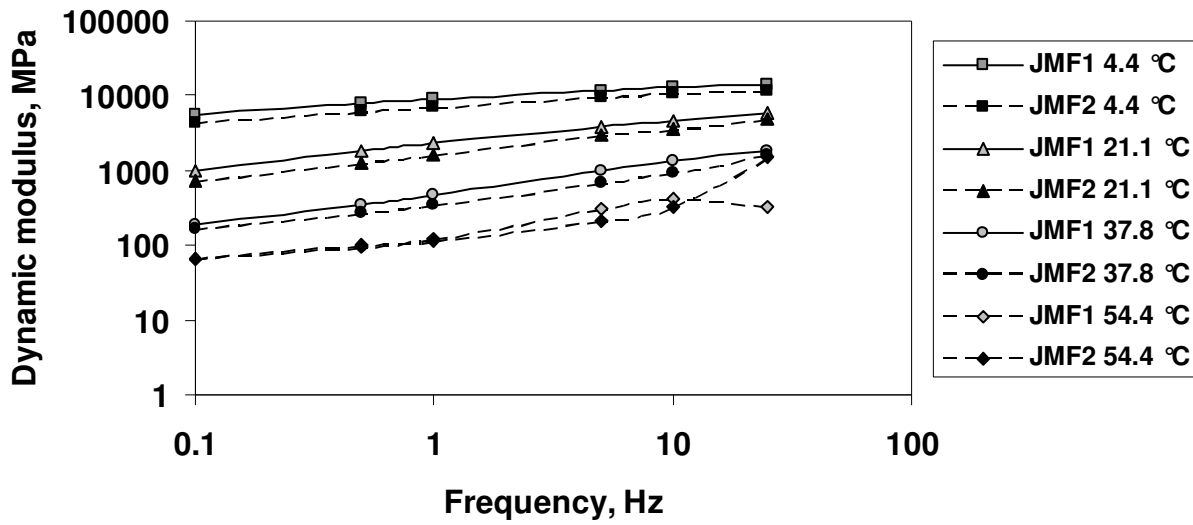
(d) Project 5373; JMF1 – 6.1% AV, JMF2 – 7.3% AV
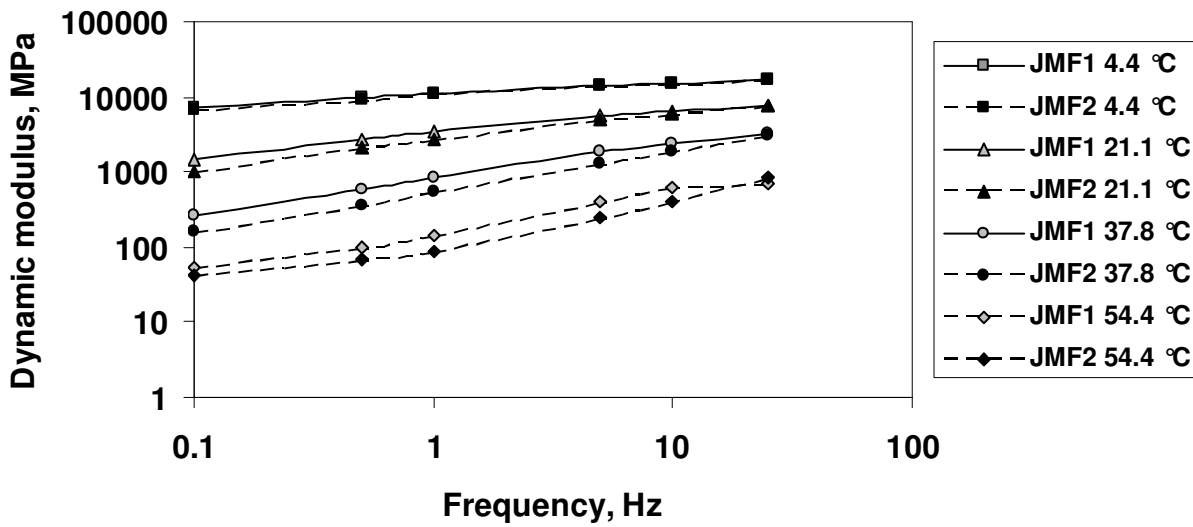
(e) Project 5627; JMF1 – 7.5% AV, JMF2 – 7.4% AV
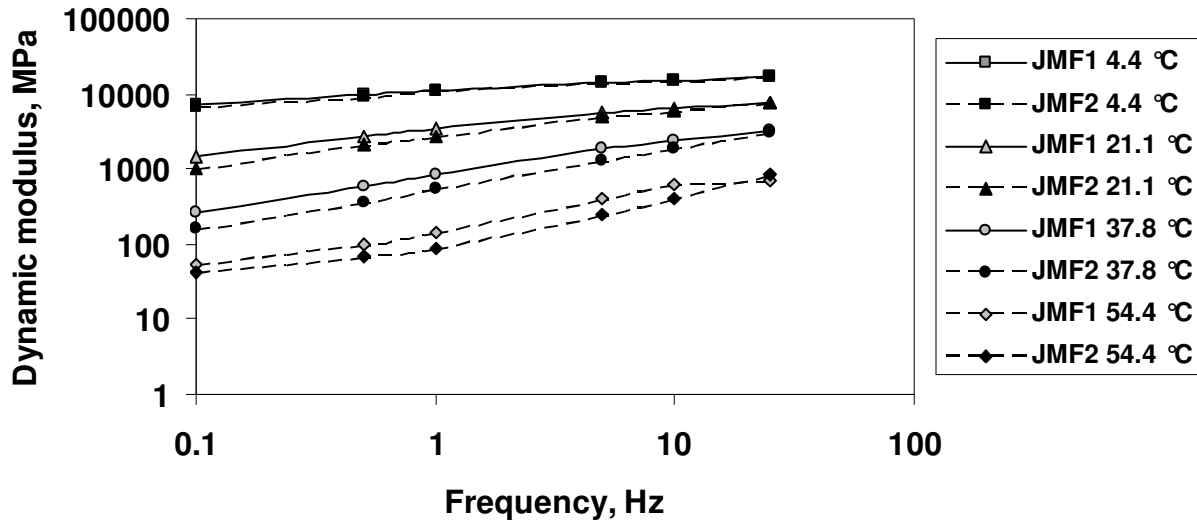
(f) Project 5364; JMF1 – 6.4% AV, JMF2 – 6.4% AV
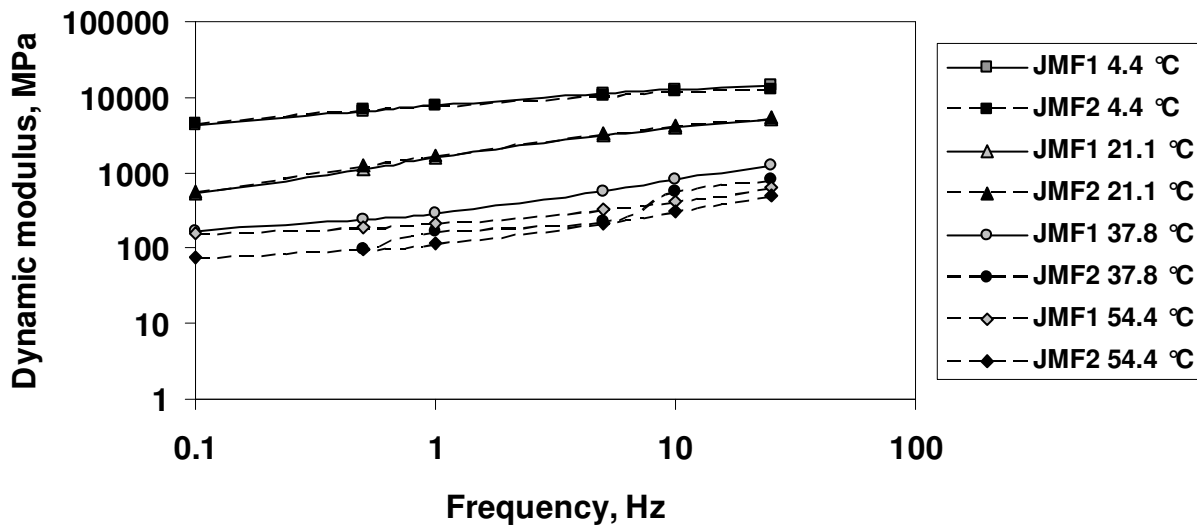
(g) Project 5408; JMF1 – 7.4% AV, JMF2 – 7.3% AV

Figure 4.2: Effect of air voids on dynamic modulus of replicates of JMF mixes

(a) 4.4 ℃
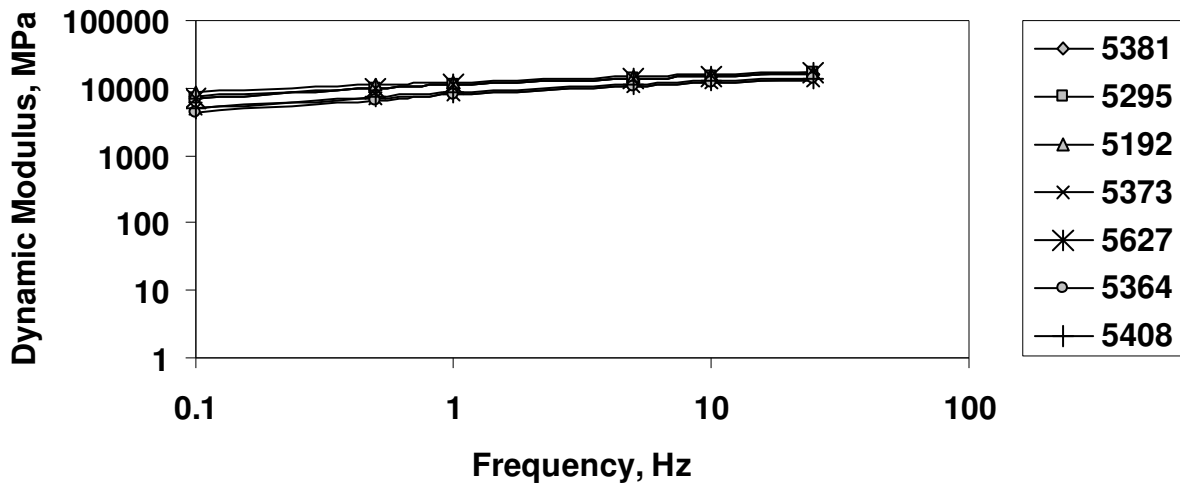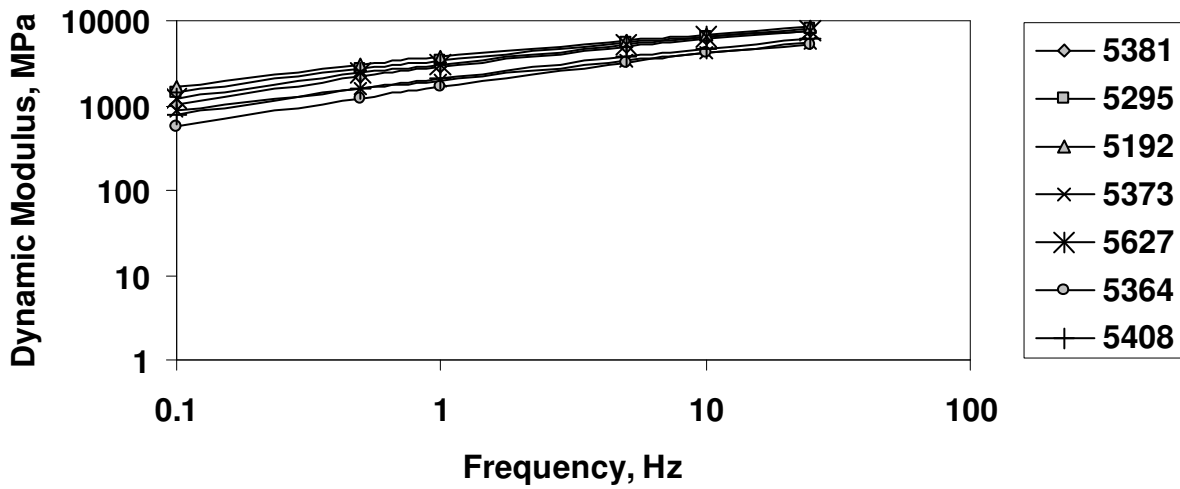
(b) 21.1 ℃
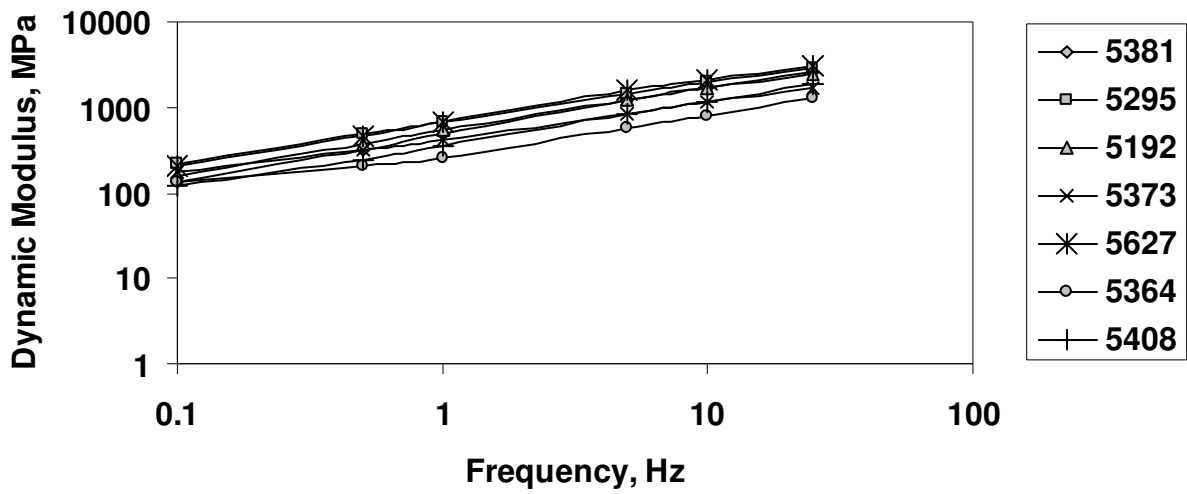
(c) 37.8 ℃
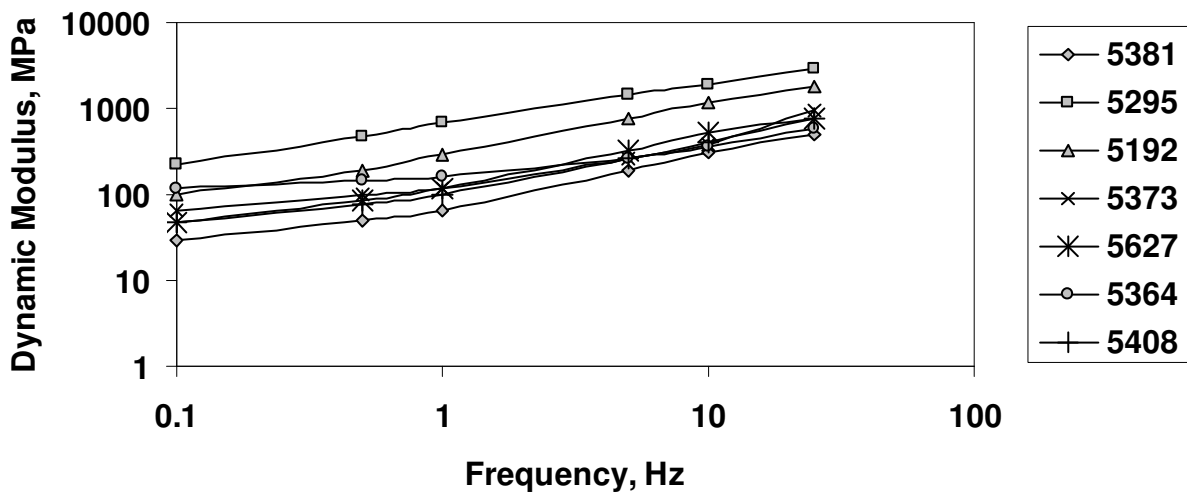
(d) 54.4 ℃

Figure 4.3: Dynamic modulus curves of JMF mixes
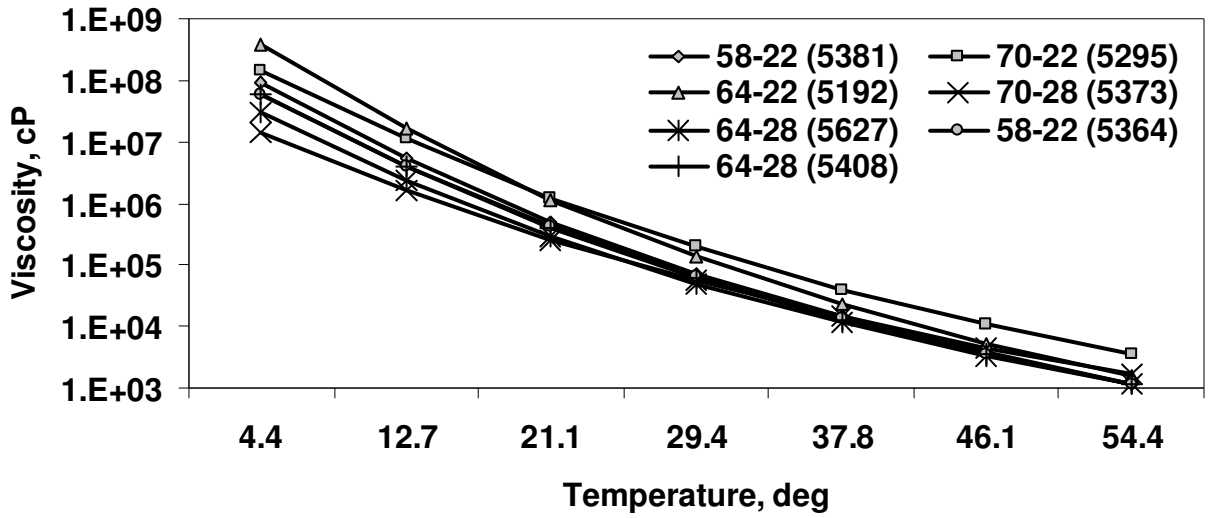
Figure 4.4: Viscosity of asphalt binders versus temperature relationship

(a) 5381

(b) 5295

(c) 5192

(d) 5373

(e) 5627

59
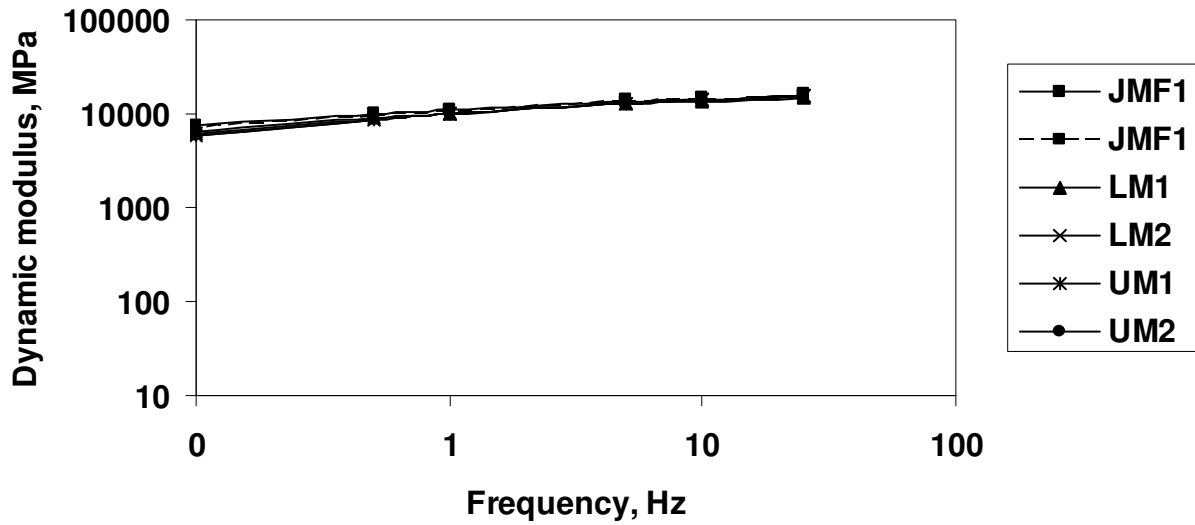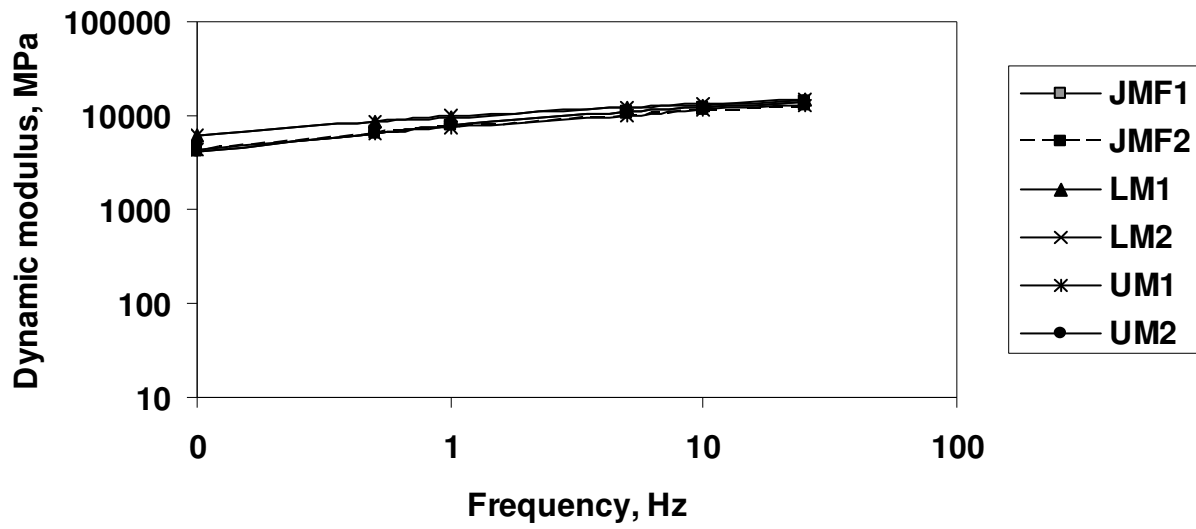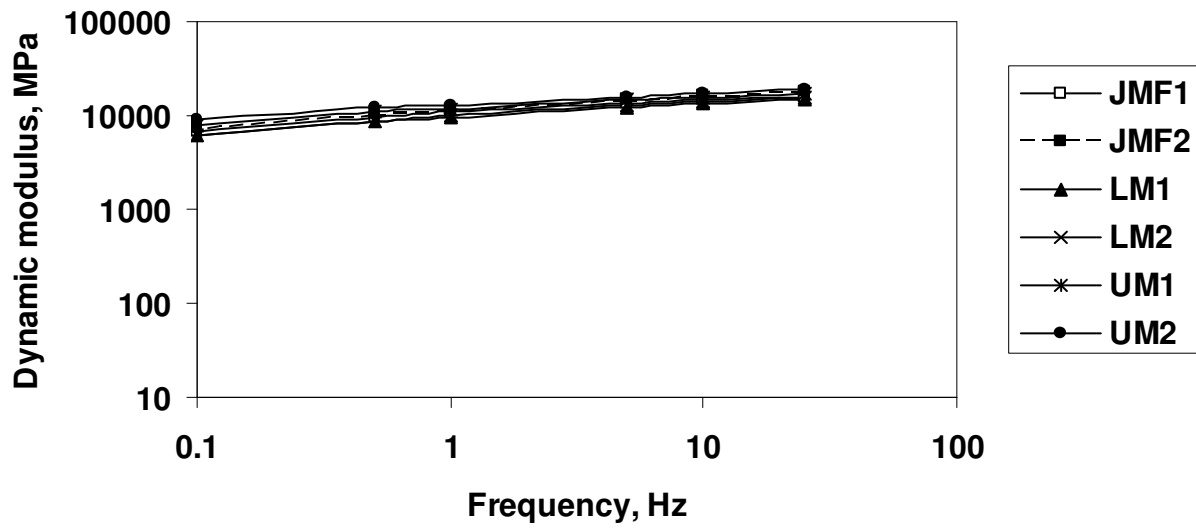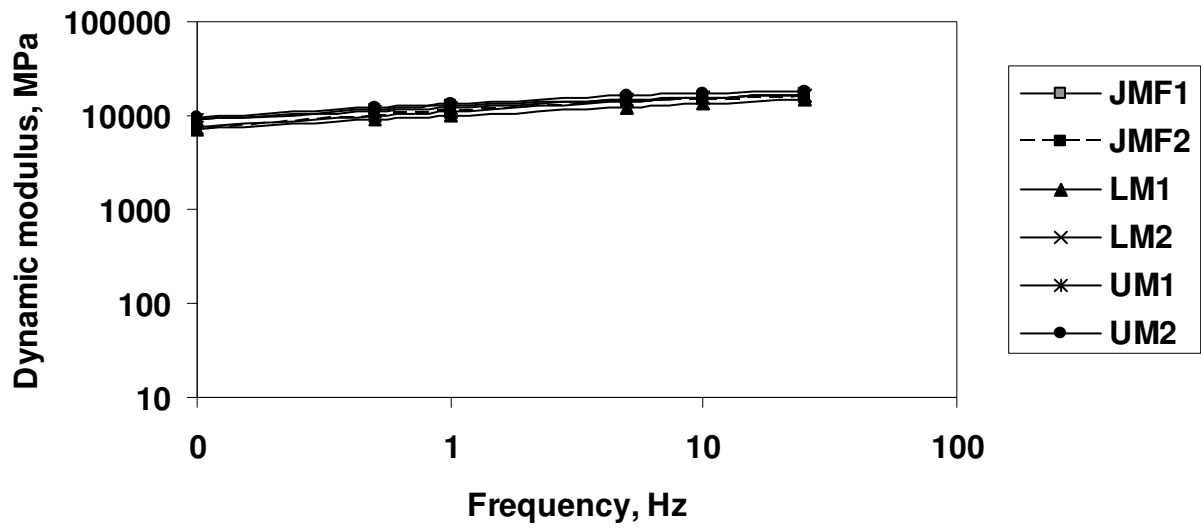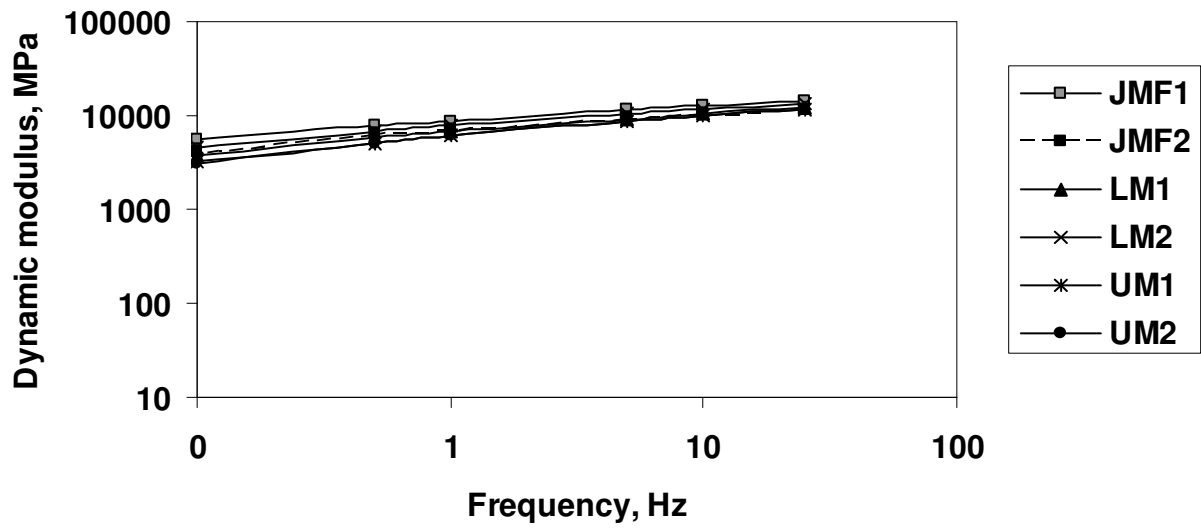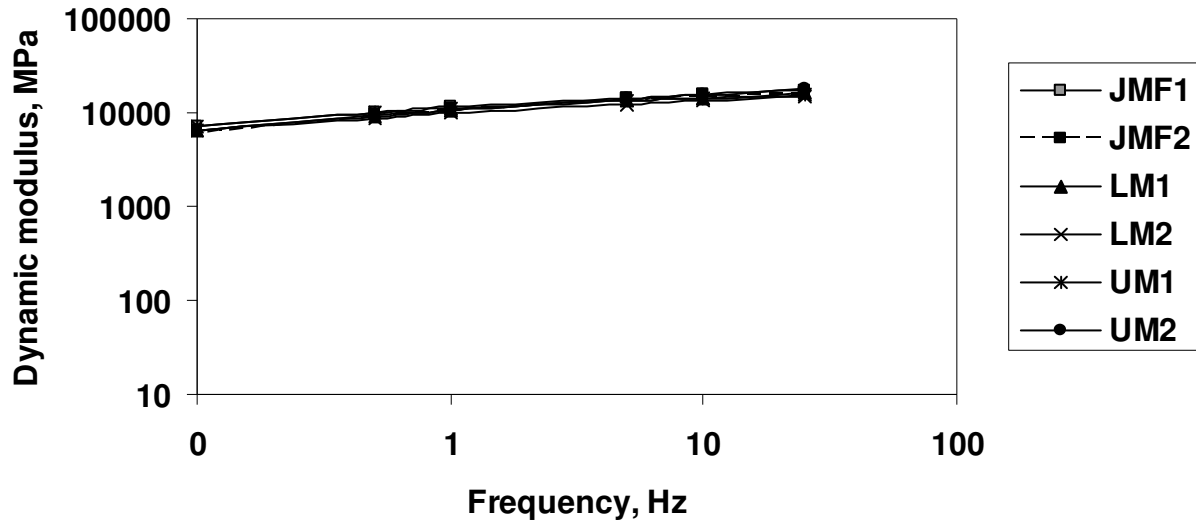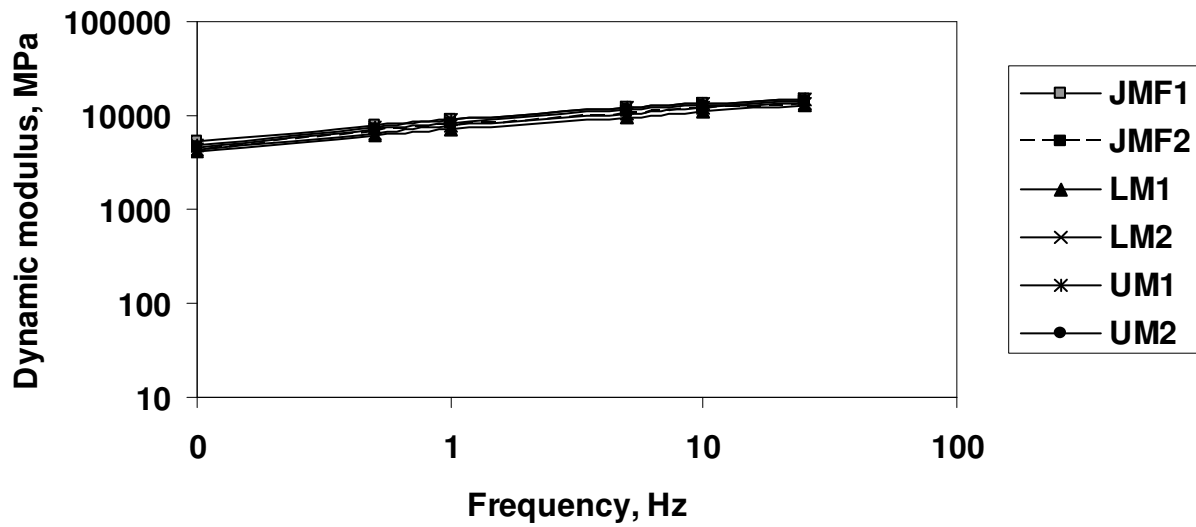
(f) 5364

(g) 5408

Figure 4.5: Dynamic modulus curves of JMF, LM and UM mixes at 4.4 °C
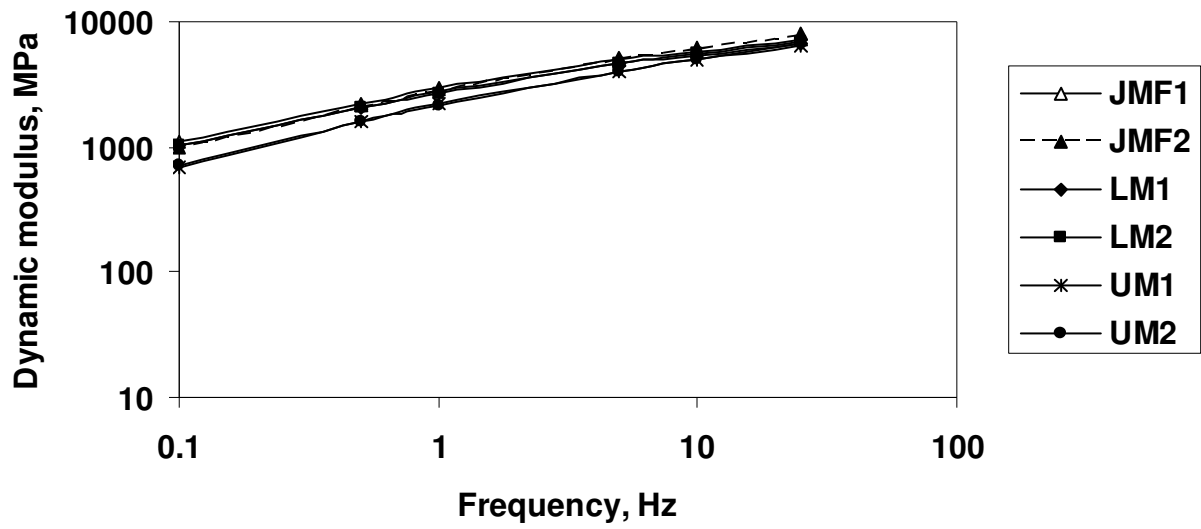
(a) 5381
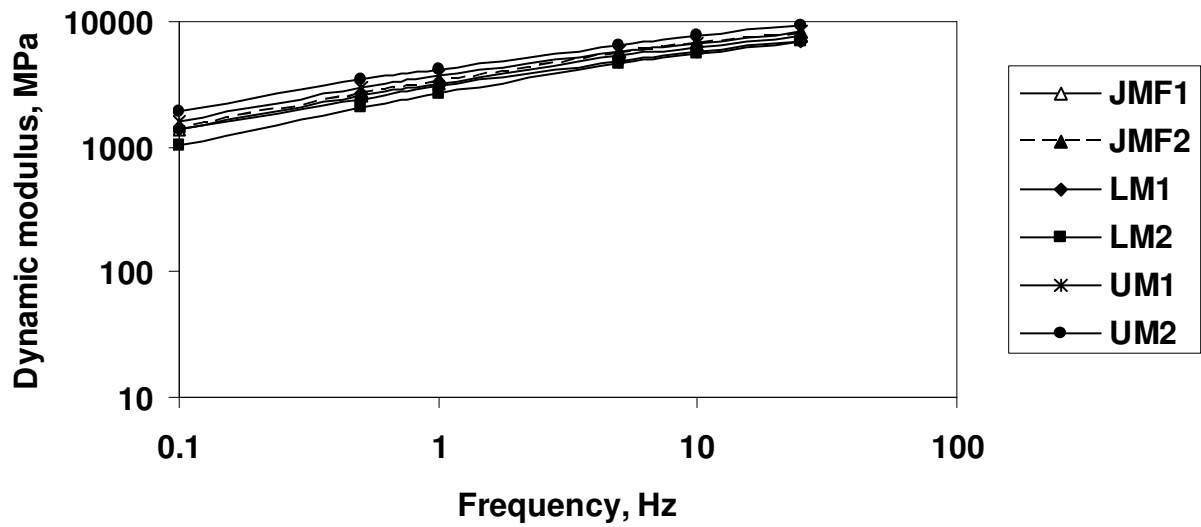
(b) 5295
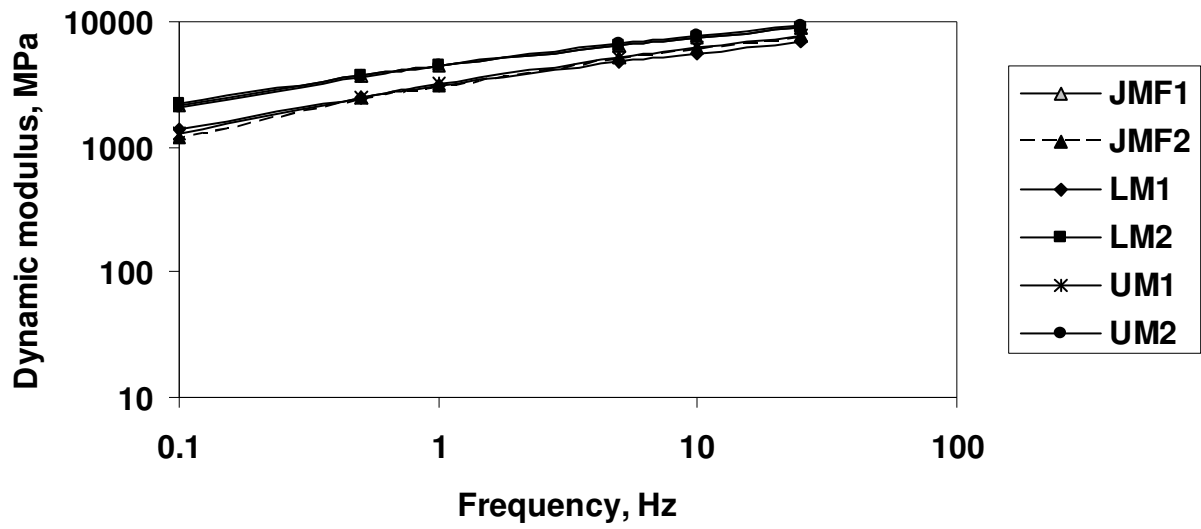
(c) 5192
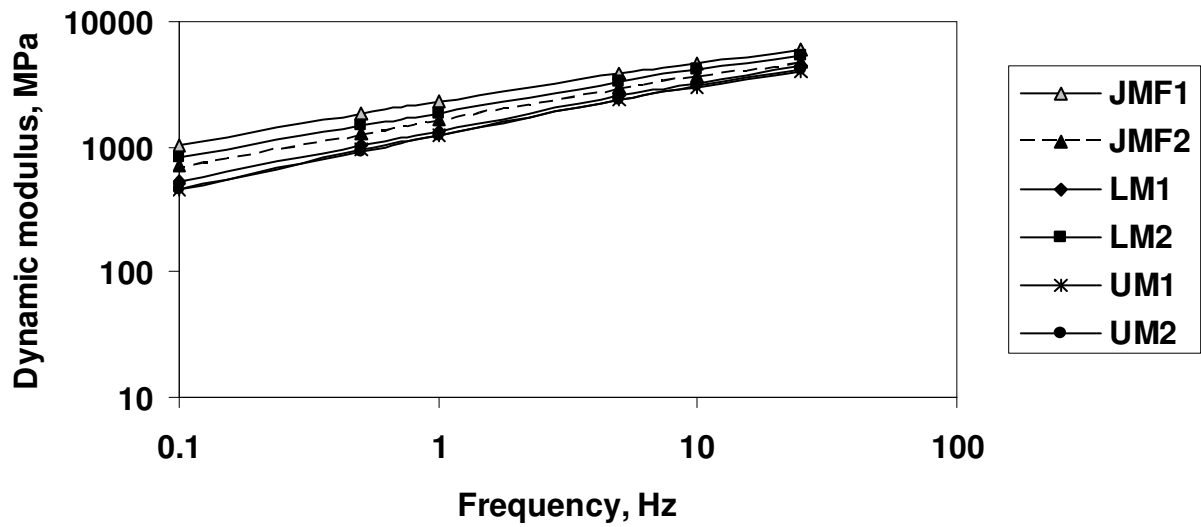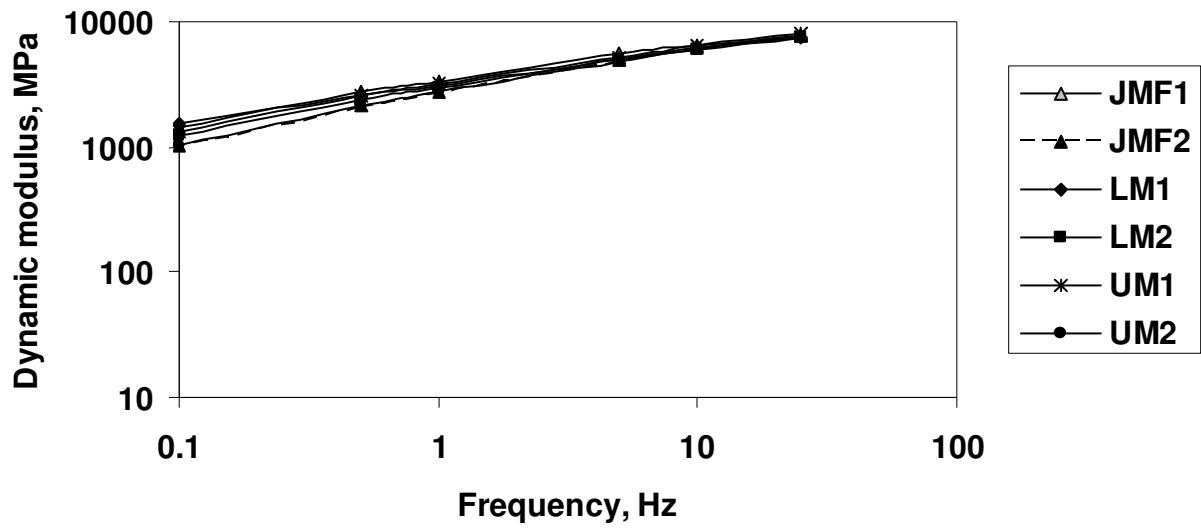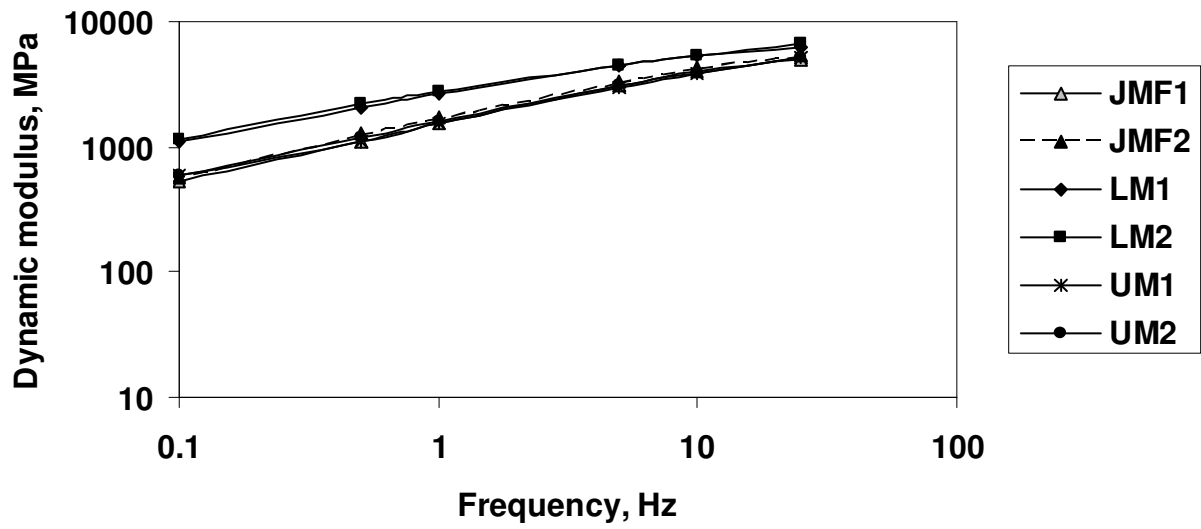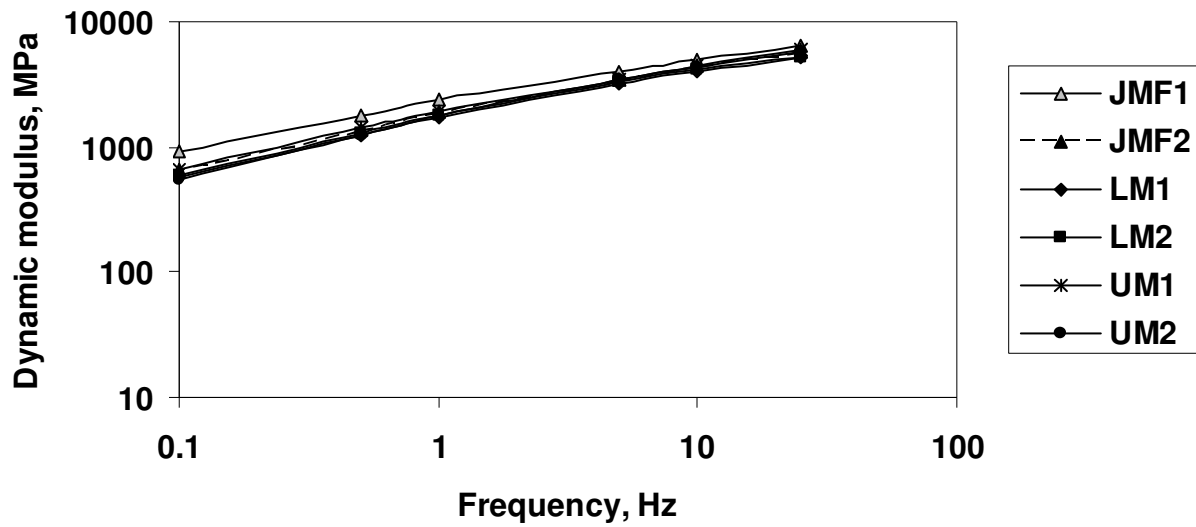
(d) 5373

(e) 5627

(f) 5364

(g) 5408

Figure 4.6: Dynamic modulus curves of JMF, LM and UM mixes at 21.1 °C

(a) 5381

(b) 5295

(c) 5192

65

(d) 5373

(e) 5627

66
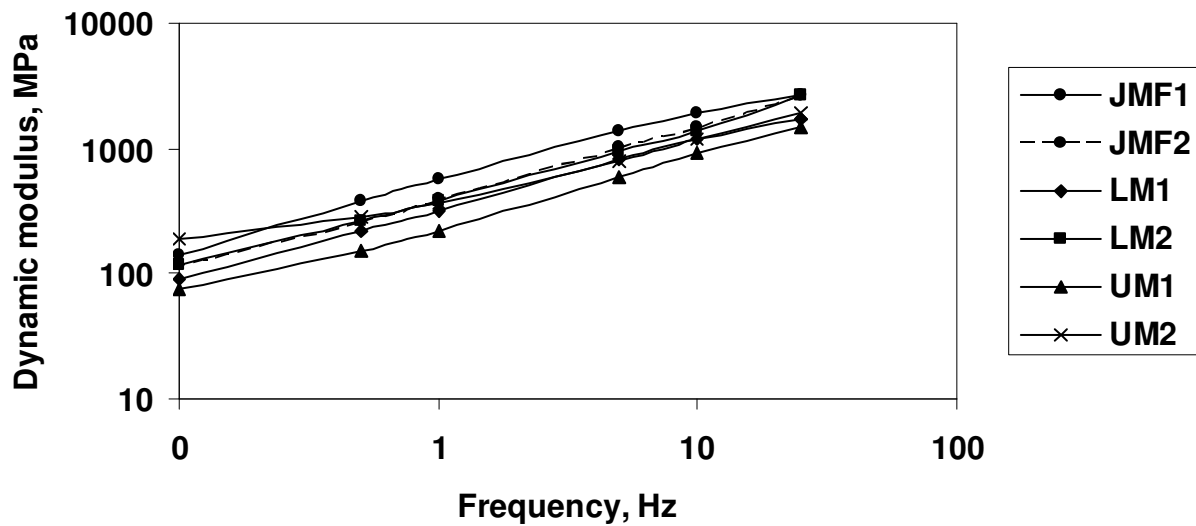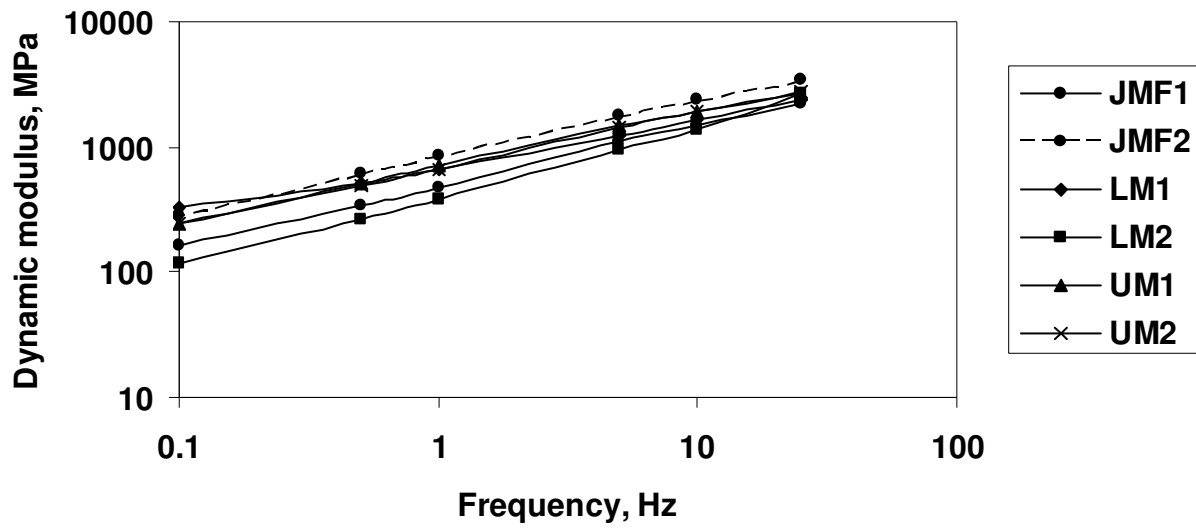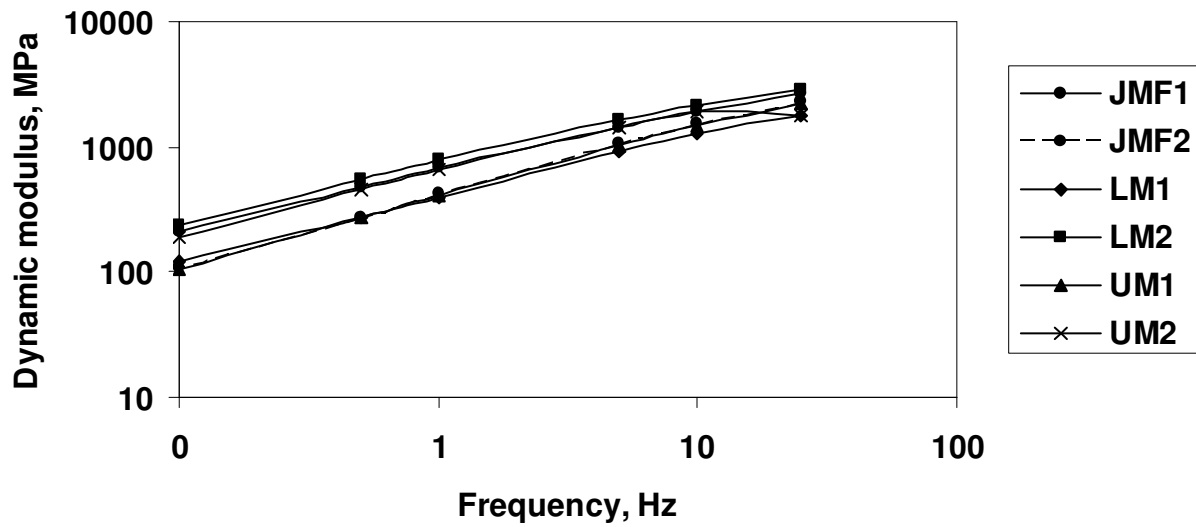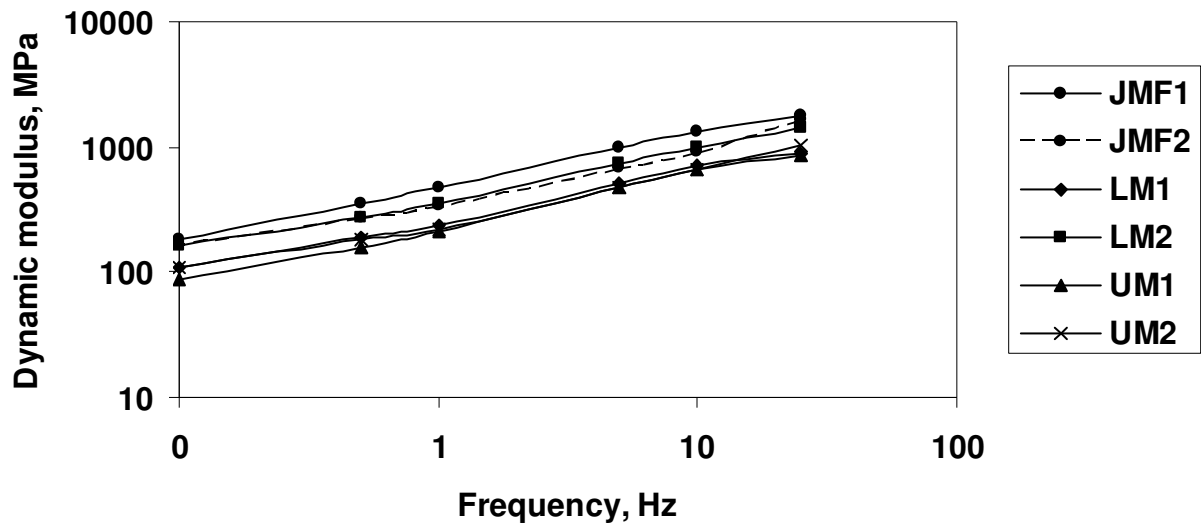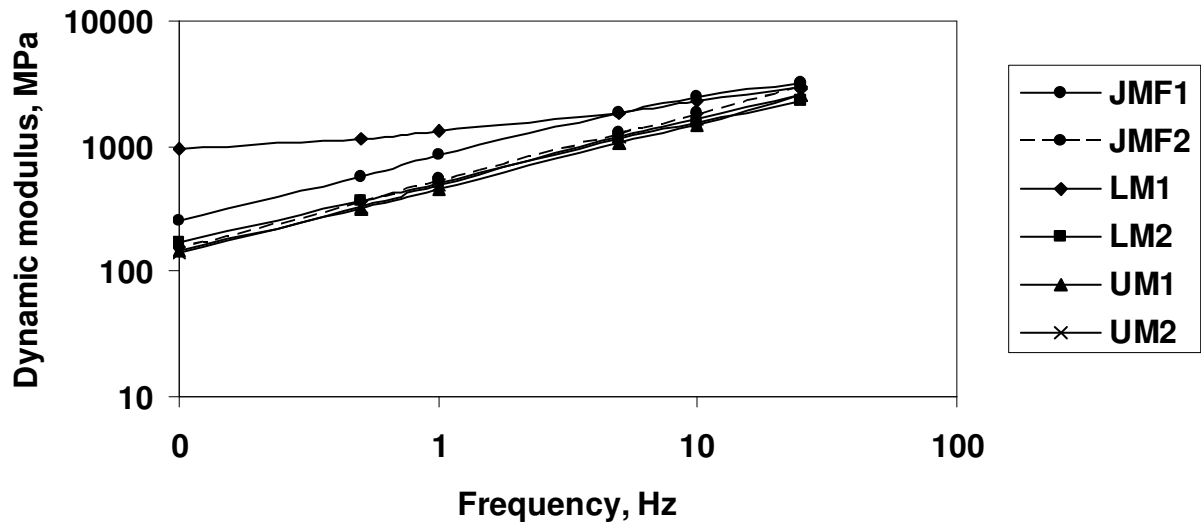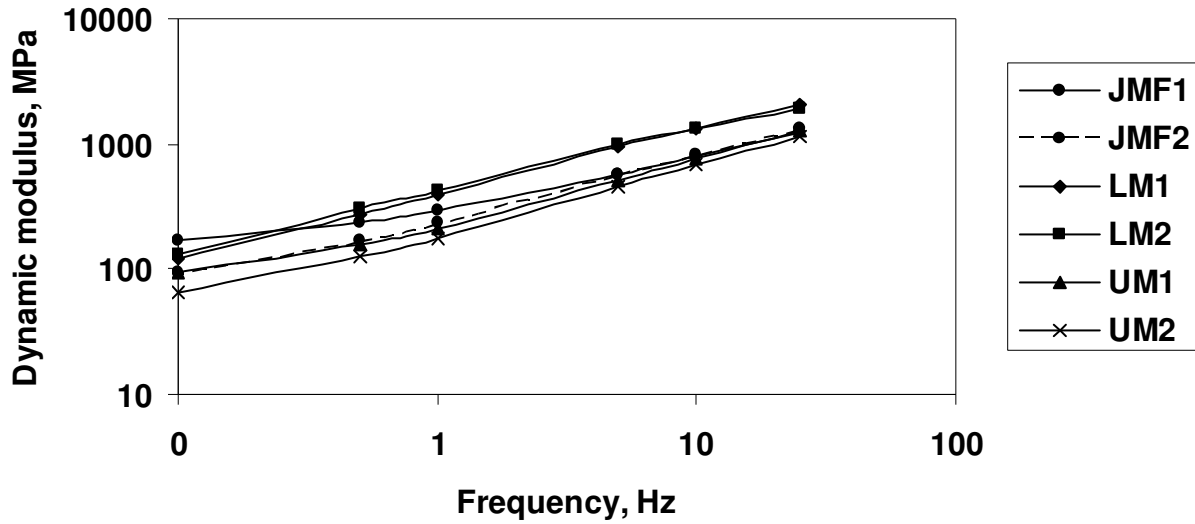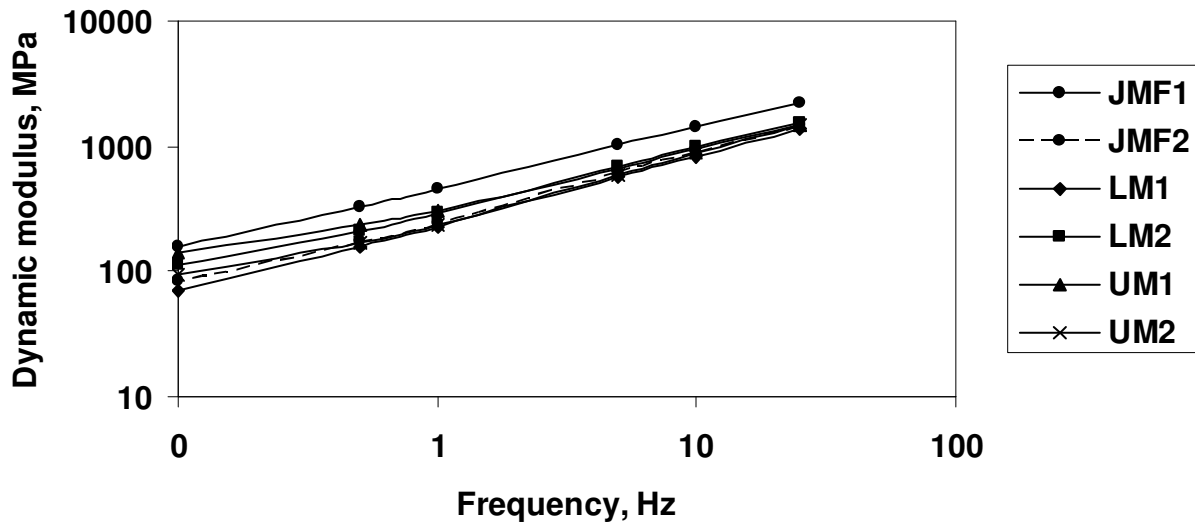
(f) 5364

(g) 5408

Figure 4.7: Dynamic modulus curves of JMF, LM and UM mixes at 37.8 °C

(a) 5381

(b) 5295

(c) 5192

(d) 5373

69
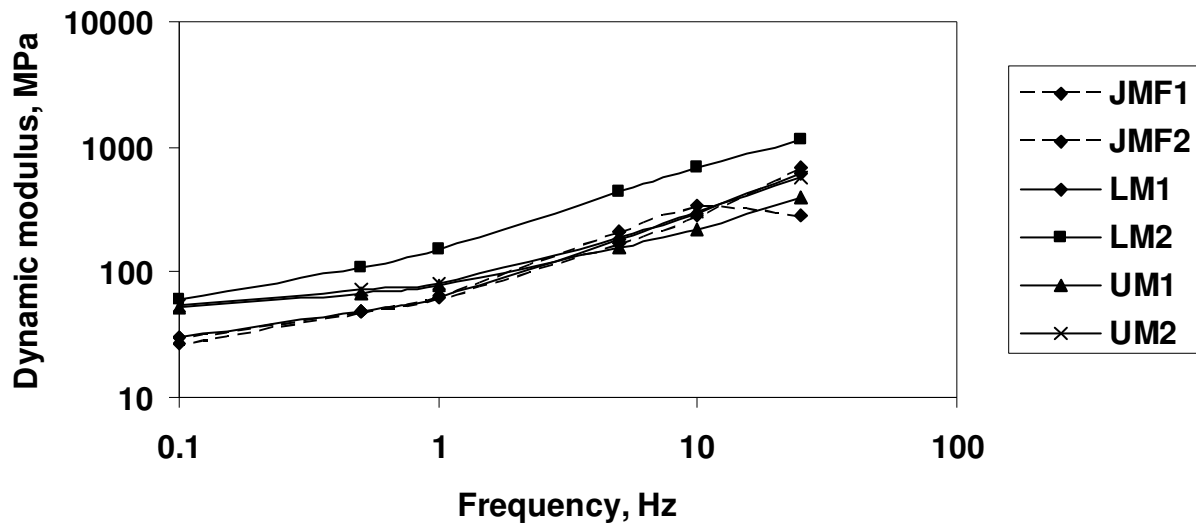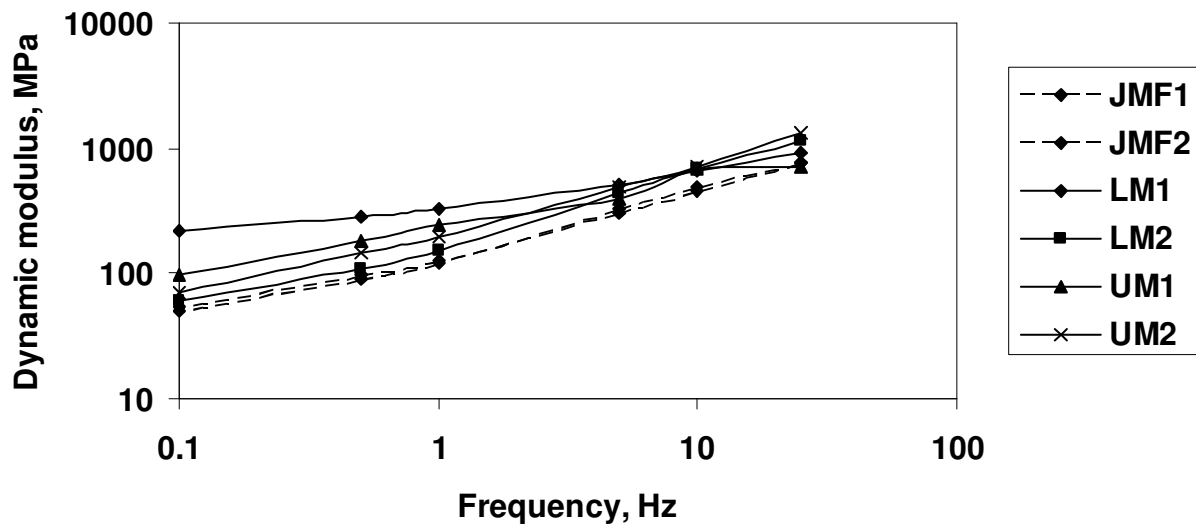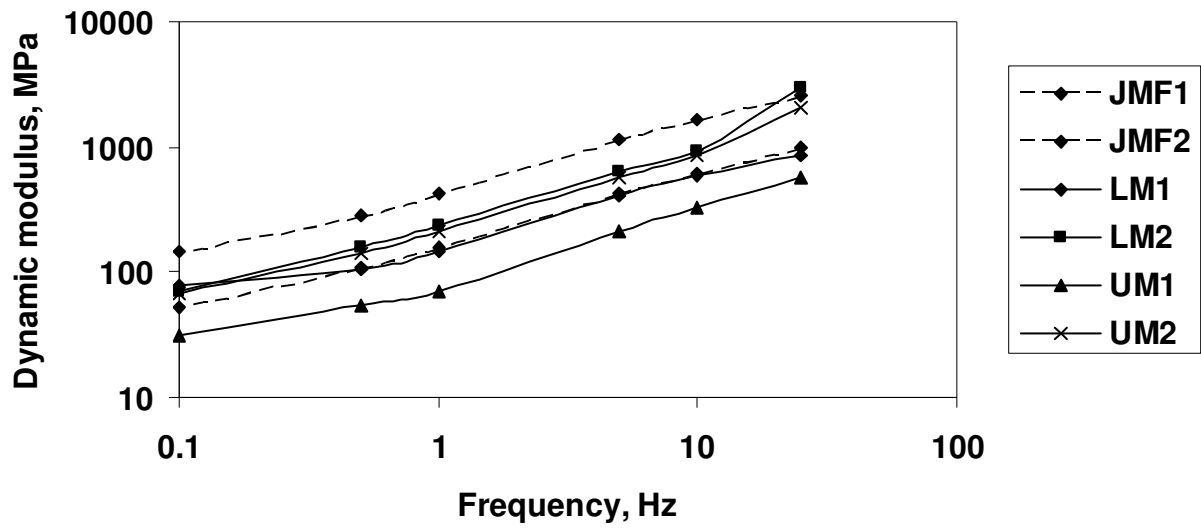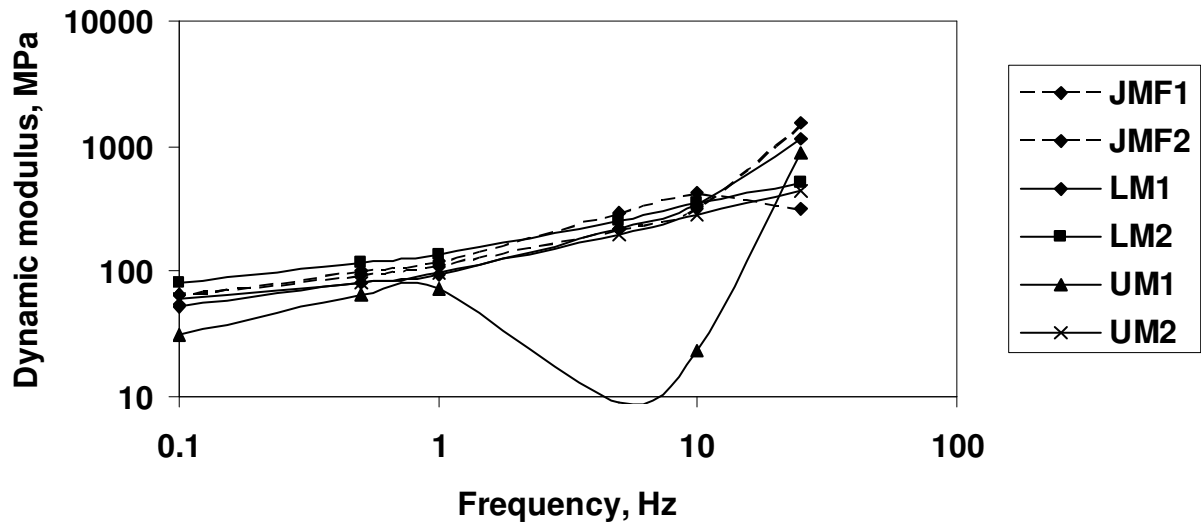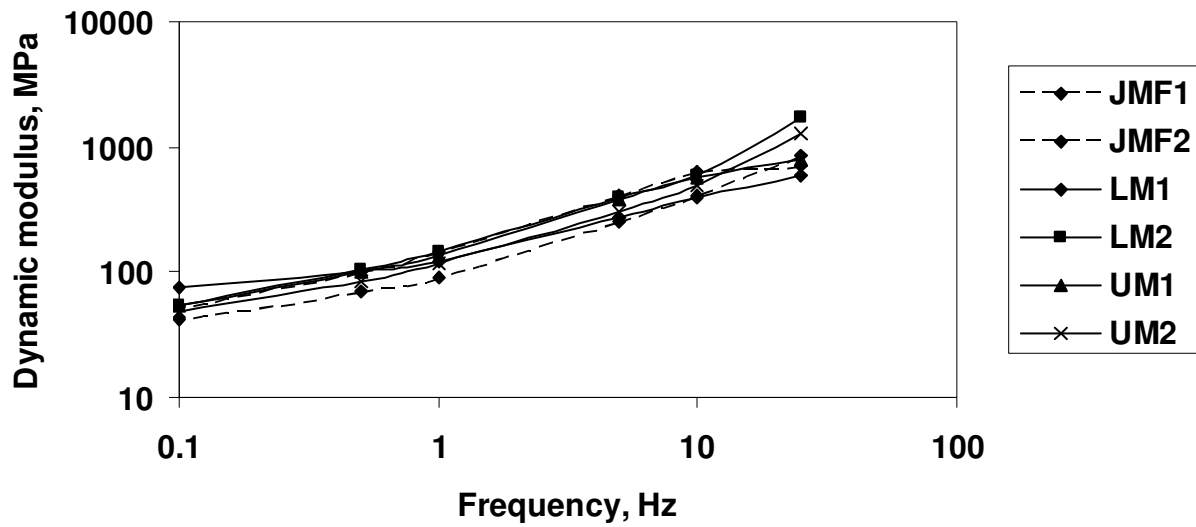
(e) 5627
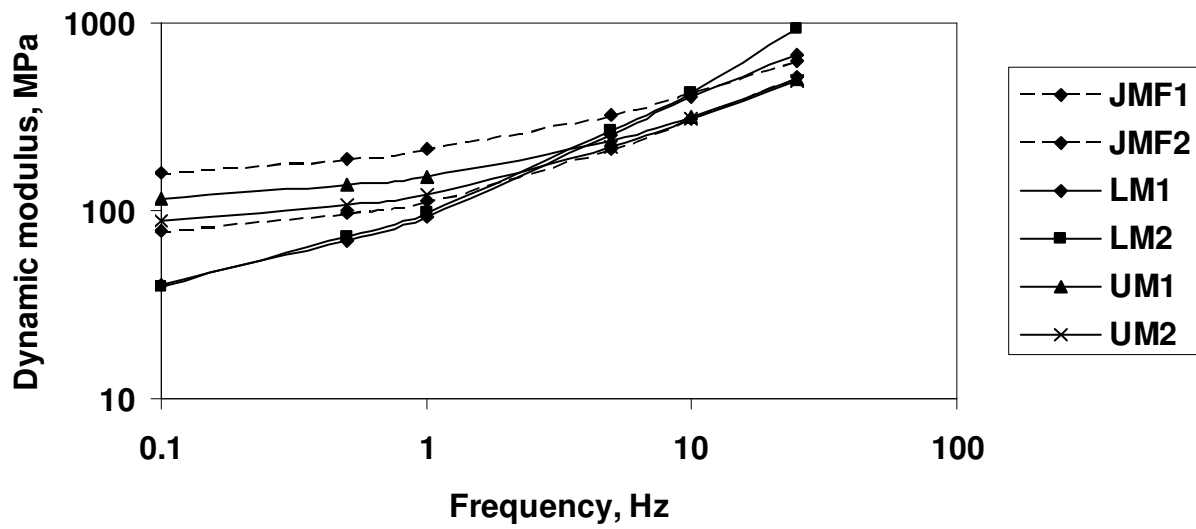
(f) 5364
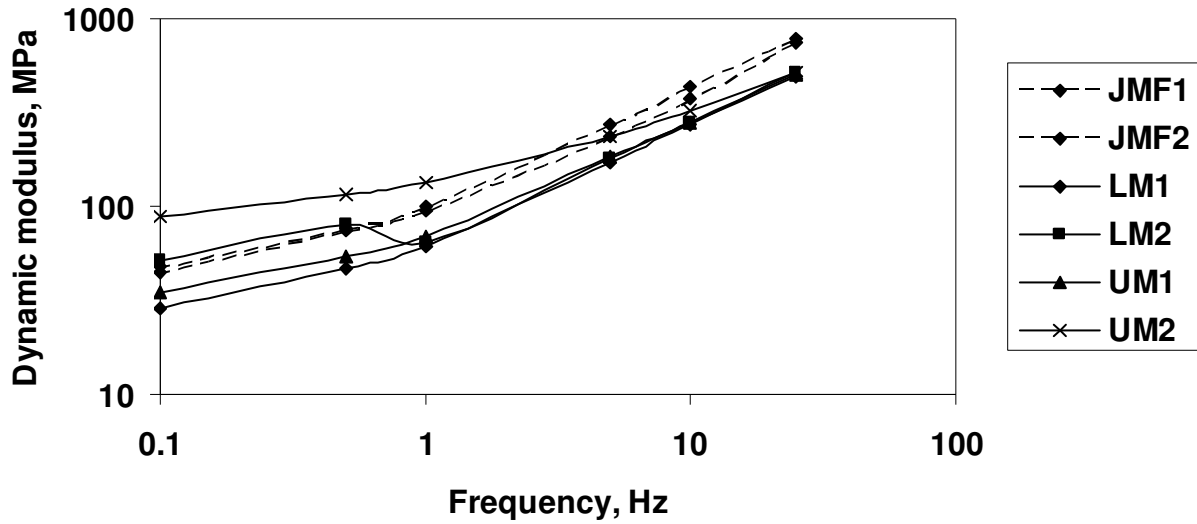
(g) 5408

Figure 4.8: Dynamic modulus curves of JMF, LM and UM mixes at 54.4 °C

Figure 4.9: Dynamic modulus trend of the JMF mixes

CHAPTER FIVE

MEPDG ANALYSIS

One of the objectives of this study was to evaluate the MEPDG, which was the next step in this study. This was done by predicting the performance of the mixes investigated in this study and comparing them with the measured (field) distresses. Performance of the mixes i.e. distresses were predicted using Design Guide (MEPDG software). A combination of site-specific data and default data in the software were used as inputs to the Design Guide. Details of the evaluation of the MEPDG are presented in this chapter.

5.1 Distress Prediction Mechanism in the MEPDG

The mechanistic models in the MEPDG divide the design life in to shorter analysis periods or increments beginning with the traffic-opening month. All factors – traffic level, asphalt concrete modulus, base-, subbase-, and subgrade modulus – that affect pavement responses and distresses remain constant within each increment. For each increment, critical stresses and strains are determined for all distress types and converted in to incremental distresses. The incremental distress could be either in absolute terms or in terms of a 'damage index', which is a mechanistic parameter representing the load-associated damage within the pavement structure. Cracking distresses (longitudinal cracking, alligator cracking, and thermal cracking) are predicted in terms of damage index, smaller the index (e.g., 0.0001) less significant will be the cracking and vice-versa. At the end of the analysis, damage is summed – calibrated models relate the cumulative damage to observable distresses. Rutting is predicted in absolute

terms allowing direct accumulation of the computed incremental distress for the entire design life.

5.2 Analysis

The objectives of the MEPDG analysis are to predict the performance of the mixes investigated in this study, to perform a simple evaluation of the distress prediction accuracy and to investigate the ability of dynamic modulus to correlate with distresses; however, calibrating the MEPDG prediction models is not in the scope of this study.

Design Guide Version 1.000 was used for predicting distresses. It gives the user the option to choose either the NCHRP 1-37A viscosity based model or the NCHRP 1-40D G* based model. The viscosity-based model was opted because the G* based model is yet to be calibrated nationally. Taking into consideration the fact that the pavement sections constructed using the selected mixes are overlays, AC over AC type of rehabilitation design was opted in all cases.

The MEPDG analysis was divided into two parts: Level 1 Analysis and Level 3 Analysis. In Level 1 Analysis, E*, G* and δ were used as Level 1 material inputs. In Level 3 Analysis, aggregate gradation and asphalt PG grade were used as Level 3 material inputs. All other inputs – traffic, climatic and materials – were a combination of site-specific data and default values in the software, which remained constant in both levels of analysis. The design life for all cases was taken as 20 years. The following distresses were predicted:

- Longitudinal cracking
- Alligator cracking
- Rutting

73

▪ International Roughness Index (IRI)

5.2.1 Inputs

Traffic data for the analyses were a combination of site-specific data, and default data in the Design Guide; Table 5.1 summarizes the site-specific traffic data. Inputs to the Enhanced Integrated Climatic Model (EICM) were the climatic files incorporated in the Design Guide – climatic data either from the nearest weather station or from a combination of weather stations proximate to the location of the pavement section; Table 5.2 lists the weather station locations. In all cases, the water table was assumed 15m below ground level. Table 5.3 summarizes the details of the pavement structural layers used in the analysis. A cement-stabilized base layer replaced the PCC layer in projects 5295, 5192 and 5364 because of insufficient data. For all unbound layers – granular bases, cement stabilized bases, and subgrade (appropriate to the AASHTO soil type used in the field) – default material properties in the Design Guide were used and were assumed 'compacted'. The existing asphalt layer (the layer below the overlay) in all cases was Class-A Type Asphalt Concrete; the properties are summarized in Table 5.4.

5.3 Field Performance Data

The performance of the pavement sections constructed using the mixes investigated in this study were obtained from recent distress data collection performed by WSDOT. Table 5.5 presents the month and year distress measurements were made on the pavement sections, and average distress values.

Typically, distress data is collected using a Pavement Condition Van (PCV), which is operated by a two-person team driving at the posted speed limit. The PCV is equipped with

cameras that capture different sections of the surface of the pavement that are used for quantifying surface distresses (cracking, patching, etc.); images are captured each 25 feet. To measure roadway profile, rutting/wear, and faulting laser sensors are mounted on the front and rear of the PCV. The data recorded by these sensors are processed using computer programs to determine roughness, faulting, and maximum wheel path wear depth. The digital images are analyzed using specially developed computer program and viewed one by one for a variety of distresses (cracking, patching, spalling, etc.), which is called as pavement distress rating, usually done in 0.10 miles increments. After completing the pavement distress rating for a pavement section, the length and type of distress are summed. The data presented in Table 5.5 were collected in this manner. More information on distress data collection is given in *Appendix 4*.

5.4 Results

The output generated by the Design Guide is a comprehensive file that contains, along with other important information, predicted incremental distress values for all distress types on a monthly basis over the entire design life. The condition of a pavement at any point during the design life is read from the output file by looking at the appropriate month and year. Table 5.6 presents the predicted performance of the mixes investigated in this study, extracted from the output file, corresponding to the month and year of distress data collection. For instance, the pavement section constructed using mix#5381 was opened to traffic in August 1998; the recent distress data collection was made in September 2006. Thereby, the predicted distress values for Mix #5381, presented in Table 5.6, correspond to September 2006 in the output file.

The type of distress data (incremental or extracted) used in the analysis depended upon the objective. For comparing the performance of the mixes, incremental distress data were used;

75

to investigate if dynamic modulus correlated with distresses, distress values at the end of the design life were used; and to evaluate the prediction accuracy of the Design Guide, data presented in Table 5.5, and Table 5.6 were used. In all cases, each distress type was analyzed separately and the inferences were validated statistically. Following are the cases analyzed statistically for validating the inferences derived from distress data analysis:

1. "Comparison of the performance of the mixes" – the distresses of the seven JMF mixes were analyzed using Two-Way ANOVA with 'Project' and 'input level' as the treatment factors; input level implies Level 1 Analysis or Level 3 Analysis.

2. "Did variation in percent passing sieve #200 affect the performance of the mixes?" – The predicted distresses of JMF, LM and UM mixes were analyzed using a Two-Way ANOVA with 'mix' and 'input level' as the treatment factors; the distress data of the three mixes in each project were analyzed separately.

3. "How accurate is the MEPDG in predicting distress?" – To test if the predicted distresses differed from the measured distresses, and if Level 1 predictions are significantly different from Level 3 Analysis predictions a One-Way ANOVA was run with 'level' (Level 1, Level 3, and Field) as the treatment factor. For all pairwise comparisons, Tukey's method was employed assuming a significance level of 0.05.

In all three statistical analyses, the data presented in Table 5.5 (measured) and Table 5.6 (predicted) were used. The results of the MEPDG analysis are presented in the following sections – each distress type separately.

5.4.1 Predicted AC rutting

Rutting is a plastic/viscoelastic deformation that manifests in the form of surface depression in the wheel path in any or the entire pavement layers including the subgrade. The main causes are heavy loads associated with high temperatures and/or poor mix. Fig.5.1 (a) and (b) illustrate the incremental rut predictions of the seven JMF mixes from Level 1 and Level 3 Analyses. Rutting predicted by both levels is relatively small in magnitude as is the variation among the mixes; also, Level 3 predictions are larger than Level 1 predictions. In general, rutting agrees with dynamic modulus trend of the JMF mixes, i.e., rutting is higher for mixes with lower dynamic modulus. For the JMF mixes investigated, dynamic modulus has correlated reasonably well with rutting. This is consistent with the results of the study conducted by Mohammad et al. (2006), who reported that the predicted rut depths followed the same trend found in the dynamic modulus test results, particularly at high temperatures.

Fig. 5.2 (a) through (g) compares predicted rutting of JMF, LM and UM mixes with measured (field) rutting, wherein each project is handled separately. In most cases, Level 3 Analysis has over-predicted rutting, and Level 1 Analysis has under-predicted rutting. However, the variation between predicted and measured is not substantial. Fig.5.2 also shows that rutting is approximately the same in JMF, LM and UM mixes invariably in all projects.

Table 5.7 (a) and (b) summarizes p-values from Tukey's pairwise comparisons of rutting of JMF mixes from Level 1 and Level 3 analyses. In majority of the cases, in both levels, p-values are larger than the significance level 0.05; hence, rutting in JMF mixes does not vary significantly. Table 5.8 summarizes the p-values from pairwise comparisons of rutting of JMF, LM and UM mixes. In most projects, the p-values are larger than 0.05 indicating that the variation in rutting is insubstantial among the three mixes.

5.4.2 Predicted longitudinal or top-down cracking

Longitudinal cracking is a type of fatigue failure associated with high tire-pressures, wheel induced stresses, and severe aging of HMA layer near the surface. Fig.5.3 (a) and (b) illustrate the incremental longitudinal cracking predictions of JMF mixes from Level 1 and Level 3 analyses. In both levels, longitudinal cracking of the mixes is approximately the same up to about 100 months from the traffic-opening month. Beyond 100 months, there is noticeable difference among the mixes, which could be attributed to aging of the pavements, especially the top HMA layers. Level 1 and Level 3 predictions show reasonable agreement; however, the predictions do not agree with the dynamic modulus trend. It appears that dynamic modulus did not correlate well with the predicting longitudinal cracking.

Fig. 5.4 (a) through (g) compares Level 1 and Level 3 predictions of longitudinal cracking of JMF, LM and UM mixes with measured cracking. Except projects 5295 and 5192, in all other projects, the predicted cracking is significantly higher than measured cracking; Level 3 predictions are higher than Level 1 predictions. Fig.5.4 also shows that longitudinal cracking of JMF, LM and UM mixes do not show variation. Kim et al. (2006) studied the impact of 20 input parameters on the MEPDG flexible pavement performance models. They found that longitudinal cracking was sensitive to HMA layer thickness, nominal maximum aggregate size, and HMA volumetrics; and very sensitive to asphalt binder PG grade.

Table 5.9 (a) and (b) summarizes *p*-values from Tukey's pairwise comparisons of the predicted longitudinal cracking of the JMF mixes from Level 1 and Level 3 analyses. In most cases, *p*-values are larger than 0.05 indicating that longitudinal cracking of the JMF mixes show insignificant difference. Table 5.10 summarizes the *p*-values of the pairwise comparisons of longitudinal cracking of JMF, LM and UM mixes. The *p*-values in most of the projects are

significantly larger than 0.05. There appears to be a minor inconsistency between Level 1 and Level 3 predictions.

5.4.3 Predicted alligator or bottom-up cracking

Alligator cracking is a type of fatigue cracking that originates in the form of short longitudinal cracks along the wheel path and quickly spreads to form a chicken mesh/alligator pattern. These cracks propagate to the surface from the bottom of the HMA layer under repeated load applications. Alligator cracking is associated with heavy traffic volumes combined with high wheel loads and tire pressures that result in high tensile strains at the bottom of the layer. Fig.5.5 (a) and (b) illustrate incremental alligator cracking predictions from Level 1 and Level 3 Analyses. The magnitude of predicted alligator cracking is relatively small as is the difference between the mixes. Like longitudinal cracking, alligator cracking of the JMF mixes do not vary up to about 100 months after traffic-opening month although it is not as prominent as in the former. The predictions of alligator cracking do not agree with the dynamic modulus trend; thus, dynamic modulus did not correlate with alligator cracking efficiently.

Fig.5.6 (a) through (g) compares Level 1 and Level 3 predictions of alligator cracking of JMF, LM and UM mixes with the measured cracking. Except in projects 5192 and 5627 predicted and measured cracking agree well. Fig.5.6 also shows that alligator cracking of JMF, LM and UM mixes does not show variation. Yang et al. (2004) in a comparative study used three different pavement sections to compare measured and predicted alligator cracking. They found that after 500,000 passes the measured alligator cracking was less than the predicted cracking in all cases. However, they concluded that the difference was not significant because of the extremely low magnitudes of cracking encountered. Taking in to consideration the fact that

79

predicted cracking is almost negligible, they felt that alligator cracking might not be a critical distress in flexible pavement design. In another study, Kim et al. (2006) concluded that alligator cracking does not seem to be a critical distress in flexible pavement structures with relatively thick HMA layers although a generalization for all cases is not plausible.

Table 5.11 (a) summarizes p-values from Tukey's pairwise comparisons of the predicted alligator cracking of the JMF mixes from Level 1 analyses – most *p*-values are larger than 0.05. Table 5.11 (b) summarizes *p*-values from Level 3 analyses. In some cases, the *p*-values are smaller than 0.05 indicating inconsistency between the two levels. However, taking in to consideration the very small magnitude of predicted cracking the inconsistency between the levels is ignored. Table 5.12 summarizes p-values from Tukey's pairwise comparisons of JMF, LM and UM mixes. In all the projects, Level 1 and Level 3 p-values are larger than 0.05 indicating that the difference between the mixes is insignificant.

5.4.4 Predicted international roughness index (IRI)

International Roughness Index (IRI), unlike the other distress types, is a functional distress parameter that depends upon rutting, bottom-up/top-down fatigue cracking, and thermal cracking, and other factors such as initial IRI, site factors, subgrade and climatic factors. IRI of a pavement is determined by first computing the initial IRI, which depends upon the as-constructed profile of the pavement and later upon the subsequent development of distresses over time. Smaller the IRI smoother is the pavement. The IRI model estimates/predicts smoothness (IRI) incrementally using distresses over time for the entire design period.

Initial IRI is highly dependent on the project smoothness specifications and has a significant impact on the long-term ride quality of the pavement. Typical values range from 50 to

100 in/mi. The initial IRI in the analysis was assumed 63 in /mi simulating field conditions. Fig.5.7 (a) and (b) illustrate the predicted IRI for the seven JMF mixes over the entire design life. In both Level 1 and Level 3 predictions, the JMF mixes show variation. The predicted IRI agree reasonably well with the dynamic modulus trend of the JMF mixes indicating that dynamic modulus correlated reasonably well with IRI.

Fig. 5.8 (a) through (g) compares IRI of JMF, LM and UM mixes from Level 1 and Level 3 predictions of each project with measured IRI. Except projects 5295 and 5192, predicted IRI is larger than measured IRI; however, the difference between Level 1 and Level 3 predictions appears to be insignificant. In addition, IRI of JMF, LM and UM mixes is almost the same in all the projects. Kim et al. (2006) reported that IRI was not sensitive to most input parameters they studied and attributed this to the nature of the IRI model in the MEPDG.

Table 5.13 (a) summarizes p-values from Tukey's pairwise comparisons of IRI of the JMF mixes from Level 1 analyses; Table 5.13 (b) summarizes similar p-values from Level 3 analyses. In both levels, majority of the p-values are smaller than 0.05 indicating that the JMF mixes exhibit significant difference in IRI. Table 5.14 summarizes p-values from Tukey's pairwise comparisons of JMF, LM and UM mixes of each project. Majority of the p-values in both levels are larger than 0.05 indicating the difference is insubstantial.

5.4.5 Level 1 versus Level 3 predictions

Table 5.15 summarizes p-values from Tukey's pairwise comparisons of Level 1 and Level 3 predictions. Essentially, the p-values in the table are an overall indication whether Level 1 and Level 3 predictions differ significantly. The table presents p-values for all projects and all

distress types. *P*-values of all distress types in most projects are larger than 0.05 indicating that Level 1 and Level 3 predictions agree reasonably well.

5.4.6 Predicted versus measured (field) distresses

Table 5.16 summarizes *p*-values from Tukey's pairwise comparisons of predicted distresses versus measured (field) distresses. The table presents all possible pairwise comparisons between Level 1, Level 3, and measured distresses. Except IRI, in all other distress types the p-values in most projects are larger than the significance level 0.05 indicating that the predicted and measured distresses do not differ significantly. It appears that the Design Guide (MEPDG software) predicted – rutting comparatively well, longitudinal cracking and alligator cracking reasonably well. Predicted IRI is significantly different from measured (field) IRI.

5.5 Summary

Predicted rutting varies significantly in the JMF mixes although it is relatively small in most mixes. Longitudinal and alligator cracking of the JMF mixes is approximately same up to about 100 months from the traffic-opening month, beyond which there is reasonable difference. Predicted alligator cracking is insignificant in most JMF mixes. IRI of the JMF mixes exhibits significant difference. Rutting and IRI agree reasonably well with the dynamic modulus trend; but not longitudinal and alligator cracking – dynamic modulus correlated well with rutting and IRI. The variation in gradation among JMF, LM and UM mixes did not have significant effect on the predicted distresses. Level 1 and Level 3 predictions all distress types exhibit reasonable agreement. The Design Guide (MEPDG software) predicted rutting and alligator cracking

comparatively well; longitudinal cracking was predicted reasonably well; predicted IRI was significantly different from measured (field) IRI.

Table 5.1: Site-specific traffic input data

Project	5381	5295	5192	5373	5627	5364	5408
SR	512	99	99	82	17	14	240
Location	Tacoma	Seattle	Tacoma	Yakima	Moses lake	Vancouver	Richland
Construction year	1998	1995	1998	1998	1999	1999	1998
Design life (years)				20			
Initial two-way AADTT	3701	900	1409	2181	1067	3473	1301
Number of lanes in design direction	4	6	4	4	2	4	6
Percent of trucks in design direction (%)	50	50	50	50	50	50	50
Percent of trucks in design lane (%)	90	70	90	90	100	90	70
Operational speed (mph)	60	40	50	60	60	60	55
Growth function				Compound growth			
Growth rate (%)	1.8	1.5	4.4	3.3	2.3	3.0	2.6

Table 5.2: Weather station locations for creating climatic files for the EICM Model

Project	Station	Elevation (ft)	Latitude (°)	Longitude (°)	Location	Months Available data
5381	Tacoma, WA	296	47.16	122.35	Tacoma Narrows airport	86
5295	Seattle, WA	450	47.28	122.19	Seattle-Tacoma International Airport	113
5192	Tacoma, WA	296	47.16	122.35	Tacoma Narrows airport	86
5373	Yakima, WA	1075	46.34	120.32	Yakima Air Terminal	116
5627	Moses Lake, WA	1180	47.13	119.19	Grant County International Airport	104
5364	Vancouver, WA	21	45.37	122.4	Pearson Field Airport	114
5408	Pasco, WA	401	46.16	119.07	Tri-Cities Airport	97

Table 5.3: Layer details of pavement sections used as inputs to the MEPDG

Project	Layer	Material	Thickness (in)
5381	1	ACP CL 12.5 mm; PG 58-22 binder	1.8
	2	ACP CL B; AC-20	7.92
	3	Crushed stone granular base (compacted)	7.2
	4	Gravelly silty sand subgrade (compacted); A-2-4	Semi-infinite
5192	1	ACP CL 12.5 mm; PG 64-22 binder	1.8
	2	ACP CL B; AC-20	6
	3	Cement Stabilized (PCCP equivalent)	6.96
	4	Crushed stone granular base (compacted)	6
	5	Gravelly silty sand subgrade (compacted); A-2-4	Semi-infinite
5295	1	ACP CL 12.5 mm; PG 70-22 binder	1.8
		Grinding	-1.8
	2	ACP CL B; AC-20	2.16
	3	Cement stabilized base layer (PCCP equivalent)	9
	4	Crushed stone granular base (compacted)	6
	5	Gravelly silty sand subgrade (compacted); A-1-b	Semi-infinite
5373	1	ACP CL 19 mm; PG 70-28 binder	2.4
		Grinding	-1.44
	2	ACP CL A; AC-20	5.16
	4	Crushed stone granular base (compacted)	8.04
	5	Silt subgrade (compacted); A-4	Semi-infinite
5627	1	ACP CL 19 mm; PG 64-28 binder	3.6
	2	ACP CL B; AC-20	5.52
	3	Crushed stone granular base	7.44
	4	Gravelly silt subgrade	Semi-infinite
5364	1	ACP CL 12.5 mm; PG 58-22 binder	1.8
	2	ACP CL A; AC-20 binder	3
	3	Cement stabilized base layer (PCCP equivalent)	8.04
	4	Crushed stone granular base (compacted)	10.08
	5	Silty sand subgrade (compacted); A-2-4	Semi-infinite
5408	1	ACP CL 12.5 mm; PG 64-28 binder	2.4
		Grinding	-0.72
	2	ACP CL B; AC-20 binder	5.16
	3	Crushed stone granular base (compacted)	11.04
	4	Subgrade (compacted); A-2-4	Semi-infinite

Table 5.4: Material properties of existing asphalt concrete layer

Cumulative % retained 3/4" sieve	0
Cumulative % retained 3/8" sieve	15
Cumulative retained #4 sieve	20
% passing #200 sieve	3
Air voids, %	4
Total unit weight, pcf	145
Poisson's ratio	0.35
Thermal conductivity, BTU/hr-ft-F°	0.67[1]
Heat capacity, BTU/lb-F°	0.23[1]

[1] Default values in the software

Table 5.5: Field performance data (averaged)

Project	5381	5295	5192	5373	5627	5364	5408
Survey date	Sep 2006	Oct 2006	Oct 2006	Sep 2006	Sep 2006	Aug 2006	Oct 2006
IRI (in/mi)	48.4	102.3	86.0	56.5	63.1	71.8	63.3
AC rutting (in)	0.15	0.04	0.073	0.16	0.06	0.33	0.14
Alligator cracking (%)	0	10.4	30.5	0.04	50.5	0	0.23
Longitudinal cracking (ft/mi)	0.62	54.5	16.4	11.3	0.92	0.79	1.7

Table 5.6: Predicted distress (a) Level 1

Mix		IRI (in/mi)	AC Rutting (in)	Longitudinal Cracking (ft/mi)	Alligator Cracking (%)
5381	JMF1	79.8	0.097	2.49	0.0208
	JMF2	75.6	0.035	0	0.0006
	LM1	81.2	0.102	1.71	0.0237
	LM2	81	0.097	1.38	0.0226
	UM1	81.4	0.105	2.22	0.024
	UM2	81.4	0.106	2.99	0.0229
5295	JMF1	77.6	0.085	11.8	0
	JMF2	77.5	0.084	5.62	0
	LM1	77.6	0.086	7.86	0
	LM2	77.5	0.086	10.2	0
	UM1	77.5	0.085	8.22	0
	UM2	77.4	0.085	5.08	0
5192	JMF1	75.7	0.039	25.2	0.0096
	JMF2	81.4	0.043	0.0074	0.0074
	LM1	82.1	0.06	0.0076	0.0076
	LM2	81.4	0.042	0.0085	0.0085
	UM1	81.6	0.048	0.0084	0.0084
	UM2	75.6	0.038	0.009	0.009
5373	JMF1	97.3	0.141	12.3	0.0032
	JMF2	97.9	0.145	30.3	0.0044
	LM1	98.2	0.154	32	0.0037
	LM2	97.8	0.148	17	0.0028
	UM1	98.5	0.153	40.3	0.0023
	UM2	98.7	0.163	38.8	0.0023
5627	JMF1	97.8	0.057	0.8	0.0141
	JMF2	97.8	0.3	0.71	0.0139
	LM1	98.7	0.075	2.84	0.0164
	LM2	97.6	0.055	0.2	0.0136
	UM1	97.7	0.056	0.28	0.0135
	UM2	97.5	0.055	0.21	0.0126
5364	JMF1	87.1	0.261	14.7	0
	JMF2	87.1	0.258	17.4	0
	LM1	86.7	0.25	24.3	0
	LM2	86.6	0.249	23.6	0
	UM1	87.2	0.26	23.7	0
	UM2	87.1	0.26	15.5	0
5408	JMF1	101.8	0.166	27.7	0.0063
	JMF2	102.1	0.173	27.7	0.0054
	LM1	102.9	0.191	49.7	0.0043
	LM2	102.8	0.188	43.8	0.0044
	UM1	102.8	0.19	26.5	0.004
	UM2	102.4	0.18	33.4	0.0053

(b) Level 3

Mix		IRI (in/mi)	AC Rutting (in)	Longitudinal Cracking (ft/mi)	Alligator Cracking (%)
5381	JMF1	84.6	0.175	21	0.0324
	JMF2	84.1	0.163	8.57	0.0314
	LM1	84.6	0.176	12.5	0.0326
	LM2	84.6	0.176	13.7	0.0327
	UM1	84.1	0.163	12.3	0.0313
	UM2	84.3	0.169	18	0.0318
5295	JMF1	78	0.095	11.3	0
	JMF2	77.9	0.094	6.08	0
	LM1	78.1	0.096	8.46	0
	LM2	78.1	0.097	12.6	0
	UM1	77.9	0.094	8.17	0
	UM2	77.9	0.093	6.23	0
5192	JMF1	83.2	0.087	29	0.0055
	JMF2	83.1	0.086	25.3	0.0052
	LM1	83.3	0.091	38.6	0.0061
	LM2	83.3	0.091	38.6	0.0061
	UM1	83.1	0.085	32.5	0.0063
	UM2	83	0.083	24.1	0.0053
5373	JMF1	105.6	0.185	46.1	0.0003
	JMF2	106.1	0.194	109	0.0002
	LM1	106.5	0.201	118	0.0001
	LM2	106.1	0.195	60.6	0.0002
	UM1	105.9	0.189	93.9	0.0003
	UM2	105.8	0.189	87.5	0.0003
5627	JMF1	101.7	0.142	6.79	0.0201
	JMF2	101.7	0.141	6.33	0.02
	LM1	102.8	0.167	17.7	0.0218
	LM2	102.9	0.168	16.1	0.022
	UM1	100.9	0.125	2.21	0.0188
	UM2	100.8	0.123	1.88	0.0187
5364	JMF1	82.9	0.19	11.3	0.0018
	JMF2	88.6	0.296	14.7	0
	LM1	89.2	0.309	26.4	0
	LM2	89.2	0.309	26.4	0
	UM1	88.6	0.294	18.8	0
	UM2	88.4	0.291	13.1	0
5408	JMF1	106.1	0.262	82	0.0001
	JMF2	106	0.261	76.8	0.0001
	LM1	107.2	0.287	131	0.0001
	LM2	107.1	0.286	123	0.0001
	UM1	105.8	0.255	67.7	0.0002
	UM2	105.9	0.258	82.1	0.0002

Table 5.7: *P*-values from pairwise comparisons of predicted rutting of the JMF mixes

(a) Level 1

Project	5381	5295	5192	5373	5627	5364	5408
5381	-	0.9984	0.9999	0.1114	1.0000	**<.0001**	0.0976
5295	0.9984	-	0.8898	0.4488	0.9685	**0.0002**	0.4072
5192	0.9999	0.8898	-	**0.0335**	1.0000	**<.0001**	**0.0291**
5373	0.1114	0.4488	0.0335	-	0.0559	**0.0126**	1.0000
5627	1.0000	0.9685	1.0000	0.0559	-	**<.0001**	0.0487
5364	<.0001	0.0002	<.0001	0.0126	<.0001	-	**0.0145**
5408	0.0976	0.4072	0.0291	1.0000	0.0487	0.0145	-

(b) Level 3

Project	5381	5295	5192	5373	5627	5364	5408
5381	-	0.3208	0.2736	0.9993	0.9973	0.0905	0.0958
5295	0.3208	-	1.0000	0.0823	0.8580	**0.0008**	**0.0009**
5192	0.2736	1.0000	-	0.0679	0.8056	**0.0007**	**0.0007**
5373	0.9993	0.0823	0.0679	-	0.7885	0.3464	0.3624
5627	0.9973	0.8580	0.8056	0.7885	-	**0.0157**	**0.0167**
5364	0.0905	0.0008	0.0007	0.3464	0.0157	-	1.0000
5408	0.0958	0.0009	0.0007	0.3624	0.0167	1.0000	-

Note: p-values in bold are smaller than the significance level 0.05.

Table 5.8: *P*-values from pairwise comparisons of rutting of JMF, LM and UM mixes

Project	Mix	Level 1		Level 3	
		LM	UM	LM	UM
5381	JMF	0.5867	0.4878	0.9985	1.0000
	LM	-	0.9999	-	0.9917
5295	JMF	0.3573	0.9913	0.1064	0.604
	LM	-	0.6040	-	0.0002
5192	JMF	0.5370	0.9993	0.9431	0.9984
	LM	-	0.7006	-	0.8059
5373	JMF	0.7102	0.1569	0.442	0.9999
	LM	-	0.6753	-	0.3585
5627	JMF	0.8014	0.9882	**0.0056**	**0.0434**
	LM	-	0.5087	-	**0.0004**
5364	JMF	0.9998	1.0000	0.3977	0.6068
	LM	-	0.9998	-	0.9965
5408	JMF	**0.0173**	0.0675	**0.0024**	0.1681
	LM	-	0.7598	-	**0.0004**

Note: p-values in bold are smaller than the significance level 0.05.

Table 5.9: *P*-values from pairwise comparisons of predicted longitudinal cracking of JMF mixes

(a) Level 1

Project	5381	5295	5192	5373	5627	5364	5408
5381	-	0.9999	0.9925	0.9805	1.0000	0.8829	0.8946
5295	0.9999	-	1.0000	1.0000	0.9999	0.9981	0.9986
5192	0.9925	1.0000	-	1.0000	0.9909	1.0000	1.0000
5373	0.9805	1.0000	1.0000	-	0.9772	1.0000	1.0000
5627	1.0000	0.9999	0.9909	0.9772	-	0.8725	0.8847
5364	0.8829	0.9981	1.0000	1.0000	0.8725	-	1.0000
5408	0.8946	0.9986	1.0000	1.0000	0.8847	1.0000	-

(b) Level 3

Project	5381	5295	5192	5373	5627	5364	5408
5381	-	0.3544	1.0000	1.0000	0.9970	0.3544	1.0000
5295	0.3544	-	0.4212	0.6763	0.0726	1.0000	0.6573
5192	1.0000	0.4212	-	1.0000	0.9911	0.4212	1.0000
5373	1.0000	0.6763	1.0000	-	0.9078	0.6763	1.0000
5627	0.9970	0.0726	0.9911	0.9078	-	0.0726	0.9184
5364	0.3544	1.0000	0.4212	0.6763	0.0726	-	0.6573
5408	1.0000	0.6573	1.0000	1.0000	0.9184	0.6573	-

Table 5.10: *P*-values from pairwise comparisons of predicted longitudinal cracking of JMF, LM and UM mixes

Project	Mix	Level 1		Level 3	
		LM	UM	LM	UM
5381	JMF	1.0000	1.0000	0.9877	1.0000
	LM	-	1.0000	-	0.9759
5295	JMF	1.0000	0.9711	1.0000	0.9711
	LM	-	0.9521	-	0.9521
5192	JMF	0.9984	1.0000	0.6292	1.0000
	LM	-	0.9993	-	0.7171
5373	JMF	1.0000	0.9864	0.9959	0.9942
	LM	-	0.5657	-	0.1939
5627	JMF	0.9777	0.9922	**<.0001**	**0.0059**
	LM	-	0.8162	-	**<.0001**
5364	JMF	0.5370	0.9619	0.0662	0.6400
	LM	-	0.9025	-	0.4331
5408	JMF	0.1559	0.9999	**0.0018**	0.8556
	LM	-	0.2020	-	**0.0009**

Note: p-values in bold are smaller than the significance level 0.05.

Table 5.11: *P*-values from pairwise comparisons of predicted alligator cracking of JMF mixes

(a) Level 1

Project	5381	5295	5192	5373	5627	5364	5408
5381	-	0.3544	1.0000	1.0000	0.9970	0.3544	1.0000
5295	0.3544	-	0.4212	0.6763	0.0726	1.0000	0.6573
5192	1.0000	0.4212	-	1.0000	0.9911	0.4212	1.0000
5373	1.0000	0.6763	1.0000	-	0.9078	0.6763	1.0000
5627	0.9970	0.0726	0.9911	0.9078	-	0.0726	0.9184
5364	0.3544	1.0000	0.4212	0.6763	0.0726	-	0.6573
5408	1.0000	0.6573	1.0000	1.0000	0.9184	0.6573	-

(b) Level 3

Project	5381	5295	5192	5373	5627	5364	5408
5381	-	**<0.0001**	**0.0006**	**<0.0001**	0.3138	**<0.0001**	**<0.0001**
5295	<.0001	-	0.8920	1.0000	**0.0036**	1.0000	1.0000
5192	0.0006	0.8920	-	0.9184	0.0631	0.9700	0.9092
5373	<.0001	1.0000	0.9184	-	**0.0041**	1.0000	1.0000
5627	0.3138	0.0036	0.0631	0.0041	-	**0.0060**	**0.0039**
5364	<.0001	1.0000	0.9700	1.0000	0.0060	-	1.0000
5408	<.0001	1.0000	0.9092	1.0000	0.0039	1.0000	-

Note: p-values in bold are smaller than the significance level 0.05.

Table 5.12: *P*-values from pairwise comparisons of predicted alligator cracking of JMF, LM and UM mixes

Project	Mix	Level 1		Level 3	
		LM	UM	LM	UM
5381	JMF	0.6111	0.5955	1.0000	1.0000
	LM	-	1.0000	-	1.0000
5295	JMF	1.0000	1.0000	1.0000	1.0000
	LM	-	1.0000	-	1.0000
5192	JMF	0.9993	0.9966	0.8745	0.9876
	LM	-	0.9649	-	0.9951
5373	JMF	0.9479	0.1553	1.0000	1.0000
	LM	-	0.3901	-	0.9999
5627	JMF	0.8613	0.8137	0.3197	0.6395
	LM	-	0.3073	-	**0.0562**
5364	JMF	1.0000	1.0000	0.5594	0.5594
	LM	-	1.0000	-	1.0000
5408	JMF	0.1420	0.3084	1.0000	1.0000
	LM	-	0.9753	-	1.0000

Note: p-values in bold are smaller than the significance level 0.05.

Table 5.13: *P*-values from pairwise comparisons of predicted IRI of JMF mixes

(a) Level 1

Project	5381	5295	5192	5373	5627	5364	5408
5381	-	1.0000	0.9969	**<.0001**	**<.0001**	**0.0001**	**<.0001**
5295	1.0000	-	1.0000	**<.0001**	**<.0001**	**0.0003**	**<.0001**
5192	0.9969	1.0000	-	**<.0001**	**<.0001**	**0.0005**	**<.0001**
5373	<.0001	<.0001	<.0001	-	**0.0011**	**<.0001**	**0.0052**
5627	<.0001	<.0001	<.0001	0.0011	-	0.4263	0.9989
5364	0.0001	0.0003	0.0005	<.0001	0.4263	-	0.1099
5408	<.0001	<.0001	<.0001	0.0052	0.9989	0.1099	-

(b) Level 3

Project	5381	5295	5192	5373	5627	5364	5408
5381	-	0.2132	0.9326	**<0.0001**	**<0.0001**	0.2416	**<0.0001**
5295	0.2132	-	0.9383	**<0.0001**	**<0.0001**	**0.0014**	**<0.0001**
5192	0.9326	0.9383	-	**<0.0001**	**<0.0001**	**0.0188**	**<0.0001**
5373	<.0001	<.0001	<.0001	-	**0.0146**	**<.0001**	0.1442
5627	<.0001	<.0001	<.0001	0.0146	-	**0.0012**	0.9724
5364	0.2416	0.0014	0.0188	<.0001	0.0012	-	**0.0001**
5408	<.0001	<.0001	<.0001	0.1442	0.9724	0.0001	-

Note: p-values in bold are smaller than the significance level 0.05.

Table 5.14: *P*-values from pairwise comparisons of predicted IRI of JMF, LM and UM mixes

Project	Mix	Level 1		Level 3	
		LM	UM	LM	UM
5381	JMF	0.6014	0.5321	0.9998	1.0000
	LM	-	1.0000	-	0.9992
5295	JMF	1.0000	0.7209	0.7209	0.7209
	LM	-	0.7209	-	0.1777
5192	JMF	0.5249	0.9998	0.9328	0.9998
	LM	-	0.6543	-	0.8414
5373	JMF	0.8124	0.0971	0.3754	1.0000
	LM	-	0.3754	-	0.3195
5627	JMF	0.8544	0.9471	**0.0129**	**0.0701**
	LM	-	0.4459	-	**0.0008**
5364	JMF	0.9999	1.0000	0.4146	0.5947
	LM	-	0.9999	-	0.9983
5408	JMF	**0.0164**	**0.0866**	**0.0034**	0.1881
	LM	-	0.6157	-	**0.0005**

Note: p-values in bold are smaller than the significance level 0.05.

Table 5.15: *P*-values from pairwise comparisons of Level 1 versus Level 3 predictions of JMF

mixes

Project	Longitudinal cracking	Alligator cracking	Rutting	IRI
5381	0.9959	**0.0031**	**0.0416**	**0.0486**
5295	1.0000	1.0000	1.0000	1.0000
5192	0.9519	0.9992	0.8000	0.9656
5373	**0.0359**	0.7205	0.9508	0.9754
5627	1.0000	0.8596	0.1156	0.2895
5364	0.9992	1.0000	1.0000	0.9999
5408	**0.0484**	0.6857	**0.0408**	0.1542

Note: p-values in bold are smaller than the significance level 0.05.

Table 5.16: *P*-values from pairwise comparisons of predicted versus measured distresses of JMF

mixes

Project	Longitudinal Cracking		Alligator cracking		Rutting		IRI	
	Field vs. Level 1	Field vs. Level 3	Field vs. Level 1	Field vs. Level 3	Field vs. Level 1	Field vs. Level 3	Field vs. Level 1	Field vs. Level 3
5381	0.9919	0.1394	0.5185	0.0693	0.2776	0.8851	**0.0100**	**0.0056**
5295	**0.0125**	**0.0125**	0.1114	0.1114	**0.0119**	**0.007**	0.0833	0.0866
5192	0.9818	0.5411	**<.0001**	**<.0001**	**<.0001**	**<.0001**	0.3956	0.8355
5373	0.9318	0.1832	0.5185	0.5185	0.9306	0.7643	**<.0001**	**<.0001**
5627	0.6965	**0.0002**	**<.0001**	**<.0001**	0.5185	0.7202	**<.0001**	**<.0001**
5364	**0.0080**	**0.0152**	**<.0001**	**<.0001**	0.5201	0.405	**0.0146**	**0.0189**
5408	**0.0026**	**<.0001**	0.4072	0.3830	0.8437	0.2495	**0.0096**	**0.0072**

Note: p-values in bold are smaller than the significance level 0.05.
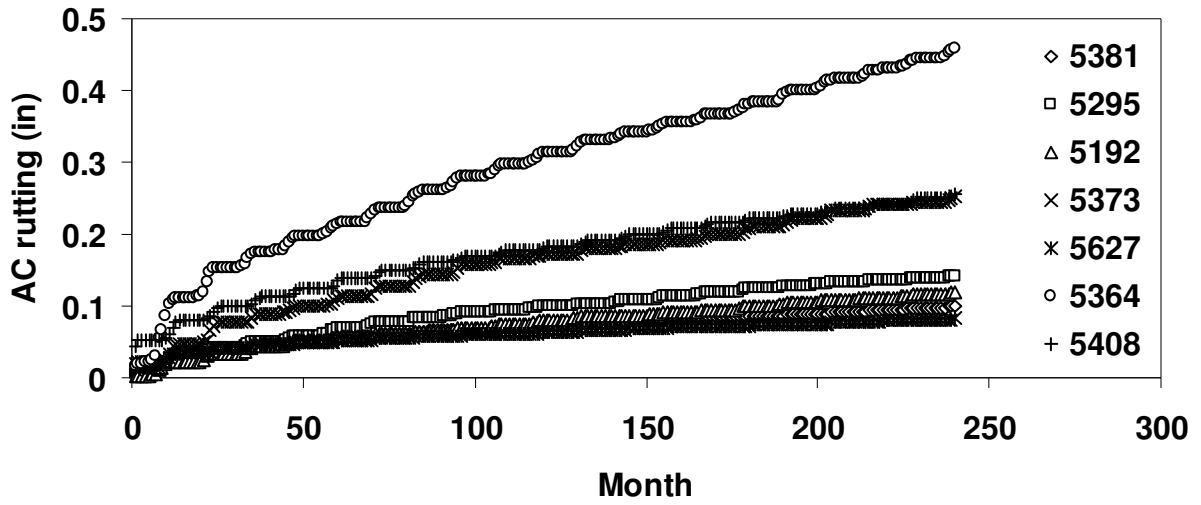
(a) Level 1
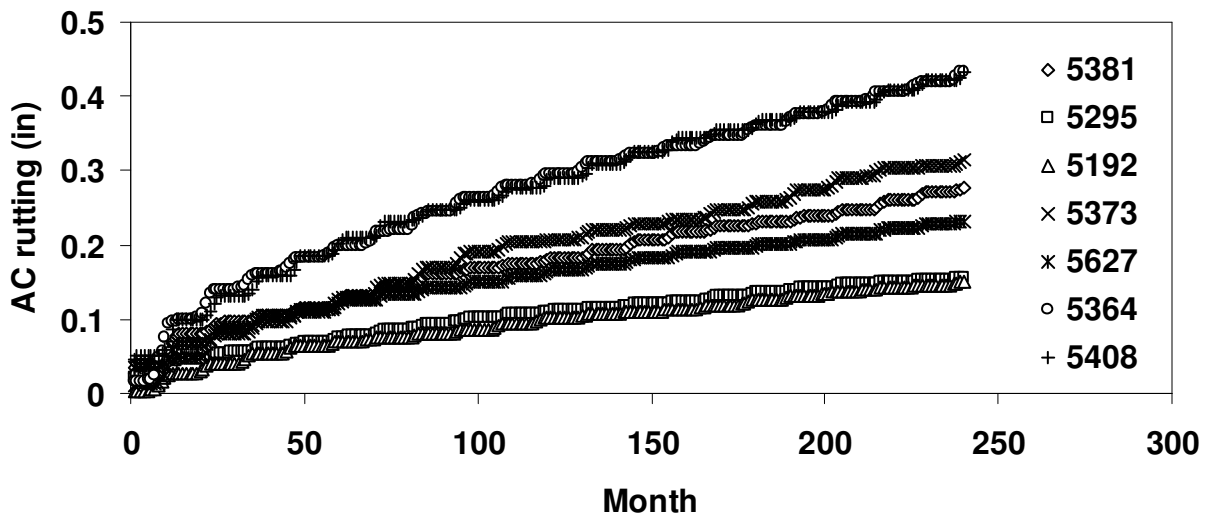
(b) Level 3

Figure 5.1: Predicted AC rutting over the design life
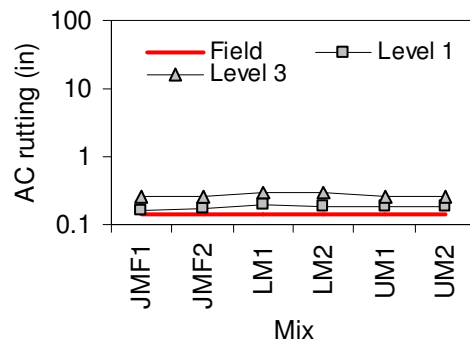
Figure 5.2: Predicted versus measured asphalt concrete (AC) rutting
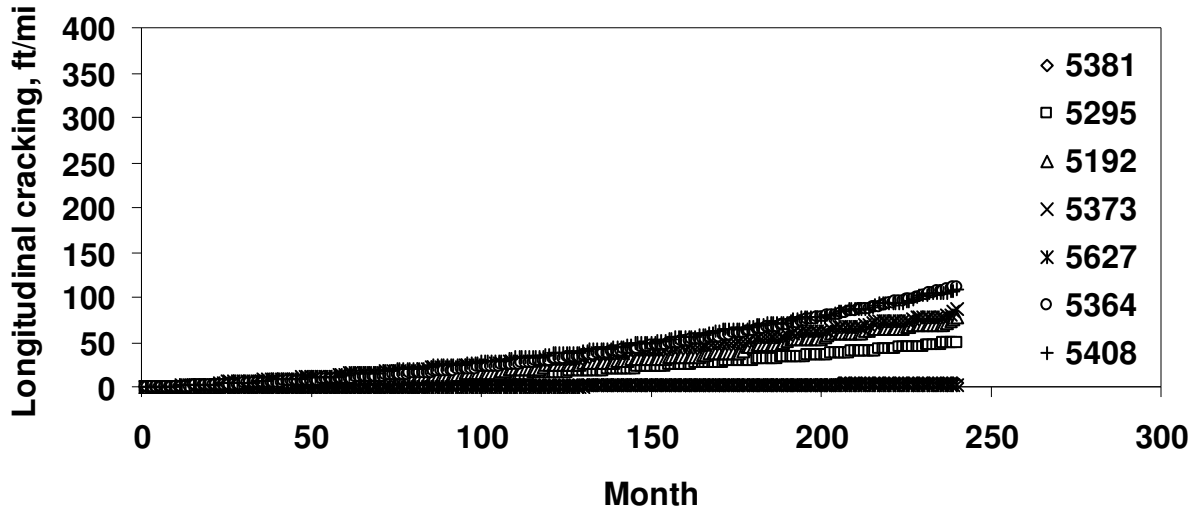
(a) Level 1
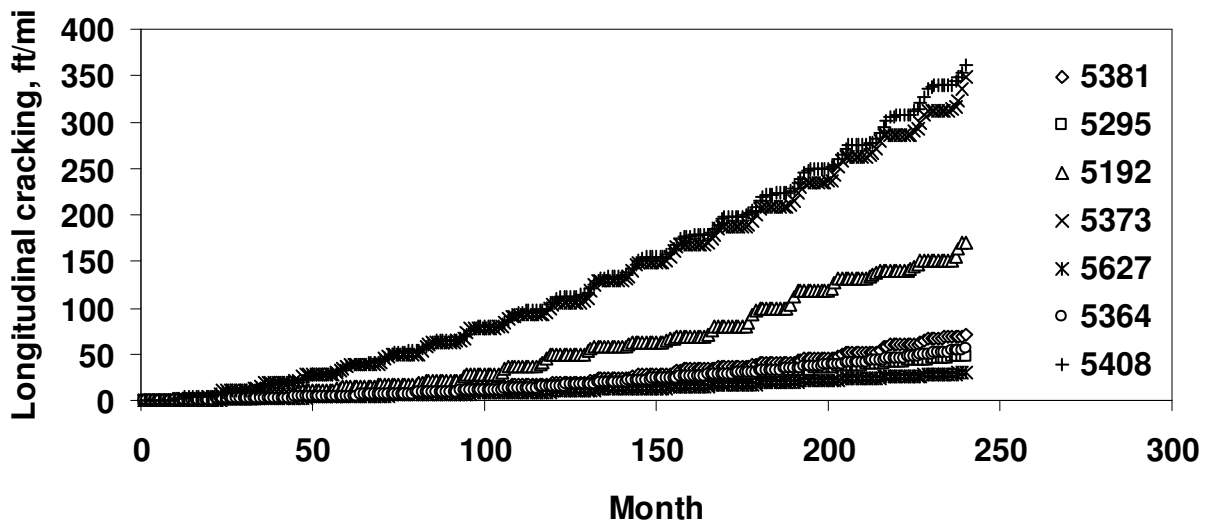
(a) Level 3

Figure 5.3: Predicted longitudinal cracking over the design life
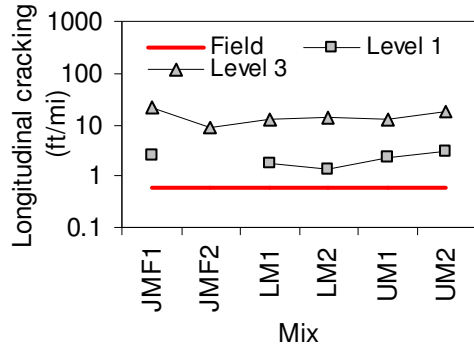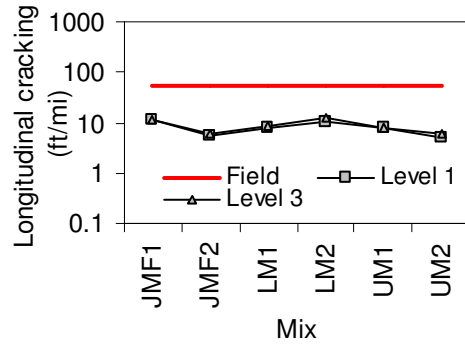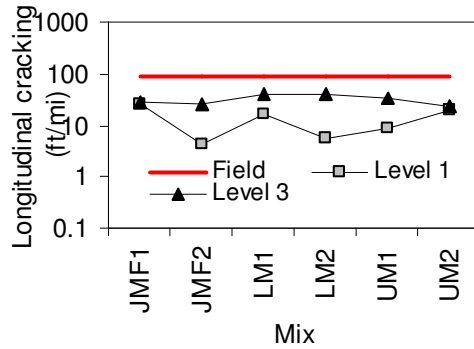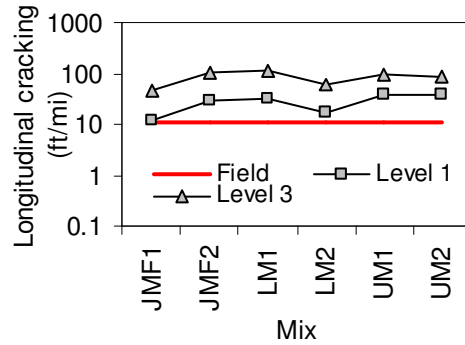
(a) 5381
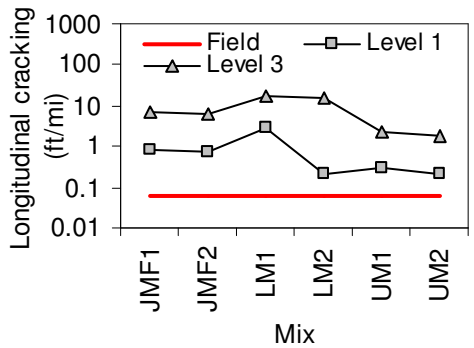
(b) 5295
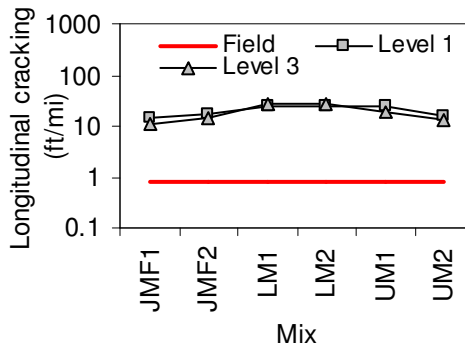
(c) 5192
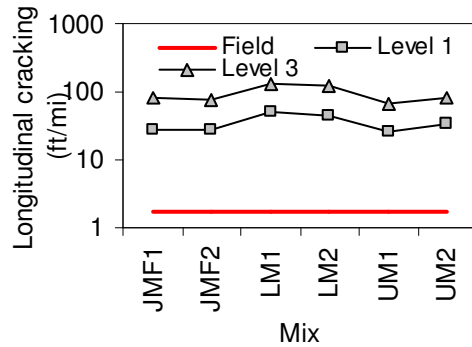
(d) 5373

(e) 5627

(f) 5364

(g) 5408

Figure 5.4: Predicted versus measured longitudinal cracking
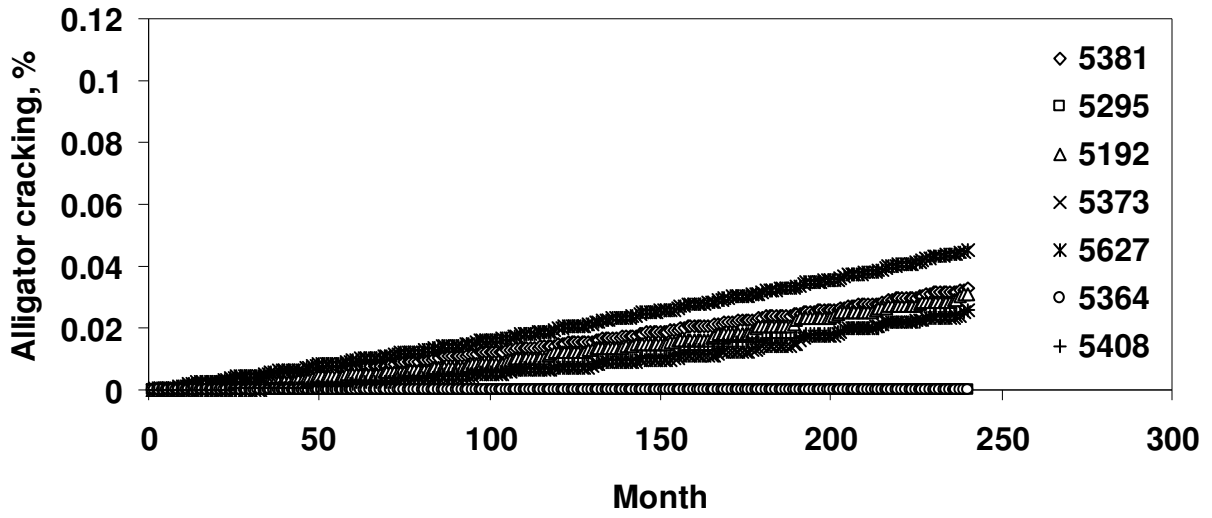
(a) Level 1
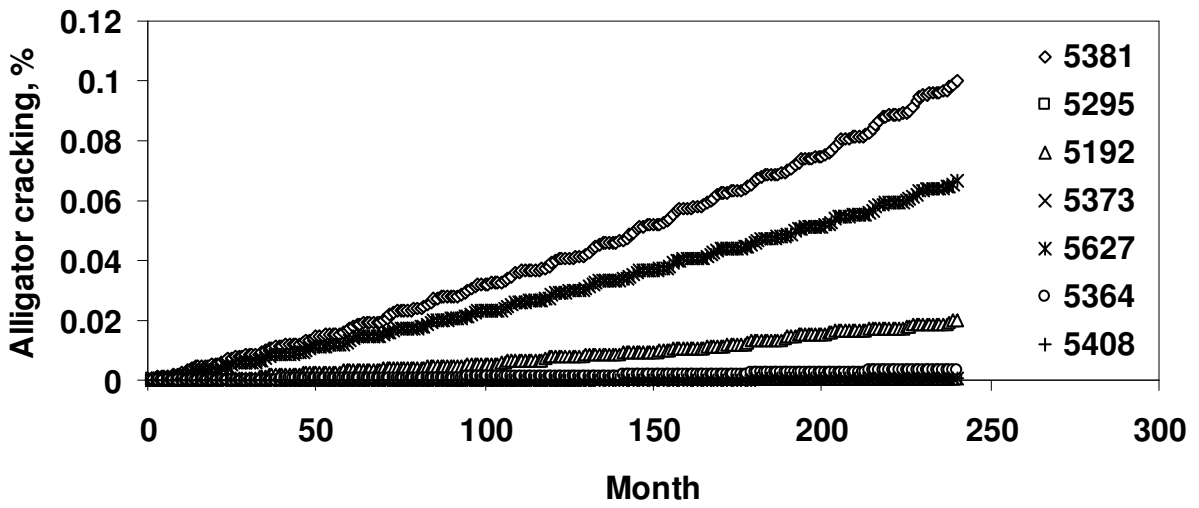
(b) Level 1

Figure 5.5: Predicted alligator cracking over the design life
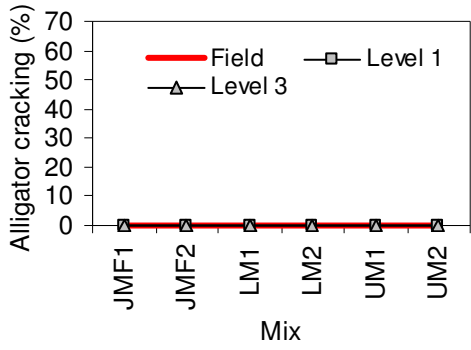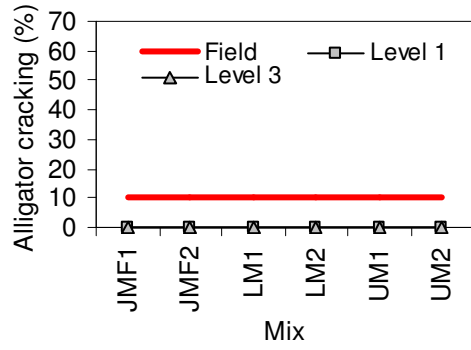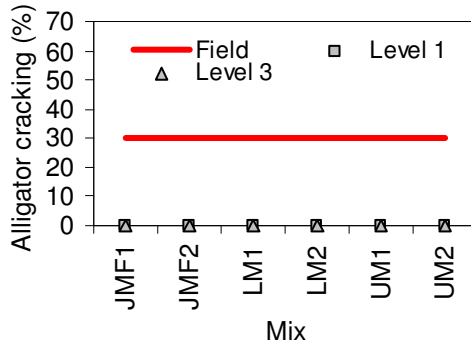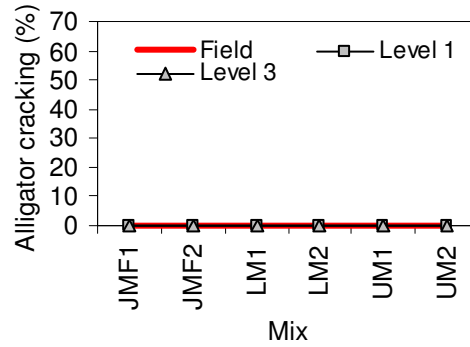
(a) 5381
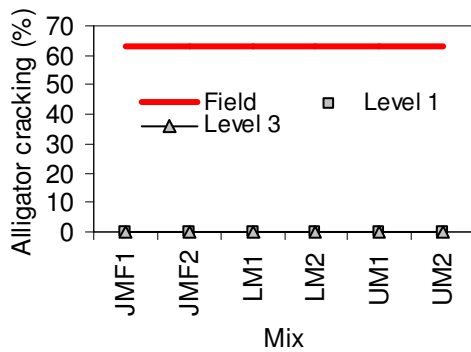
(b) 5295
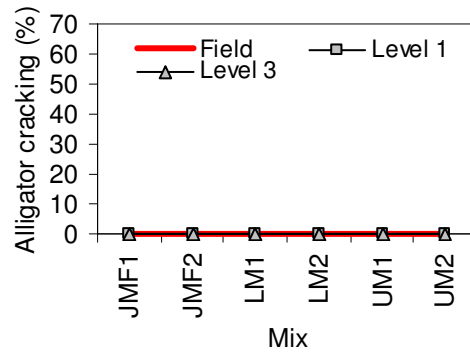
(c) 5192
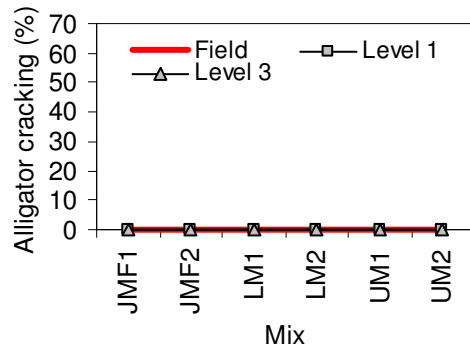
(d) 5373

(e) 5627

(f) 5364

(g) 5408

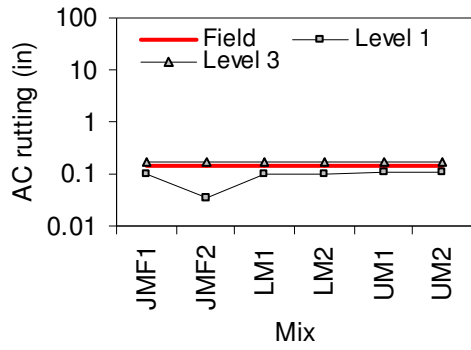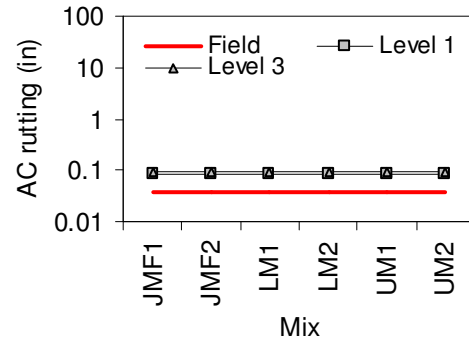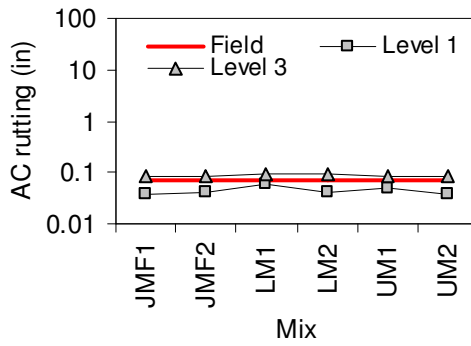**Figure 5.6:** Predicted versus measured alligator cracking
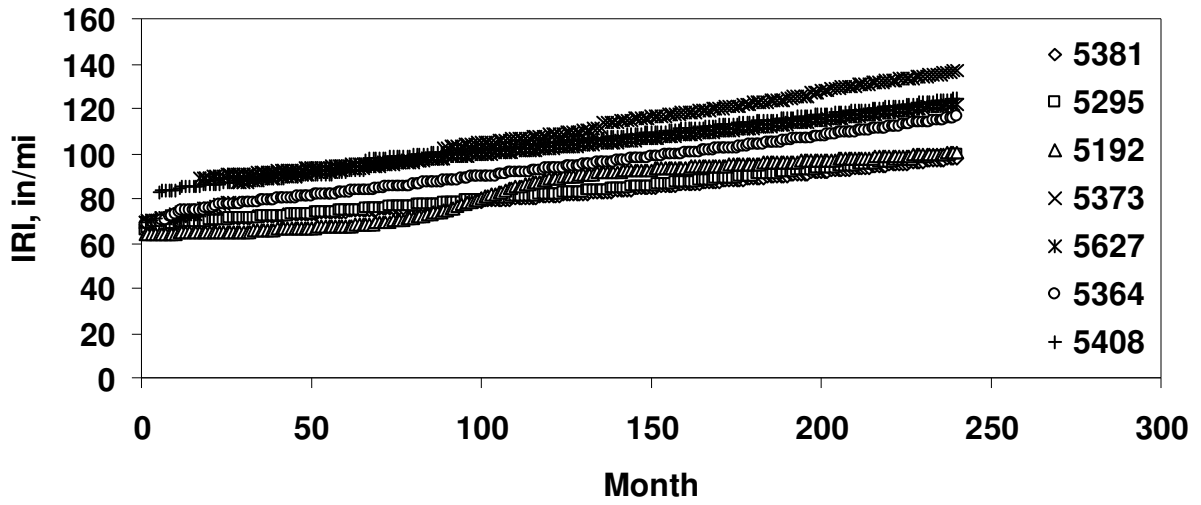
(a) Level 1
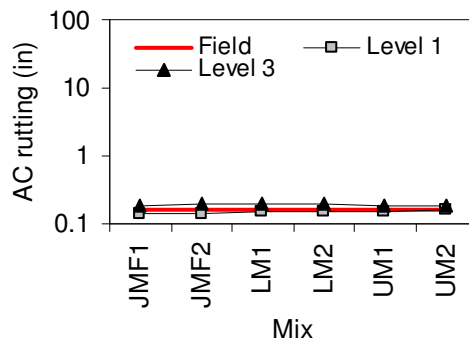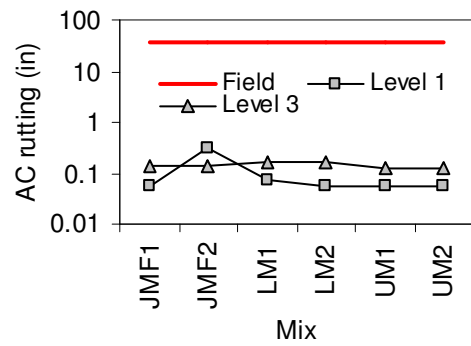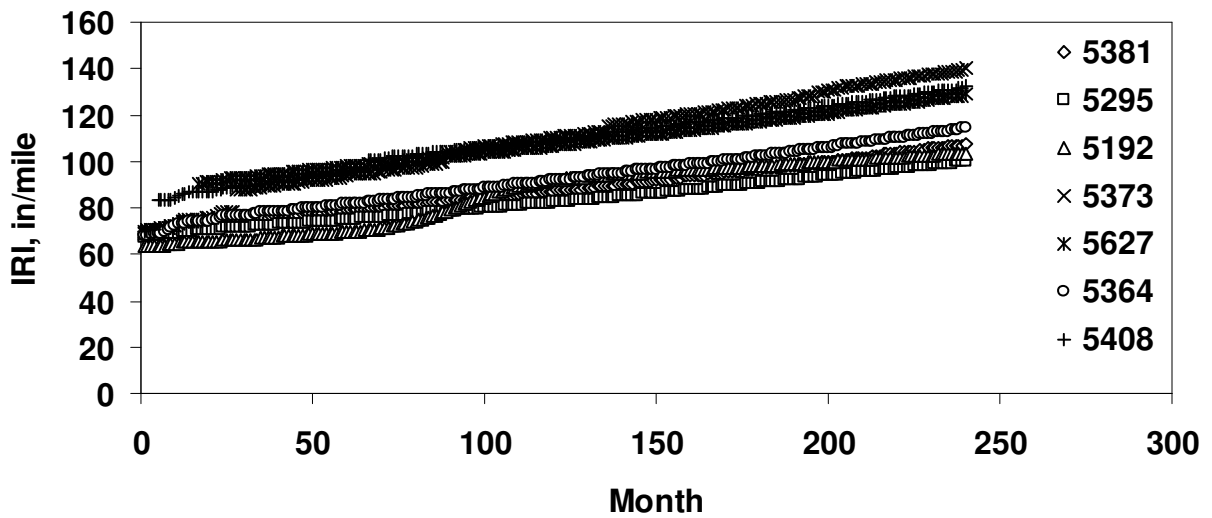

(b) Level 3

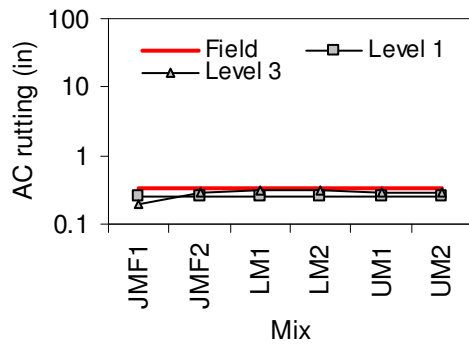**Figure 5.7:** Predicted IRI over the design life
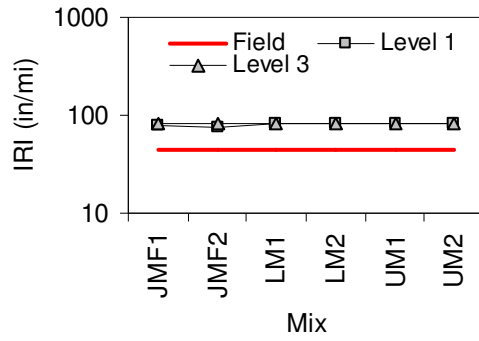
(a) 5381
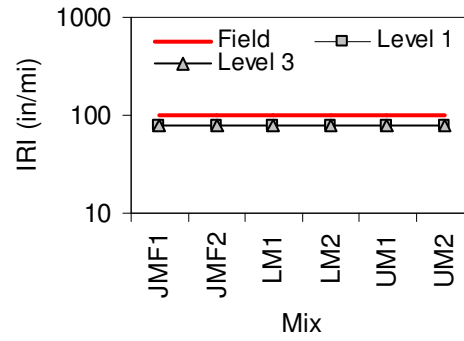
(b) 5295
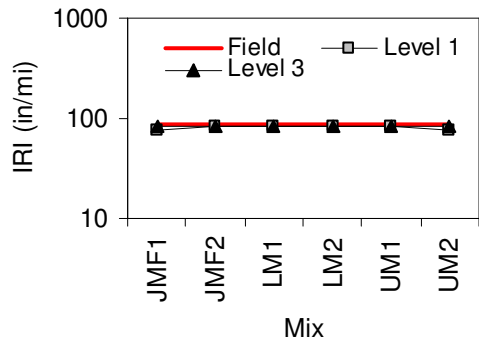
(c) 5192
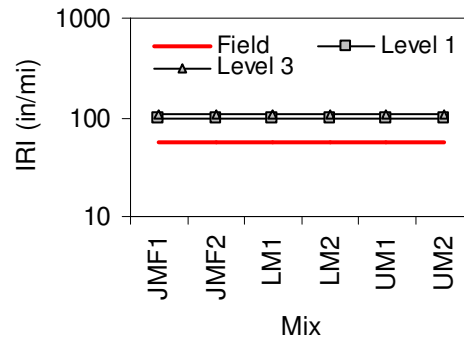
(d) 5373
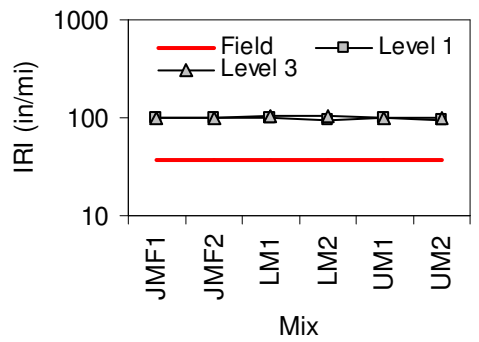
(e) 5627
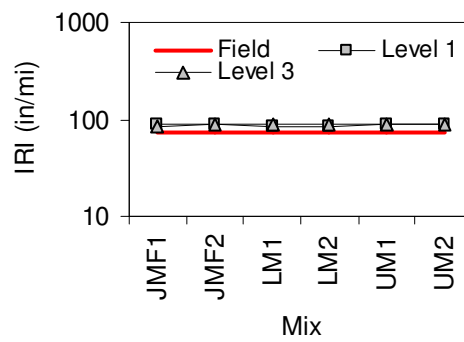
(f) 5364
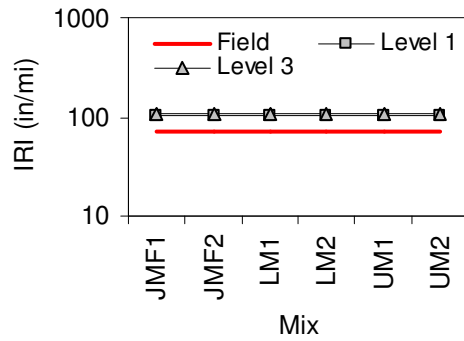
(g) 5408

Figure 5.8: Predicted versus measured IRI

CHAPTER SIX

CONCLUSIONS

6.1 Summary of the Study

Seven HMA mixes widely used in the State of Washington, designated as Job Mix Formula (JMF) mixes, were first selected for this study. Two additional mixes – lower modified mix (LM) and upper modified mix (UM) – were prepared from each JMF mix; percent-passing sieve #200 was decreased by 2% in the LM mix and increased by 2% in the UM mix. Dynamic modulus was measured and master curves were constructed for all the mixes. The performance of the mixes were predicted using Design Guide (MEPDG software) Version 1.000; longitudinal cracking, alligator cracking, rutting and IRI were the distresses predicted. The predicted distresses were compared with the measured distresses to evaluate the MEPDG. The conclusions derived from this study are summarized in the following sections.

6.2 Sensitivity of Dynamic Modulus

Dynamic modulus of the seven JMF mixes showed significant variation at 37.8 and 54.4 °C, but not at 21.1 and 4.4°C. Aggregate gradation and interlocking between particles appear to be the most influential parameters at high temperatures causing variation in dynamic modulus. At low temperatures, even though stiffness of asphalt binder governs dynamic modulus, air voids and interlocking between particles seem to suppress the variation in dynamic modulus caused by stiffness of asphalt binder. Dynamic modulus of JMF, LM and UM mixes do not vary and no definite trend was observed between them.

103

In the field, under a constant loading, the behavior of the mixes at low temperatures might be similar; however, there can be considerable difference at high temperatures. As dynamic modulus was not sensitive to the ±2% variation in the percent-passing sieve #200, during HMA operations, a similar variation might not affect dynamic modulus, or behavior of a mix under load.

6.3 Prediction Accuracy of MEPDG

The performance of the seven HMA mixes predicted by MEPDG varied depending upon the type of distress. Rutting was relatively small, as was the variation among the mixes. Longitudinal cracking and alligator cracking of the mixes showed little variation up to about 100 months from the traffic-opening month, beyond which there was considerable difference. However, the magnitude of both predicted and measured alligator cracking was negligible in most mixes that shows alligator cracking may not be a critical distress in flexible pavements. Unlike the other distress types, IRI of the mixes varied significantly. The predicted distresses of JMF, LM and UM mixes in all seven projects did not show significant variation; thus, varying percent-passing sieve #200 by ±2% did not affect performance of the mixes.

The MEPDG predicted rutting and alligator cracking reasonably well; predicted IRI varied significantly from measured IRI, and longitudinal cracking were inconsistent. One of the issues encountered while using the Design Guide was that the thermal cracking module did not work when inputs to this model were predicted using HMA layer properties; therefore, default values in the software were used as inputs to the model in all cases investigated. Thus, the variations in predicted and measured IRI could be the result of the malfunctioning of the thermal cracking model.

Level 1 and Level 3 predictions agree reasonably well although there is inconsistency in longitudinal and alligator cracking i.e. the levels either over-predicted or under-predicted these distresses. It indicates that aggregate gradation and asphalt binder PG grade (Level 3 inputs) predicted distresses as efficiently as E^*, G^* and δ (Level 1 inputs). However, the thickness of the HMA overlays in the pavement sections investigated in this study were comparatively thin, which could be another reason for the agreement between Level 1 and Level 3 predictions. This could be further investigated by analyzing a full depth pavement rather than an overlay.

Rutting and IRI of the JMF mixes followed the dynamic modulus trend i.e. higher modulus produced lower distress. On the other hand, longitudinal and alligator cracking did not follow the dynamic modulus trend. For the cases studied, dynamic modulus has correlated reasonably well with rutting and IRI, but not with longitudinal and alligator cracking.

BIBLIOGRAPHY

Ali, O. (2005). "Evaluation of the Mechanistic Empirical Pavement Design Guide (NCHRP 1-37A)." National Research Council Canada. Research Report 216.

Andrei, D., Witczak, M.W., and Mirza., M.W., (1999). "Development of a Revised Predictive Model for the Dynamic (Complex) Modulus of Asphalt Concrete Mixtures." NCHRP 1-37A Inter Team Report, University of Maryland, March 1999.

Carvalho, R. L. (2006). "Mechanistic-Empirical Design of Flexible Pavements: A Sensitivity Study" M. S. Thesis, University of Maryland.

Carvalho, R. L., Schwartz, C.W. (2007). "Evaluation of Mechanistic-Empirical Design Procedure." Implementation of the NCHRP 1-37A Design Guide, Final Report, Volume 2, Maryland State Highway Administration, February 2007.

Ceylan, H., Gopalakrishnan, K., and Coree, B. (2005). "A Strategic Plan for Implementing the Mechanistic-Empirical Pavement Design Guide in Iowa." Presented at the 84th Annual Meeting of the Transportation Research Board, Washington, D.C., 2005.

Christensen, D., Pellinen, T., and Bonaquist, R. (2003). "Hirsch Model for Estimating the Modulus of Asphalt Concrete." Proceedings of the Association of Asphalt Paving Technologists, 72, 2003, 97-121.

Dongré, R., Myers, L., D'Angelo, J., Paugh, C., and Gudimettla, J. (2005). "Field Evaluation of Witczak and Hirsch Models for Predicting Dynamic Modulus of Hot-Mix Asphalt." Journal of the Association of Asphalt Paving Technologists, 74, 381-442.

Mohammed, L.N., Saadeh, S., Obulareddy, S., Cooper, S. (2007). "Characterization of Louisiana Asphalt Mixtures Using Simple Performance Tests." 86th Transportation Research Board Annual Meeting, 2007, January 21-25, Washington, D.C.

NCHRP 1-37A Draft Document. *2002 Guide for the Design of New and Rehabilitated Pavement Structures*. ERES Division of ARA Inc., Champaign Illinois, May 2002. http://www.trb.org/mepdg/guide.htm

Hall, K. D., and Beam, S., (2005). "Estimating the Sensitivity of Design Input Variables for Rigid Pavement Analysis with a Mechanistic-Empirical Design Guide." *Transportation Research Record*, 1919, 65 – 73.

Hirsch, T.J., (1961). "The Effects of the Elastic Moduli of the Cement Paste Matrix and Aggregate on the Modulus of Elasticity of Concrete." Ph.D. Thesis, agricultural and mechanical college of Texas (Texas A&M), College Station Texas, January 1961, pp.105.

Kim, S., Ceylan, H., Gopalakrishnan, K., and Heitzman, M., (2006). "Sensitivity Study of Iowa Flexible Pavements Using the Mechanistic-Empirical Pavement Design Guide." presented at the 85th Annual Meeting of the Transportation Research Board, Washington, D.C., 2006.

Memorandum of American Association of State Highway and Transportation Officials, Committee Correspondence, AASHTO Joint Task Force on Pavements, June 2004. http://www.trb.org/mepdg/AASHTO_memorandum.pdf.

Mohammad, L. N., Wu, Z., Obulareddy, S., Cooper, S., and Abadie, C., (2006). "Permanent Deformation Analysis of Hot-Mix Asphalt Mixtures with Simple Performance Tests and 2002 Mechanistic-Empirical Pavement Design Software." *Transportation Research Record*, 1970, 133 – 142.

Nantung, T., Chehab, G., Newbolds, S., Galal, K., Li, S., and Kim, D. H., (2005). "Implementation Initiatives of the Mechanistic-Empirical Pavement Design Guides in Indiana." *Transportation Research Record*, 1919, 142 – 151.

Robinette, C., and Williams, R. C. (2006). "The Effects of the Testing History and Preparation Method on the Superpave Simple Performance Test." *Journal of the Association of Asphalt Paving Technologists*.

Shah, A., McDaniel, R., and Gallivan, V., (2005). "Evaluation of Mixtures using Dynamic Modulus Tester: Results and Practical Considerations." *Journal of the Association of Asphalt Paving Technologists*, 74E.

Tandon, V., Bai, X., and Nazarian, S. (2006). "Impact of Specimen Geometry on Dynamic Modulus Measurement Test Setup." *Journal of Materials in Civil Engineering*, Vol. 18, No. 4, 477-484.

Tarefdar, R.A., Stormont, J.C., and Zaman, M.M. (2007). "Evaluating Laboratory Modulus and Rutting Potential of Asphalt Concrete." Transportation Research Board, 86th Annual Meeting, Washington, D.C.

Witczak, M., Kaloush, K., Pellinen, T., El-Basyouny, M., and Von Quintus, H. (2002). *Simple Performance Test for Superpave Mix Design*. NCHRP Report 465, National Cooperative Highway Research Program, Transportation Research Board, Washington D.C.

Yang, J., Wang, W., Petros, K., Sun, L., Sherwood, J., and Kenis, W., (2005). "Test of NCHRP 1-37A Design Guide Software for New Flexible Pavements." Presented at the 84th Annual Meeting of the Transportation Research Board, Washington, D.C., 2005.

Zhou, F., and Scullion, T. (2003). "Preliminary Field Validation of Simple Performance Tests for Permanent Deformation." *Transportation Research Record No. 1832*, p. 209-216. Transportation Research Board, National Research Council, Washington, DC, 2003.

"Design and Analysis of Experiments." Springer Texts in Statistics. Dean, A., and Voss, D. (1999). ISBN 0-387-98561-1.

APPENDIX 1

DYNAMIC MODULUS DATABASE

A1.1 Introduction

Two databases are presented in this section: a database of dynamic modulus values of the mixes investigated in this study and a database of fitting parameters for a sigmoidal function that can be used for computing dynamic modulus of the mixes investigated in this study at any temperature and frequency. These databases are cornerstones for a comprehensive database of mixes used in the State of Washington.

A1.2 Database of Dynamic Modulus of the Mixes Investigated

Table A1.1 (a) through (g) presents dynamic modulus data measured at different temperatures and frequencies for JMF, LM and UM mixes and their replicates in each project. The test-specimen properties asphalt content, percent air voids and unit weight are also presented. The mix properties in the replicates do not vary except the air voids; in some cases, it differs by approximately 1%. However, in Section 4.3, Chapter 4 it was shown that variation in air voids did not affect dynamic modulus of replicates.

The database will be useful for the evaluation of existing pavement sections listed in Table 3.1, Chapter 3 if air voids in the existing field HMA layer does not vary substantially from the air voids in the database. In addition, the dynamic modulus values in the database are representative of the mixes that are widely used in the State of Washington for usage in preliminary/trial designs. They can also be used as input parameters to the MEPDG to predict distresses in actual or trial designs. The dynamic modulus values of LM and UM mixes can be

used for evaluation purposes when variability in the percent-passing sieve #200 is expected or noticed. However, in Section 4.5.4, Chapter 4 it was shown that dynamic modulus of JMF, LM and UM mixes do not vary significantly. Even though a general conclusion is not plausible, variation in percent-passing sieve #200 within the tolerance limits might not affect dynamic modulus significantly.

It must be understood that the database can be used only if the air voids in the field do not differ significantly from the air voids in the database, or can be used where air voids is expected to be within the range 6±1%. If the air voids differ substantially, computation of approximate shift factors might be required in order to use the database. Other factors like aggregate and asphalt content in the study were same as in the field.

A1.3 Database of Sigmoidal Fitting Parameters for Determining Dynamic Modulus

The dynamic modulus data presented in Table A1.1 (a) through (g) are only valid for the conditions (i.e. temperatures and frequencies) tested in the laboratory. Dynamic modulus of the mixes at other conditions can be determined with the help of master curves. Section 4.4, Chapter 4 presents the concept of master curves and construction procedure. Dynamic modulus at any temperature and frequency can be determined using Eq.A1.1. A database of sigmoidal fitting parameters is presented in Table A1.3. The parameter $\log (t_r)$ is unknown in the equation and can be computed using Eq.A1.2. In order to use this equation viscosity of asphalt at the temperature in question and at the reference temperature, in most cases 21.1 °C, is required. Table A1.2 summarizes the viscosities of the asphalt binders at different temperatures. For any other temperature, Eq.A1.3 can be used. The regression parameters, A and VTS, in Eq.A2.3 are constant for a particular asphalt binder. Table A1.4 summarizes A and VTS for the asphalt

binders used in this study. The parameters of Eq.A1.1 through A1.3 are explained in Section 4.4, Chapter 4.

$$\log |E^*| = \chi + \frac{\alpha}{1 + e^{\beta + \gamma \log t_r}} \quad \text{... (A1.1)}$$

$$\log(t_r) = \log(t) - c[\log(\eta) - \log(\eta_{T_r})] \quad \text{............................ (A1.2)}$$

$$\log\log\eta = A + VTS \log(T_R) \quad \text{... (A1.3)}$$

A1.4 Sample Computation of Dynamic Modulus Using Sigmoidal Fitting Parameters

This section presents a sample E* prediction for Mix 5381 at a temperature of 45 °C and a frequency of 35 Hz.

Step 1: Compute time of loading

Time of loading, $t = \dfrac{1}{f}$

where, f is the frequency in Hz.

Here, f = 35 Hz. Then, t = $\dfrac{1}{35}$ = 0.03 sec

log(t) = log(t$_{35}$) = log(0.03) = -1.523

Step 2: Compute viscosity at 45 °C

The asphalt binder grade in Mix 5381 is PG 58-22.

$$loglog\eta = A + VTS\log(T_R)$$

Temperature in Rankine, $T_R = \frac{9}{5} \times T_c + 491.69$, where T_C is the temperature in Celsius

Here, $T_C = 45\ °C$

$T_R = \frac{9}{5}$ x 45 + 491.69 = 572.69

$logT_R = 2.76$

A = 16.4394, VTS = -5.7574 (read from Table A1.4)

$log(log(\eta_{45})) = 16.4394 + (-5.7574)$ x (2.76) = 0.5609

Taking anti-logarithm twice, $\eta_{45} = 4.4$ x 10^3 cP

$log(\eta_{45}) = log(4.4$ x $10^3) = 3.64$

Step 3: Compute time of loading at the reference temperature $log(t_r)$

The reference temperature is 21.1 °C.

$log(t_r) = log(t_{35}) - c\ [log(\eta_{45}) - log(\eta_{21.1})]$

c = 1.237558 (read from Table A1.3; JMF1)

$\eta_{21.1} = 5.05x10^5$ cP (read from Table A1.2)

$log(\eta_{21.1}) = log(5.05x10^5) = 5.703$

$log(t_r) = -1.544 - 1.237558\ [3.64 - 5.703] = 1.011$

Step 4: Compute E*

$$\log | E^* | = \chi + \frac{\alpha}{1 + e^{\beta + \gamma \log t_r}}$$

$\chi = 0.429752$; $\alpha = 3.760578$; $\beta = -1.53895$; $\gamma = 0.604881$ (read from Table A1.3; JMF1)

Plug in log(t$_r$) from Step 3

$$\log |E^*| = 0.429752 + \frac{3.760578}{1 + e^{-1.53895+0.604881\times1.011}} = 3.124399$$

Taking anti-logarithm, $|E^*| = 10^{\wedge 3.124399} = 1332$ MPa

*The dynamic modulus of Mix 5381 (JMF1) at 45 °C and 35 Hz is **1332 MPa**.*

Table A1.1 Dynamic modulus of the mixes investigated in this study

(a) Mix ID 5381

Temp (°C)	Freq (Hz)	E*, MPa					
		JMF1	JMF2	LM1	LM2	UM1	UM2
4.4	25	15794	16215	15059	15534	15459	15694
	10	14387	14859	13514	14015	13799	14097
	5	13311	13753	12646	12697	12600	12835
	1	10796	11089	10118	9919	9789	10087
	0.5	9778	10221	9042	8748	8468	8828
	0.1	7367	7331	6553	6253	5784	5866
21.1	25	7216	7884	6641	6943	6459	6704
	10	5856	6250	5393	5537	4973	5065
	5	4888	5082	4586	4633	3959	4000
	1	2985	2888	2754	2709	2179	2155
	0.5	2254	2141	2093	2093	1593	1592
	0.1	1106	972	1023	1027	690.1	697.4
37.8	25	2681	2638	1691	2635	1490	1939
	10	1907	1490	1192	1376	903.4	1182
	5	1389	1012	834.3	939.9	594.9	801
	1	577.2	390.8	321.7	379.6	220.3	361.3
	0.5	378.1	267.7	215.3	263.9	151	283.7
	0.1	143.3	118.8	89.4	116.4	74.7	190.1
54.4	25	282.3	692.3	609.9	1162	388.8	574.5
	10	339.1	287.5	292.6	694.4	222.6	302.6
	5	210.7	168.3	182.2	447.3	157.2	191.9
	1	65.1	62.6	63.8	153.9	78.3	82.7
	0.5	49.2	48.4	48.8	109	66.9	73.5
	0.1	26.9	30.2	30.5	61.3	52.3	53.7
Asphalt (%)				5.7			
Air voids (%)		7.9	6.6	7.0	7.1	7.2	7.8
Unit wt. (pcf)		143	145	145	145	144	143

(b) Mix ID 5295

Temp (°C)	Freq (Hz)	E*, MPa					
		JMF1	JMF2	LM1	LM2	UM1	UM2
4.4	25	15922	17732	14672	15534	17137	18463
	10	14553	16061	13300	14015	15633	16909
	5	13496	14804	12280	12697	14583	15694
	1	10839	11750	9633	9919	11831	13014
	0.5	9608	10371	8582	8748	10812	11876
	0.1	6870	7559	6259	6253	8010	8934
21.1	25	7688	8461	6930	6943	8357	9190
	10	6208	6837	5710	5537	6685	7613
	5	5330	5672	4832	4633	5702	6551
	1	3255	3468	3035	2709	3676	4210
	0.5	2564	2750	2399	2093	2943	3444
	0.1	1351	1473	1375	1027	1612	1932
37.8	25	2255	3431	2346	2635	2676	2761
	10	1496	2392	1660	1376	1922	1912
	5	1095	1805	1238	939.9	1482	1415
	1	482.2	860	647.6	379.6	710.8	658.2
	0.5	339.4	619.5	510.9	263.9	507.5	483.7
	0.1	161.1	284.4	323.8	116.4	240.8	242.3
54.4	25	759.8	776.7	931.6	1162	701.1	1322
	10	491.3	456.9	651.1	694.4	693.6	701.5
	5	331.6	305.6	513.1	447.3	394.2	482.6
	1	123.2	126.3	328.4	153.9	247.2	199.3
	0.5	91.1	98.4	286	109	182.5	144.6
	0.1	49.5	54.9	222.7	61.3	97.2	70.9
Asphalt (%)				5.3			
Air voids (%)		8.1	7.1	7.5	8.2	7.6	7.2
Unit wt. (pcf)		142	144	144	142	143	144

(c) Mix ID 5192

Temp	Freq	E*, MPa					
(°C)	(Hz)	JMF1	JMF2	LM1	LM2	UM1	UM2
4.4	25	16649	17185	14458	16550	16458	18428
	10	15454	15718	13230	15519	15181	17001
	5	14561	14581	12283	14651	13932	15939
	1	12511	11703	10059	12310	11259	13389
	0.5	11581	10419	9234	11248	10136	12240
	0.1	9229	7610	7004	8908	7545	9585
21.1	25	8855	7729	6925	8799	7730	9250
	10	7452	6236	5602	7368	6303	7721
	5	6530	5113	4802	6403	5182	6739
	1	4425	3068	3101	4438	3174	4426
	0.5	3665	2473	2447	3701	2516	3536
	0.1	2172	1206	1365	2190	1296	2087
37.8	25	2654	2292	1747	2861	2218	1798
	10	1916	1521	1294	2100	1456	1885
	5	1438	1065	926.4	1649	1032	1423
	1	679.1	417.4	390.8	779.8	403.9	658.1
	0.5	481.5	276	273.2	554.1	268.4	450.9
	0.1	209.2	110.1	123.6	236	105.3	191.2
54.4	25	975.6	2558	847.3	2956	571.3	2037
	10	618	1677	583.4	906.5	332.5	844.2
	5	426.1	1145	407.7	638.6	208.6	575.2
	1	154.5	428	147.7	238.8	70.3	208.5
	0.5	107.4	281.1	104.5	156.2	53.7	140
	0.1	52.2	145.7	78.3	68.9	31	67.4
Asphalt (%)				5.1			
Air voids (%)		7.0	6.8	7.3	7.3	7.2	6.8
Unit wt. (pcf)		144	144	144	144	144	145

(d) Mix ID 5373

Temp (°C)	Freq (Hz)	E*, MPa					
		JMF1	JMF2	LM1	LM2	UM1	UM2
4.4	25	14193	11702	11996	13146	11428	11658
	10	12844	10648	10486	11550	9868	10067
	5	11433	9671	9251	10353	8729	8765
	1	8804	7260	6640	7687	6079	6002
	0.5	7778	6284	5717	6614	5126	5020
	0.1	5497	4242	3712	4505	3245	3097
21.1	25	5911	4863	4450	5279	3957	4082
	10	4636	3666	3246	4121	3001	3058
	5	3878	2923	2554	3272	2347	2389
	1	2333	1652	1343	1869	1243	1213
	0.5	1833	1288	1024	1456	938.2	910.1
	0.1	1015	716.6	522.3	808.7	455.8	464.3
37.8	25	1781	1630	888.2	1420	859.1	1042
	10	1344	933.1	703.1	983.9	652.5	663.1
	5	1005	677.7	503.4	724.7	478.4	474.8
	1	472.2	345.2	236.5	352.4	209.6	220.9
	0.5	354.9	276.6	188.3	277.9	159.6	179.3
	0.1	184.2	170.5	107.5	160.8	88.4	109.8
54.4	25	320	1549	1132	502.8	888.1	440.9
	10	416.6	330.2	344.4	353.7	23.5	285.1
	5	297.7	217.8	220.4	257.7	8.9	192.8
	1	123.5	112.4	93.5	138.2	72.5	96.8
	0.5	101.5	95.7	79.8	118.3	64.5	82.1
	0.1	66.2	64	52.3	82.6	31.1	59.9
Asphalt (%)				5.4			
Air voids (%)		6.1	7.3	7.2	6.3	7.2	7.1
Unit wt. (pcf)		149	148	148	149	148	148

(e) Mix ID 5627

Temp	Freq	E*, MPa					
(°C)	(Hz)	JMF1	JMF2	LM1	LM2	UM1	UM2
4.4	25	17178	16522	15992	15036	15324	17668
	10	15315	15222	14371	13480	14070	15832
	5	14240	13827	13155	12362	13350	13901
	1	11347	10767	10263	9760	10943	10655
	0.5	9866	9382	9212	8782	9789	9391
	0.1	7103	6574	6539	6402	7106	6522
21.1	25	7707	7676	7555	7389	7879	7461
	10	6488	6139	6177	5893	6415	5916
	5	5523	4914	5055	4912	5135	4713
	1	3364	2732	3070	3021	3174	2780
	0.5	2731	2103	2560	2358	2554	2132
	0.1	1427	1009	1540	1251	1327	1023
37.8	25	3175	3044	3002	2341	2531	2593
	10	2442	1834	2323	1538	1491	1660
	5	1841	1293	1856	1133	1064	1194
	1	841.4	541.7	1346	507.6	453.5	490.9
	0.5	576.2	365	1153	362.2	318.1	333.5
	0.1	257.9	159.3	953.5	168.3	148.1	140.2
54.4	25	716.5	849.7	590.5	1732	788.7	1285
	10	631.3	414.7	390.6	586.5	574.9	486.5
	5	408.1	252.8	274.1	396.6	379.7	308.5
	1	144.3	90	120.2	146.2	134.9	115.9
	0.5	99.8	69.4	99.8	106.1	99.8	83.2
	0.1	52.6	41.4	74.3	55	55	48.5
Asphalt (%)				4.5			
Air voids (%)		7.5	7.4	8.6	5.7	6.2	6.0
Unit wt. (pcf)		151	151	149	154	153	154

(f) Mix ID 5364

Temp (°C)	Freq (Hz)	E*, MPa					
		JMF1	JMF2	LM1	LM2	UM1	UM2
4.4	25	14418	12964	14495	14663	13084	13895
	10	12247	11738	13070	13345	11587	12199
	5	10944	10696	11985	12319	10211	10889
	1	7815	7831	9548	9868	7405	7852
	0.5	6541	6756	8535	8790	6477	6571
	0.1	4202	4475	6227	6278	4410	4183
21.1	25	5040	5393	6298	6755	5178	5174
	10	3950	4286	5261	5442	3899	3800
	5	3088	3273	4385	4426	3004	3054
	1	1554	1729	2642	2747	1515	1601
	0.5	1121	1262	2073	2211	1105	1166
	0.1	526.5	579.1	1089	1154	582.7	581.5
37.8	25	1244	1332	2029	1899	1258	1139
	10	797.4	819.1	1315	1321	759.9	679.3
	5	572.6	560.4	935.9	972	508.3	449.3
	1	292.5	232.3	392.6	424.7	212.2	173.1
	0.5	239.3	171	273.4	299.8	158.8	128.1
	0.1	167.4	95.8	123.8	132.2	95.2	66.2
54.4	25	635.3	511.4	670.8	936.9	498.5	492.9
	10	425.7	306.3	400.1	426.3	317.3	306.6
	5	324.2	214.2	254.8	265.7	237.5	219.1
	1	213.6	114.2	93.6	98.7	151.2	123
	0.5	191.1	98.4	69.2	72.3	137.7	108.8
	0.1	157.5	77.8	40.3	39.8	117.2	88.6
Asphalt (%)				5.3			
Air voids (%)		6.4	6.4	7.1	7.1	6.8	6.3
Unit wt. (pcf)		146	146	145	145	146	146

(g) Mix ID 5408

Temp	Freq	E*, MPa					
(°C)	(Hz)	JMF1	JMF2	LM1	LM2	UM1	UM2
4.4	25	14747	13904	12472	13676	14998	13988
	10	13186	12285	11050	11917	13193	12800
	5	12006	10915	9724	10613	11982	11522
	1	9140	8073	7039	7783	8876	8188
	0.5	7891	7022	6100	6520	7581	6944
	0.1	5317	4649	4088	4268	4806	4519
21.1	25	6378	5699	5189	5244	5967	5728
	10	4918	4436	4040	4159	4491	4304
	5	4025	3497	3242	3333	3497	3426
	1	2348	1904	1702	1763	1923	1756
	0.5	1793	1386	1252	1287	1449	1245
	0.1	907.8	659.5	564.1	596.2	663.1	541.1
37.8	25	2217	1490	1359	1544	1502	1459
	10	1425	929.8	834	982.3	950.5	885.6
	5	1022	636.4	563.8	678.9	664.5	593.5
	1	452	247.3	226.4	291.4	304.8	238
	0.5	324.1	172.8	158.3	212.9	234.5	172.4
	0.1	157.8	83.8	71.2	113.6	140.6	92.9
54.4	25	741.8	785.4	490.1	513.5	500.8	516.3
	10	376.4	434.8	271.3	281	280	327.5
	5	236.7	275.6	172.7	178.9	184.7	236.2
	1	95.9	100.2	60.8	64.6	68.6	133.4
	0.5	73.7	76.5	46.5	79.4	54.2	115.4
	0.1	45.1	47.6	28.6	51	35	88.7
Asphalt (%)				5.3			
Air voids (%)		7.4	7.3	7.9	7.8	7.2	7.5
Unit wt. (pcf)		146	146	145	145	146	146

Table A1.2 Viscosity of asphalt binders at standard test temperatures

Temp °C	Viscosity (cP)						
	5381	5295	5192	5373	5627	5364	5408
	58-22	70-22	64-22	70-28	64-28	58-22	64-28
4.4	9.51×10^7	1.45×10^8	3.78×10^8	1.43×10^7	2.94×10^7	6.04×10^7	6.01×10^7
12.7	5.51×10^6	1.10×10^7	1.60×10^7	1.66×10^6	2.40×10^6	4.03×10^6	3.98×10^6
21.1	5.05×10^5	1.20×10^6	1.14×10^6	2.57×10^5	2.87×10^5	4.11×10^5	4.03×10^5
29.4	7.27×10^4	1.94×10^5	1.36×10^5	5.45×10^4	5.03×10^4	6.40×10^4	6.26×10^4
37.8	1.42×10^4	4.03×10^4	2.29×10^4	1.42×10^4	1.14×10^4	1.33×10^4	1.30×10^4
46.1	3.70×10^3	1.08×10^4	5.31×10^3	4.58×10^3	3.32×10^3	3.61×10^3	3.52×10^3
54.4	1.19×10^3	3.45×10^3	1.56×10^3	1.71×10^3	1.16×10^3	1.20×10^3	1.17×10^3

Table A1.3: Master curve fitting parameters

Mix	Fitting parameter	JMF1	JMF2	LM1	LM2	UM1	UM2
5381	χ	0.429752	0.723597	0.685327	1.094173	1.412442	1.107084
	α	3.760578	3.505684	3.522654	3.18061	2.771668	3.190491
	β	-1.53895	-1.29788	-1.23332	-0.96776	-0.75969	-0.84595
	γ	0.604881	0.706093	0.665885	0.715226	0.829887	0.62152
	c	1.237558	1.0693	1.088817	0.858737	1.04894	1.053801
5295	χ	0.754426	0.739572	2.097732	1.115056	1.349815	0.850646
	α	3.540724	3.525531	2.121062	3.174893	2.97311	3.516116
	β	-1.21295	-1.4508	-0.57006	-0.94547	-1.04119	-1.26753
	γ	0.589617	0.584911	0.717185	0.713823	0.580509	0.571712
	c	1.118277	1.210963	1.089971	0.895927	1.173026	1.112086
5192	χ	0.717671	1.577324	1.32258	0.838219	0.611667	0.82866
	α	3.532344	2.795282	2.882083	3.415631	3.61956	3.512376
	β	-1.54077	-0.68855	-1.01487	-1.4876	-1.37461	-1.30994
	γ	0.605617	0.759926	0.698459	0.677857	0.653291	0.611534
	c	1.070714	0.65738	0.939002	0.862534	1.040376	0.921389
5373	χ	0.951054	1.06223	0.984625	1.462069	0.94939	1.356004
	α	3.352918	3.211286	3.395035	2.799761	3.128716	2.925591
	β	-0.9497	-0.73676	-0.52767	-0.58053	-0.82761	-0.34539
	γ	0.492612	0.587209	0.560918	0.59849	0.597303	0.627483
	c	1.446028	1.113646	1.086728	1.289935	1.576219	1.151558
5627	χ	0.720986	0.61706	0.870989	0.740363	1.010413	0.685796
	α	3.527131	3.665471	3.433698	3.5238	3.251023	3.653522
	β	-1.43743	-1.26066	-1.19168	-1.21507	-1.15226	-1.12177
	γ	0.604239	0.638959	0.578819	0.636242	0.659386	0.635165
	c	1.194188	1.101545	1.05	1.015378	1.121583	1.016377
5364	χ	2.062348	1.629383	0.657738	0.599883	1.875792	1.692657
	α	2.171295	2.533179	3.573183	3.642303	2.264939	2.491587
	β	0.010771	-0.48116	-1.20807	-1.24136	-0.24289	-0.31901
	γ	0.871458	0.831703	0.607851	0.60718	0.91855	0.865757
	c	0.936438	0.982732	1.095646	1.072552	0.969752	0.969007
5408	χ	0.654177	1.076748	0.724261	1.170639	0.544068	1.719066
	α	3.604997	3.182946	3.460911	3.039655	3.798391	2.475911
	β	-1.12988	-0.74576	-0.92331	-0.74213	-0.93878	-0.38433
	γ	0.585194	0.699142	0.663697	0.679031	0.53111	0.878477
	c	1.051831	0.907786	0.987328	1.012931	1.096855	0.939319

Table A1.4: Viscosity regression coefficients

| Mix	Binder grade	A	VTS
5381	PG 58-22	16.4394	-5.7574
5295	PG 70-22	14.5301	-5.0462
5192	PG 64-22	17.039	-5.9679
5373	PG 70-28	13.7993	-4.7966
5627	PG 64-28	15.3901	-5.3792
5364	PG 58-22	16.0001	-5.5986
5408	PG 64-28	16.0605	-5.6210

SAMPLE DYNAMIC MODULUS CURVES
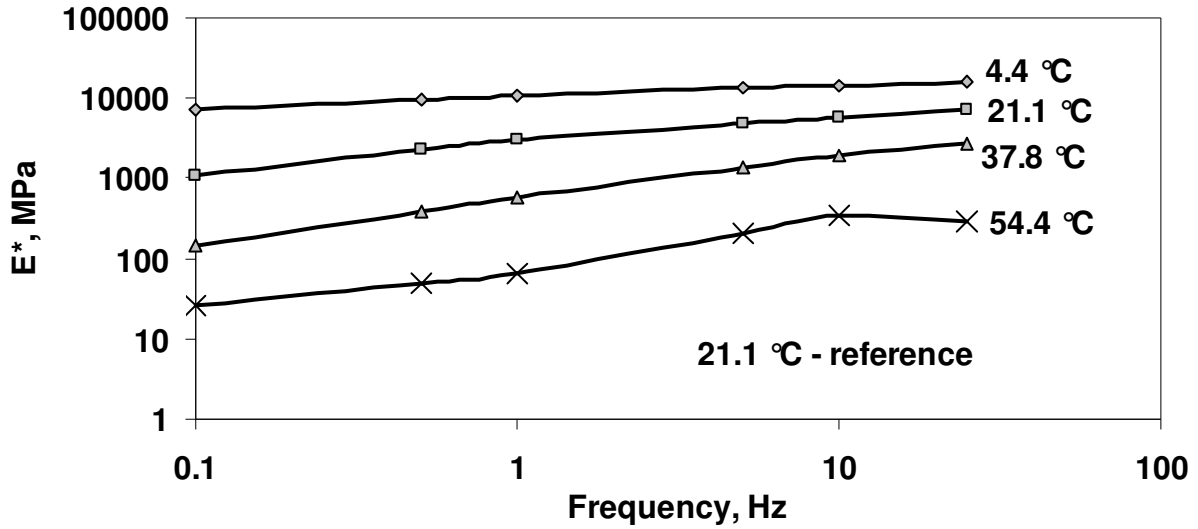
Figure A2.1: Typical raw dynamic modulus data measured at different temperatures and

frequencies
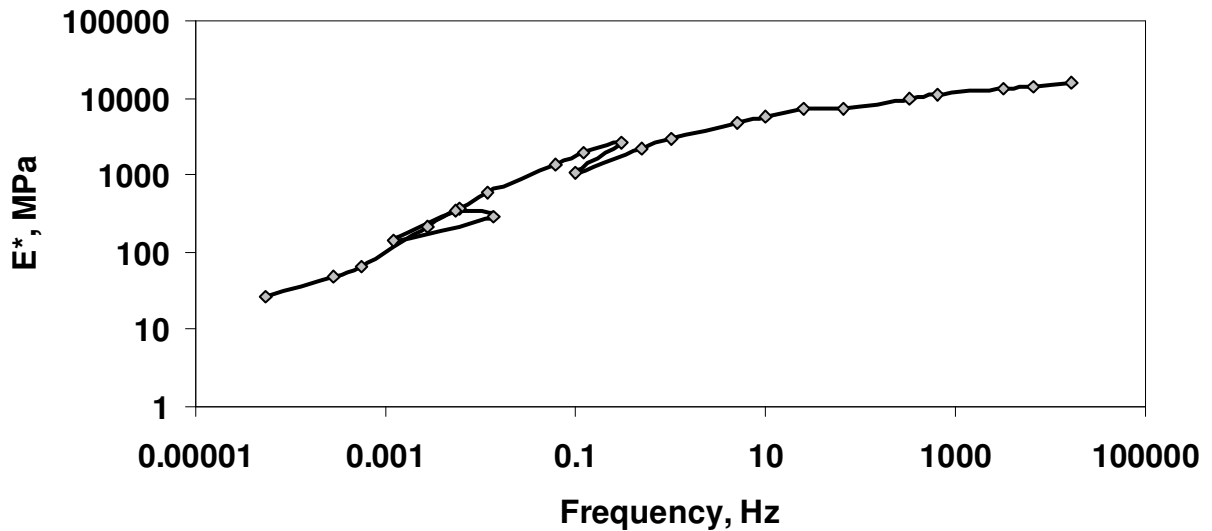
Figure A2.2: Master curve constructed by shifting the curves in Fig. A1.1 with reference to

21.1°C
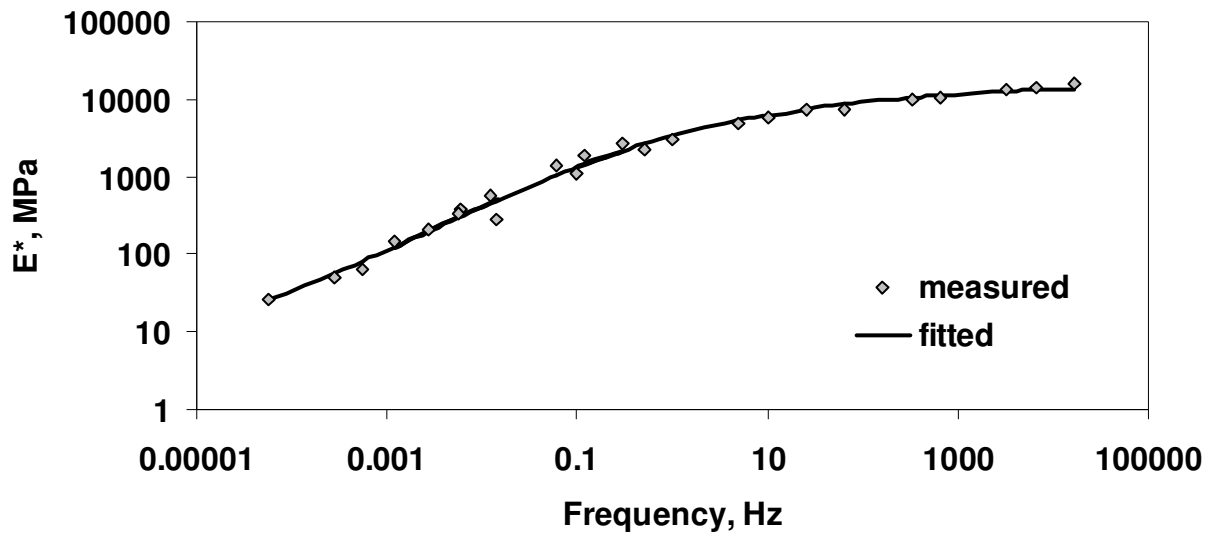
Figure A2.3: Master curve after sigmoidal curve fitting

APPENDIX 3

ANALYSIS OF VARIANCE – BASIC TERMINOLOGIES

A3.1 Treatment Factor

Treatment factor is any substance or item whose effect on the data is studied. The *levels* are the specific types or amounts of the treatment factor in the experiment. For example, a treatment factor might be a drug in a study whose levels are the different amounts of the drug studied. In an experiment, there can be one or many treatment factors each having its own levels. If two or more treatment factors are involved in an experiment then the combination of treatment factors is a 'treatment combination' or simply 'treatment'. For example, in a dynamic modulus test, temperature and frequency are the two treatment factors. Each temperature and frequency combination, say 4.4 °C and 25 Hz, is a treatment combination or treatment.

A3.2 Response

Response or response variable is the outcome of the study. Obviously, it is dependent upon the levels of the treatment factors. For instance, dynamic modulus is a response dependent on temperature and frequency.

A3.3 Experimental Units

Experimental units are the "material" to which the levels of the treatment factor(s) are applied. For example, HMA test specimens are the experimental units in a study investigating dynamic modulus of different mixes.

A3.4 Model

A model is a mathematical representation of the dependence of the response variable upon the levels of the treatment factors. The model expresses the response variable (Y) as a linear sum of the *true response*, denoted by μ, and the *error variable* or *residual error*, denoted by ε. Linear models provide reasonably good approximations and are used extensively. Eq.A3.1 shows the mathematical form of a typical linear model.

$$Y = \mu + \varepsilon \quad\text{.. (A3.1)}$$

Any model that takes the form similar to Eq.A3.1 is a *linear model*. This model is valid for a case involving a single treatment factor. If two or more treatment factors are involved, the model takes the form shown in Eq.A3.2.

$$Y_{it} = \mu_i + \varepsilon_{it} \quad\text{... (A3.2)}$$

where,

$t = 1,\ldots, r_i, i = 1,\ldots, v.$

v is the number of treatments, t is the experimental unit in question, and r_i is the number of observations taken on the ith treatment.

For example, if dynamic modulus (E*) is the response, temperature and frequency are the treatment factors, and two replicates were tested, the model can be written as,

$$E^*_{it} = \mu + \varepsilon_{it}$$

$i = 1, 2$ (1 – temperature; 2 – frequency); $t = 1, 2$ (two replicates); $r_i = 2$ (two replicates)

A3.5 Testing Equality of Treatment Effects

In an experiment involving many treatments, a common objective is to test whether or not the treatments differ in terms of their effects on the response variable. Two hypotheses are possible – null hypothesis and alternative hypothesis. Null hypothesis (H_0) exists if the treatment effects are all equal; alternative hypothesis (H_A) exists if the treatment effects differ (at least two of the treatment effects differ). For example, if dynamic modulus of different mixes is compared, null hypothesis will exist if dynamic modulus of the mixes does not vary (i.e., $E_{mix1} = E_{mix2} = \ldots = E_{mix7}$). If dynamic modulus of all or at the least two of the mixes differs then alternative hypothesis exists (i.e., $E_{mix1} \neq E_{mix2} \neq \ldots \neq E_{mix3}$). H_0 is either accepted or rejected depending upon p-value. If the computed p-value is less than the significance level (α) (see section A3.6), H_0 is rejected.

i.e., reject H_0 if $p < \alpha$.

A3.6 Significance Level (α)

It is the probability of rejecting H_0 (i.e., the treatment effects are equal) when it is actually true (H_A) – this is called a Type I error. Generally, α is set before testing the hypothesis. It should be small if it is important not to commit a Type I error (typical choices are $\alpha = 0.01$ and 0.001); otherwise, a larger value can be chosen (typical choices are $\alpha = 0.01$ and 0.05).

A3.7 *P*-value

In simple terms, *p*-value is the smallest level of significance that would lead to rejection of the null hypothesis H_0; most computer programs for statistical analysis report *p*-values. For example, if the specified level of significance (α) is 0.01 and if p-value from the software is

0.0001, H_0 exists. In this study, the statistical software SAS Version 9.1 is used for computing p-values. Any textbook on analysis and design of experiments will explain the procedure for computing p-value.

A3.8 Analysis of Variance (ANOVA)

Section A3.4 showed that any observed response can be expressed as the linear sum of true response μ and residual error ε. If in an experiment, there are n responses each response will differ/deviate from the true response μ by some error ε_t (where t refers to the response under question). Obviously, the question of interest would be "How big are the errors?" *Analysis of Variance* or *ANOVA* is the method used for measuring the error size important in p-value computations. If the experiment involves a single treatment factor, it is a case of single-factor ANOVA. If more than one treatment factor is involved, it is a case of multi-factor ANOVA. ANOVA can be performed using statistical software like SAS, which is used in this study.

A3.9 Repeated Measures ANOVA

It is a special case when the experiment involves testing of all treatment factors or all levels of the treatment factor(s) on a single experimental unit; the treatment factors are called repeated measures. For example, in a dynamic modulus test a single specimen is tested under all temperatures and frequencies. This requires a different statistical approach, which is the repeated measure ANOVA. On the other hand, if the test uses a different specimen for different temperatures and frequencies, say one specimen for 4.4°C and 25 Hz, and a different specimen for 4.4°C and 10Hz, it becomes a case of standard ANOVA explained in Section A2.6.

A3.10 Tukey's Multiple Comparison Method

This method is best for all pairwise comparisons. Pairwise comparison means comparing each item with the rest of the items in the population. For example, in this study one of the objectives was to test if the seven JMF mixes produced significantly different dynamic modulus. Pairwise comparison here means comparing the dynamic modulus of each JMF mix with the dynamic modulus of the other mixes i.e. JMF1 vs. JMF2, JMF1 vs. JMF3 etc.

Tukey's method computes p-values by first computing confidence intervals for all pairwise comparisons. Confidence interval is the upper and lower limit within which the response of one treatment will differ from the other treatment. For example, consider a study conducted to determine the effect of number of revolutions per minute (rpm) of a pump on the fluid flow rate (in liters per minute). If after comparing 75 rpm and 50 rpm the confidence interval was found to be (0.53, 0.64). Here, 0.64 is the upper limit and 0.53 is the lower limit indicating that the fluid flow rate at 75 rpm will vary between 0.53 and 0.64 liters per minute greater than at 50 rpm. This is confidence interval for a single contrast. If many contrasts are involved, confidence intervals for all the pairwise comparisons can be determined using Tukey's multiple comparison method. Tukey's method uses the confidence intervals of all pairwise comparisons to determine p-values for each pairwise comparison.

APPENDIX 4

DISTRESS DATA COLLECTION[1]

A4.1 Data Collection

Pavement condition data is collected using a specialized pavement condition van (PCV), illustrated in Fig. A4.1. A two-person team, driving at the posted speed limit, operates the PCV. The PCV is equipped with six cameras that capture digital images of the driver's perspective, the right shoulder view, and the full width of the pavement surface. The driver's perspective and right shoulder view cameras are placed above the windshield of the PCV; two pairs of cameras capture the roadway surface, placed on extension arms at the front and at the rear of the PCV. The arrangement of the cameras is illustrated in Figure A4.2. The pavement image is captured using one pair of cameras, each photographing half of the 12-foot lane. Each camera captures an image 5x6.5 ft wide; images are captured every 25 feet. Depending on the angle of the sun, either the front cameras or the rear cameras are selected to minimize shadows on the pavement surface images. This arrangement of cameras and the captured images are used for characterizing surface distresses (cracking, patching, etc.).

In addition to surface distress, it is also important to quantify the surface characteristics that affect the roadway user. These characteristics are a measure of roadway roughness (roadway profile in the longitudinal direction), rutting/wear (variation of roadway surface in the transverse direction), and faulting. The roadway profile and rutting/wear measurements are collected via laser sensors mounted on the front and rear of the pavement condition van. The PCV is equipped with a profile bar, illustrated in Figure A4.2-(a), comprising laser sensors and accelerometers for

---

[1] Pierce, L.M. (2008). Washington State Department of Transportation, State Pavement Engineer, Personal Communication, May 2008.

measuring the longitudinal profile, from which roughness and faulting are calculated. The INO laser illustrated in Figure A4.2-(b) measures rutting/wear transversely across the pavement surface. The INO laser system consists of two laser line profilers (each capturing one-half of the roadway width) and a special camera for measuring deformations (rutting or wear) of the laser line profile.

A4.2 Data Analysis

The pavement profile and INO data is processed via computer programs, for determination of roughness, faulting and maximum wheel path wear depth. Processing of the digital images is a much more time consuming operation, since it requires review of each pavement image by trained pavement rating staff. Review of pavement condition images are accomplished via a specially developed computer program (PathView II) that allows the pavement rating staff to view images for the driver's perspective, the right shoulder view and the pavement view on one screen, illustrated in Figure A4.3. In Figure A4.3, the upper left hand image is the driver's perspective view, the upper right hand image is the right shoulder view, and the lower images are of the full lane width of the pavement surface.

The digital images are viewed one by one for a variety of pavement distress (cracking, patching, spalling, etc.) types. The pavement rating staff, using a specially coded keyboard, views the digital image for any pavement distress and use keystrokes that correspond to the noted distress. The computer program records the keystroke and beginning and ending milepost locations of each distress. Once the pavement distress rating is complete, the data is processed for determination of type and length of distress and summed of 0.10 mile increments.

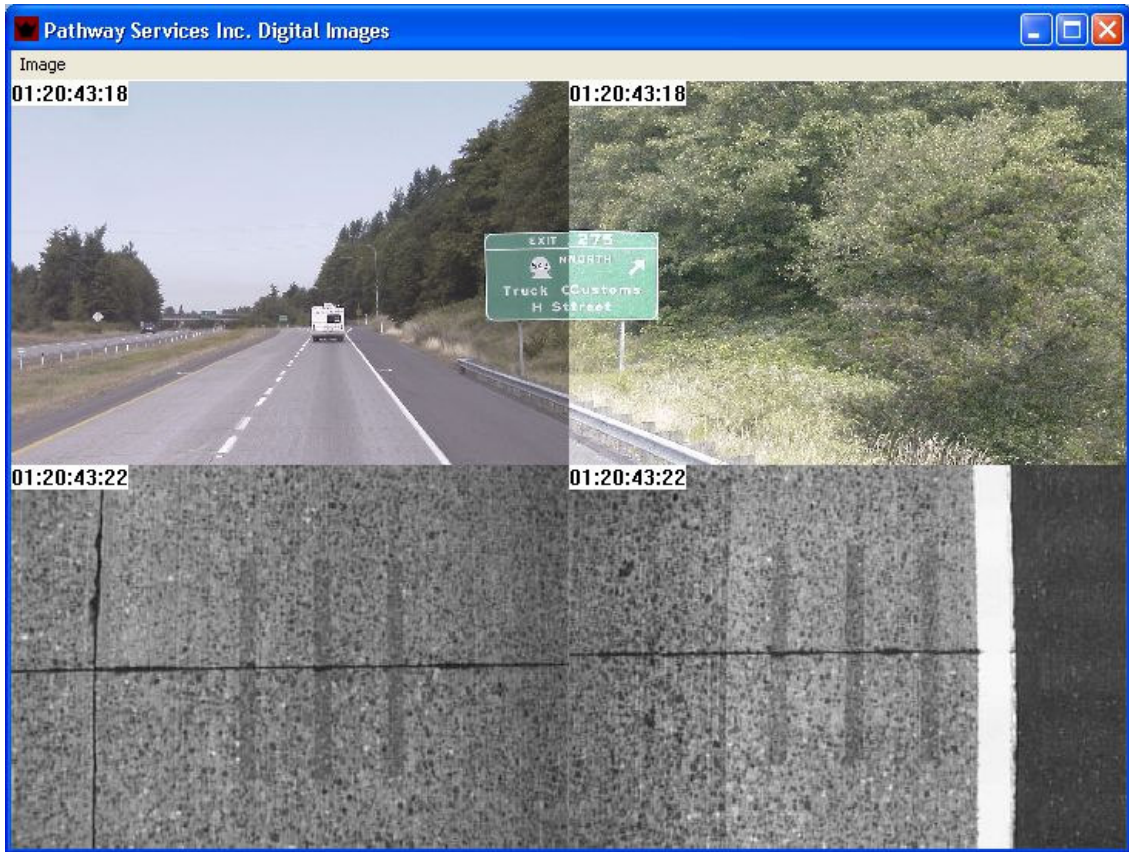**Figure A4.1** WSDOT pavement condition van.
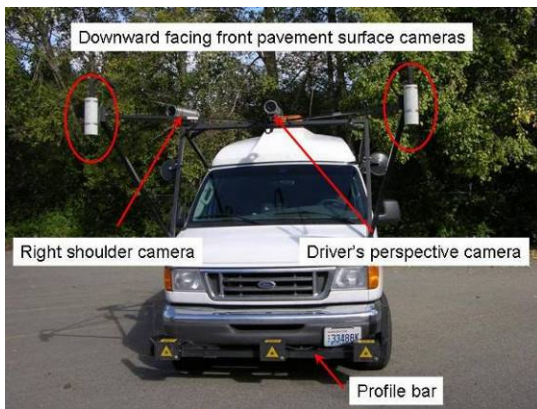
(a) Front of van

(b) Rear of van

Figure A4.2 Arrangement of cameras and sensors.

Figure A4.3 Sample image of pavement condition survey.